THEORY OF OUTER-SPHERE ELECTRON-TRANSFER REACTIONS

Thesis by

Paul David Siders

In Partial Fulfillment of the Requirements

for the Degree of

Doctor of Philosophy

California Institute of Technology

Pasadena, California

1983

(Submitted May 16, 1983)

Acknowledgments

I thank Vicky Hodgson Siders for her patience and support during my graduate research. It is a pleasure to acknowledge Professor R. A. Marcus' direction and support of that research. I am grateful for interactions with colleagues, especially with Robert Cave and Robin Lucchese. Chapter 5 of this thesis describes work done in collaboration with Robert Cave.

I remain indebted to Professors J. Kirk Romary and Charles McCoy who have communicated to me a taste for science that I hope to explore through many years.

ABSTRACT

Classical, semiclassical and quantum theories of outer-sphere electron-transfer reactions in polar media are discussed. For each, the Franck-Condon overlap factors for the hexaamminecobalt, hexaaquoiron and hexaammineruthenium self-exchange rates and for the cross-reaction of hexaaquoiron(II) with tris(2,2'-bipyridine)ruthenium(III) are evaluated and compared. The quantum effect on the rates is small in the region of moderate driving force; the "normal" ΔG^{o} region. Direct-sum and saddle-point evaluations of the quantum Franck-Condon factors are made and compared. The saddle-point approximation is shown to be an excellent approximation in the cases considered.

Quantum effects in homogeneous outer-sphere electron-transfer reactions in the region of large negative ΔG^{o} (the "inverted" region) are considered. The results of quantum, semiclassical and classical calculations on model systems are presented. A sequence of highly exothermic photoinduced reactions of tris(2,2'-bipyridyl) complexes is discussed with regard to the possible importance of quantum effects and of alternate reaction pathways in understanding the failure of the sequence of reactions to exhibit pronounced "inverted" behavior.

A mechanism leading to electronically excited products provides a possible explanation for the large discrepancy.

The theory of highly exothermic homogeneous outer-sphere electron-transfer reactions is discussed for transfers occurring over a range of distances. A finite rate of diffusion of reactants and their long-range force are treated by solving the reaction-diffusion equation numerically for the reactant pair distribution function. Steady-state solutions are compared with experimental data. On the basis of short-time solutions it is proposed that experiments which measure electron-transfer rates at short times following the onset of reaction improve the possibility of observing the inverted effect in bimolecular systems.

The effect of the reactants' relative orientation on the electron-transfer rate is considered. Reactants are modeled as oblate-spheroidal potential wells of constant, finite depth. Energy levels and wavefunctions are obtained for an electron localized in such a well. The electronic matrix elements that govern electron transfer within a nonadiabatic quantum theory are evaluated. Significant orientational preferences are predicted for electron transfer between nonspherical donor and acceptor sites.

TABLE OF CONTENTS

INTRODUCTION

This thesis is concerned with the rate of electron-transfer reactions such as reaction 1 occurring in a polarizable medium. The reactants are supposed to be sufficiently dilute that they interact pairwise only. Simultaneous interactions of more than two reactants (electron sites) will not be treated. The medium may be a polar solvent such as water, or some more highly organized structure such as a membrane or protein. The reactants A and B may be metal complexes (e.g., $Fe(H_2O)_6^{3+}$ or Ru(2,2'-bipyridine)$_3^{2+}$) or molecular ions or neutrals (e.g., porphyrin, anthracene, quinone). Thus reactions described by equation 1 include the hexaaquoiron self-exchange reaction in water and the reduction of pheophytin by chlorophyll in photosynthetic reaction centers. The reactants A and B may even be distinct chromophores in the same molecule; two sites which are to a significant extent electronically isolated from one another. In such a case the electron transfer of reaction 1 is an intramolecular electron transfer.

$$A^- + B \xrightarrow{k} A + B^- \qquad (1)$$

Reaction 1 is said to be "homogeneous" if it occurs in a single phase. Electron transfers between solvated ions are clearly homogeneous. Oxidation-reduction reactions at electrodes, for example, are "heterogeneous" reactions and so are not in the domain of the present discussion.

Reaction 1 is said to be an "outer-sphere" reaction if the chemical identities (apart from charge-types, of course) of species A and B are preserved throughout the reaction. "Inner-sphere" electron transfers, which involve concerted bond-breaking and/or bond-forming, will not be considered.

The object of theories of electron transfer is to predict the electron-transfer rate. It is the forward rate that will be dealt with throughout this thesis. The reverse rate can be obtained of course from the forward rate and the equilibrium constant. The rate of a reaction such as reaction 1 is to be calculated within an idealized model of the electron-transfer system. The system, which consists of an A-B pair and the surrounding medium, is described by a conceptually simple model in order that a theoretical treatment be feasible. A discussion of the features of a theoretical model of the electron-transfer system follows.

The reaction involves an electron moving from a solvated donor site to a solvated acceptor. Even if the reactants are neutral, the products will be charged, or vice versa. Thus at some time in the course of the reaction the electrostatic interaction between the medium and at least one charge must be considered. As the electrostatic fields change about the reactants the polarization field must change in response. Conversely, a fluctuation in the polarization state of the medium can induce a change in the source. That is, a polarization fluctuation in the solvent medium can prepare the reactants in a configuration favorable for electron transfer. The treatment of the role of the polar medium is one of the most important aspects of an electron-transfer theory.

The first successful treatment of the role of the polar medium in electron transfer is due to Marcus (1). In this theory the solvent is treated as a classical dielectric continuum. In case a reactant is an unligated ion, e.g., Fe^{2+}, the continuum approximation is applied only outside the first coordination shell. The polarization $\underline{P}$ of the solvent is conceived of as the sum of two components, $\underline{P}_{op}$ and $\underline{P}_{ir}$. The electronic polarization $\underline{P}_{op}$ arises from electronic motions in components of the medium. $\underline{P}_{op}$ is assumed to respond

instantaneously to electrical perturbations and so is always in equilibrium with the local electric field. The second component, $\underline{P}_{ir}$, arises from collective librations and vibrations of the components of the medium. This component of the polarization responds relatively slowly (with characteristic times on the order of 10^{-11} sec (2)) to electric fields and so need not be in equilibrium with the charge distribution on the reactants. Fluctuations of $\underline{P}_{ir}$ from equilibrium can bring the system to the transition state. These fluctuations and their implications for the rate constant were analyzed by Marcus (1,2,3).

The medium polarization has also been treated quantum-mechanically (4,5). (See especially chapter 2 of reference 6 for a discussion of the quantum treatment of the medium polarization.) In the quantum-mechanical treatment of the medium, the state of polarization is represented as a set of harmonic oscillators corresponding to the Fourier components of $\underline{P}_{ir}$. This treatment does not assume that the solvent molecules move harmonically. Rather it corresponds to an expansion of the polarization in a harmonic basis. (Section 7 of reference 7 contains a discussion of the implications of the quantum-mechanical treatment of the medium.)

The nuclear degrees of freedom internal to species A and B (or describing the first coordination sphere in the case when A or B is an atomic ion) have been treated both classically by Marcus (8,9) and quantum-mechanically by Levich and Dogonadze (4,10) and others (11,12). In the quantum theory there is no formal distinction between such "inner-sphere" modes and medium ("outer-sphere") modes. The term "inner-sphere" is used here (and subsequently in this thesis) to classify nuclear degrees of freedom. This use is distinct from its use to indicate an electron-transfer mechanism which involves making or breaking bonds. "Nuclear coordinates," in the context of this thesis, refers either to the positional coordinates of nuclei, or to the coordinates describing solvent polarization, but not to other degrees of freedom such as nuclear spins or the motion of subatomic particles within nuclei.

In principle it is possible to treat all of the inner-sphere nuclear vibrational modes. In practice of course only a few may be considered. The equilibrium values of the nuclear coordinates of some inner-sphere vibrational modes may shift upon electron transfer. It is important to consider such modes having large coordinate changes since a coordinate shift may, depending upon the vibration frequency, contribute a

significant energy barrier to the electron transfer. The importance of inner-sphere vibrations and the nature of the energy barrier are discussed in more detail in Chapter 1.

Common to all of the discussion and calculations in this thesis is the assumption that immediately prior to electron transfer the nuclear modes are relaxed. That is, it is assumed that vibrational states of the reactants are thermally populated, or in the classical picture, that the nuclear-phase-space distribution is at thermal equilibrium. Electron transfer from non-equilibrium initial-state distributions has been considered theoretically (13) but experimental evidence for such behavior is still lacking.

The motion of reactants A and B along the coordinate $\underline{r}$ which describes the location of B relative to the center of A ($r = |\underline{r}|$ = distance between the centers of A and B), and the rotations of A and B which determine their relative orientations $\underline{\Omega}$, are considered separately from the inner-sphere and medium-polarization nuclear coordinates. This separation is based on time scales. The characteristic times for reactants' tumbling and diffusion in a condensed medium are expected to be much greater than the periods of polarization fluctuations and inner-sphere vibrations. The rate constant

calculated first is thus a unimolecular rate constant for a "super-molecule" consisting of the medium and reactants A and B at fixed ($\underline{r}$,$\underline{\Omega}$). The observable rate constant, which is a weighted average of $k(\underline{r},\underline{\Omega})$ with respect to $\underline{r}$ and $\underline{\Omega}$, can be either obtained through thermodynamic arguments (1,13) or calculated using a reactant-pair distribution function (14,15,16,17). A particular form of the latter approach, one which is appropriate to reactions in homogeneous fluids, is discussed and employed in Chapters 3 and 4 of this thesis.

The type of averaging that is appropriate depends on the nature of the reacting system and whether it is a steady-state rate constant or a time-dependent rate constant (as in certain fluorescence-quenching studies) that is observed. For reactions in fluids diffusion may occur relatively freely so that $\underline{r}$ and $\underline{\Omega}$ sample a large domain. In intramolecular electron transfers and in biological electron-transfer systems the reactant sites may have only limited freedom of orientation and separation. Electron transfers between sites in glassy matrices involve reactants whose motion is even more severely inhibited. The analysis in this last case is complicated by the time-dependent nature of the observed rate.

Thus far this introduction has dealt with the role of nuclear degrees of freedom in the electron-transfer rate. Chapters 1 through 4 of this thesis focus on that role. However, electronic degrees of freedom are also important in the electron-transfer step. The discussion now turns to that aspect of electron-transfer theory.

A pair of Born-Oppenheimer potential curves is depicted schematically in Figure 1. The full potential surfaces are multidimensional, defined in principle over the space of all nuclear coordinates of both the inner-spheres of A and B and of the medium (but not $(\underline{r},\underline{\Omega})$, as discussed above). Figure 1 represents a cut through the potential surfaces along some hypothetical nuclear coordinate R. Two electronic states are considered; one in which the 'transferable' electron is localized on A (the "reactant" state corresponding to $A^- + B$), and one in which the electron is localized on site B (the "product" state corresponding to $A + B^-$). If the two electronic states could be prevented from interacting, for instance by separating the reactants to $r = \infty$, then the product and reactant states would be degenerate at $R = R_o$. But in general the two states do interact and are split in energy by $\sim 2 V_{AB}$ at $R = R_o$. V_{AB} is the matrix element $|\langle B|V|A\rangle|$ of the perturbing

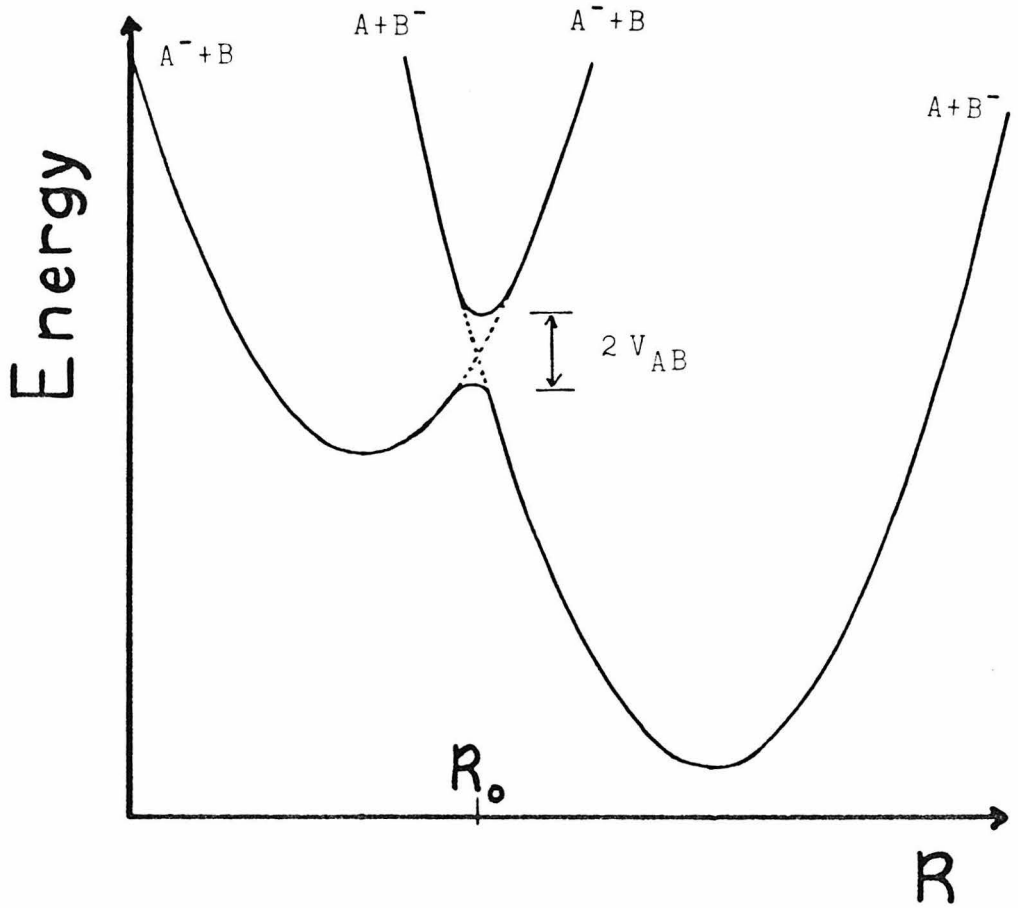

Figure 1. Profile of potential energy surfaces versus a generalized nuclear coordinate. The dashed lines indicate the potential energies in the limit $V_{AB} = 0$.

potential V between the localized states $|B\rangle$ (which corresponds to products, $A + B^-$) and $|A\rangle$ (which corresponds to reactants, $A^- + B$). An explicit example of V_{AB} is given in Chapter 5 for a particular model of an electron-transfer system.

The terms "adiabatic" and "nonadiabatic" as they apply to electron transfers may be discussed in terms of Figure 1. A reaction for which the electronic interaction V_{AB} is large is said to be adiabatic. In this limit the upper surface is irrelevant and the reacting system moves solely on the lower potential surface. If on the other hand V_{AB} is very small, then the reaction is said to be nonadiabatic. Classically, as $V_{AB} \to 0$ it becomes possible for the reactant system to move from $R < R_o$ to $R > R_o$ with a significant probability of remaining on the reactant $(A^- + B)$ potential surface. Thus the frequency factors (in an Arrhenius rate constant) for nonadiabatic reactions are likely to be smaller than those for adiabatic reactions. A more quantitative distinction between adiabatic and nonadiabatic reactions is drawn in reference 18. According to a criterion given there, a room-temperature reaction in a polar fluid will be adiabatic for $V_{AB} \gtrsim 0.01$ eV and nonadiabatic for $V_{AB} \lesssim 0.01$ eV.

References 7 and 19 contain general discussions of the meaning for electron-transfer reactions of the terms "adiabatic" and "nonadiabatic." A distinction between adiabatic and nonadiabatic reactions is not easily drawn in practice. A single electron-transfer system may even exhibit both types of behavior, since V_{AB} may differ along various reaction paths through the coordinate space.

The classical theory of Marcus was derived for adiabatic reactions, although a "nonadiabaticity factor" κ was incorporated into the pre-exponential factor of the rate constant. For an adiabatic reaction $\kappa = 1$. For nonadiabatic reactions κ is less than unity and has been evaluated using the Landau-Zener theory of curve crossing. (See (8) or pages 68-72 of reference 7.)

The quantum-mechanical theory of electron-transfer due to Levich and Dogonadze was derived using time-dependent perturbation theory and is valid when V_{AB} is small. The quantum-mechanical theory is thus a nonadiabatic theory. The interaction V_{AB} must diminish as the reactants are drawn apart, so all reactions become nonadiabatic at sufficiently large separation r. Thus the nonadiabatic quantum theory is suitable for the study of distance effects in electron transfers

and is used to that end in Chapters 3 and 4 and especially in Chapter 5 of this thesis.

The specific problems addressed in each of Chapters 1 through 5 are described in the remainder of this introduction.

Inner-Sphere Quantum Effects

As discussed earlier in this introduction, an outer-sphere electron-transfer reaction in a polar solvent is characterized by changes in the force constants and bond lengths and bond angles of the reactants and by fluctuations in the surrounding solvent. In many systems the inner-sphere changes are very small, so that the reaction is controlled by fluctuations in the solvent polarization (e.g., $Ru(NH_3)_6^{3+/2+}$ (20) and Cr(2,2'-bipyridyl)$_3^{3+/2+}$ (21)). On the other hand, some redox systems involve substantial internal reorganization (e.g., $Fe(H_2O)_6^{3+/2+}$ (20) and $Co(NH_3)_6^{3+/2+}$ (22)). In such systems inner-sphere effects are important.

In Chapter 1 classical, semiclassical and quantum theories of electron transfer are discussed. It has been suggested that reactions in which inner-sphere reorganization is important are not adquately described by classical theory but require a quantum-mechanical

treatment (11,12,23). The nature and magnitude of quantum effects in the particular cases of the very slow hexaamminecobalt self-exchange reaction, the hexaaquoiron self-exchange reaction, the hexaammine ruthenium self-exchange reaction, and the Fe^{2+} - $Ru(2,2'\text{-bipyridine})_3^{3+}$ cross-reaction are discussed in Chapter 1.

One of the differences between the classical and the quantum theories of electron transfer is that the latter theory allows for tunneling in the nuclear-coordinate space of the reacting system. The meaning of nuclear tunneling is conveniently discussed in terms of Figure 1, where R is now taken to be the reaction coordinate. Classically, the reacting system begins in the left-hand potential well. Reaction occurs when the system passes over the energy barrier at $R = R_o$. But the quantum-mechanical theory allows the reacting system to pass <u>through</u> (as well as over) the barrier. Tunneling appears in the quantum theory's rate expression in the form of Franck-Condon overlaps of reactant and product vibrational wavefunctions that lie below the barrier maximum at $R = R_o$.

It is expected that if nuclear tunneling is to be important, it will be so for systems in which a high-frequency mode undergoes a significant displacement. For example, in the hexaamminecobalt self-exchange reaction the equilibrium position of the symmetric stretching mode, $h\nu \simeq 431\ cm^{-1}$, is displaced by 0.18 Å (see Chapter 1), and in electron-transfer reactions in which an electronically excited bipyridyl complex is quenched, a ring mode, $h\nu \simeq 1300\ cm^{-1}$, undergoes a substantial equilibrium displacement.

In Chapter 1 it is found that a reasonable order-of-magnitude estimate for the contribution of configurational changes of high-frequency quantum modes in the first coordination layer, for typical metal-ligand frequencies, to the reaction rate constant can be provided by a classical expression.

Quantum Effects in the Inverted Region

It has been predicted that the rate constant of a sequence of homogeneous electron-transfer reactions in which the reactants A and B are varied (but with A and B chosen so that the nature of medium-polarization and inner-sphere vibration effects is constant) should first increase with increasingly negative standard free energy of reaction ΔG° at small ΔG°. It should then achieve a maximum at some value of ΔG° and thereafter decline as ΔG° continues to become still more negative. The region of decline was termed the "inverted" region (8). The existence of an inverted region was first predicted on the basis of a classical theory (8,24). The quantum-mechanical theory predicts a smaller but nevertheless nonzero inversion (12,25).

The experimental evidence of an inverted region is sparse. Some evidence for the effect is available for the reactions of electrons with different solutes, where the ΔG° for a given solute was varied by varying the hydrocarbon solvent and, thereby, the electron-solvent binding energy (26). Supporting data appear in the reactions of micelle-trapped pyrene with various anion radicals and in reactions of hydrated electrons with organic molecules trapped in micelles (pages 163-4

of reference 6), and (a small decrease) in the reduction of electronically excited bipyridyl complexes of Ru(II) by various metal-bipyridyl complexes (21). In the two micellar examples, the ΔG^{o}'s are uncertain, however. Evidence has also been offered in studies (27) of the rate of fluorescence quenching of trapped electrons in a glass at 77 K by various aromatic acceptors.

On the other hand, many studies of highly exothermic reactions have found a diffusion-limited rate constant which extends to quite negative ΔG^{o}'s, rather than the predicted declining rate constant (e.g. (28)). These studies frequently involve measuring the rate of quenching of fluorescence by a series of reactants, where quenching was presumed or demonstrated to proceed by electron transfer. In most cases, the reason for the absence of decrease in the rate is unknown. Several possible explanations are offered in Chapters 3 and 4.

The prediction of classical theory for the inverted region, and the quantum-mechanical corrections thereto, are examined in Chapter 2, first for a model system and then for an actual system using realistic vibration frequencies and bond-length changes for the data of Creutz and Sutin (21). The discrepancy between the experimental results and the theoretical predic-

tion is found to be very large, some quantum effects notwithstanding. An alternate pathway of forming an electronically excited product is explored in Chapter 2. It reduces the discrepancy considerably.

In Chapter 3 the relationship of the unimolecular rate constant to an 'observable' bimolecular rate constant for a reaction in a polarizable fluid medium is discussed. A reactant-pair distribution function $g(r)$, where r is the distance between reactants A and B, is obtained as a solution to a reaction-diffusion equation. The bimolecular rate constant calculated in this way explicitly contains contributions from electron transfer over large separations. The inclusion of reaction-at-a-distance has special implications for the inverted region. Those implications are also discussed in Chapter 3. Chapter 4 constitutes an elaboration of the material in Chapter 3.

Orientation Effects

The relative orientation (specified earlier by $\underline{\Omega}$) of the donor A^- and the acceptor B may affect the electron-transfer rate, inasmuch as V_{AB} may depend on $\underline{\Omega}$. For example, the photoinduced electron transfer in photo-

synthetic reaction centers may be influenced by the orientation of the reactants. In plant photosystem II the acceptor is probably a pheophytin (29,30) and the donor may be a substituted chlorophyll a (30,31). Both of those molecules are large and asymmetric which suggests that there may be one or more preferred orientations for electron transfer. For another electron transfer, that between hemes in cytochromes, there is evidence that the rate constant depends strongly on the mutual orientation of the hemes' porphyrin rings (32).

A model theoretical electron-transfer system is presented and discussed in Chapter 5. This system is designed for studying the effects of orientation and distance on electron-transfer rates. The donor and acceptor in the model are three-dimensional oblate-spheroidal square-well potentials. They are inherently orientable because of their nonspherical shape. Matrix elements V_{AB} are presented in Chapter 5 for a few cases. Significant orientation effects are found.

References:

(1) R. A. Marcus, J. Chem. Phys. 1956,24,966-978.

(2) R. A. Marcus, J. Chem. Phys. 1956,24,979-989.

(3) R. A. Marcus, J. Chem. Phys. 1965,43,679-701.

(4) V. G. Levich and R. R. Dogonadze, Doklady Adak. Nauk SSSR 1959,124,123. (English translation pages 9-13).

(5) R. R. Dogonadze, A. M. Kuznetsov, and A. A. Chernenko, Russian Chemical Reviews 1965,34,759-775. (English translation).

(6) J. Ulstrup, "Charge Transfer Processes in Condensed Media," Lecture Notes in Chemistry, Volume 10, (Springer, New York, 1979). This is a detailed review of the nonadiabatic quantum theory of electron transfer.

(7) P. P. Schmidt, Spec. Period. Repts. Electrochem. 1975,5,21-131. This is an excellent, highly readable review.

(8) R. A. Marcus, Disc. Faraday Soc. 1960,29,21-31. This is a review of the early classical developments in electron-transfer theory.

(9) R. A. Marcus, J. Phys. Chem. 1963,67,853-857 and 2889.

(10) V. G. Levich in "Physical Chemistry: An Advanced Treatise," Volume 9B, H. Eyring, Ed., (Academic, New York, 1970) Chapter 12, pp.985-1074.

(11) N. Kestner, J. Logan, and J. Jortner, J. Phys. Chem. 1974,78,2148-2166.

(12) J. Ulstrup and J. Jortner, J. Chem. Phys. 1975, 63,4358-4368.

(13) N. Sutin and B. S. Brunschwig in "Mechanistic Aspects of Inorganic Reactions," ACS Symposium Series No. 198, D.B. Rorabacher and J. F. Endicott, Eds., (American Chemical Society, Washington, 1982) pages 105-125.

(14) R. A. Marcus, Disc. Faraday Soc. 1960,29,129-130.

(15) M. Inokuti and F. Hirayama, J. Chem. Phys. 1965,43,1978-1989.

(16) R. A. Marcus, Int'l J. Chem. Kinet. 1981,13,865-872.

(17) R. K. Huddleston and J. R. Miller, J. Phys. Chem. 1982,86,200-203.

(18) N. Sutin, Accts. Chem. Research 1982,15,275-282.

(19) General discussion in "Tunneling in Biological Systems," B. Chance, D. C. DeVault, H. Frauenfelder, J. R. Schrieffer, and N. Sutin, Eds., (Academic, New York, 1979) pages 295-299.

(20) N. Sutin, ibidem, pages 201-224.

(21) C. Creutz and N. Sutin, J. Am.Chem. Soc. 1977, 99,241-243.

(22) D. Stranks, Disc. Faraday Soc. 1960,29,116.

(23) E. Buhks, M. Bixon, J. Jortner, and G. Navon, Inorganic Chemistry 1979,18,2014-2018.

(24) R. A. Marcus, J. Chem. Phys. 1965,43,2654-2657.

(25) R. P. VanDuyne and S. F. Fischer, Chem. Phys. 1974,5,183-197.

(26) S. Lipsky, J. Chem. Ed. 1981,58,93-101.

(27) J. V. Beitz and J. R. Miller, J. Chem. Phys. 1979,71,4579-4595.

(28) D. Rehm and A. Weller, Israel J. Chem. 1970,8,259-271.

(29) V. V. Klimov, A. V. Klevanik, V. A. Shuvalov, and A. A. Krasnovsky, FEBS Letters 1977,82,183-186.

(30) J. Fajer, M. S. Davis, A. Forman, V. V. Klimov, E. Dolan, and B. Ke, J. Am. Chem. Soc. 1980,102,7143-7145.

(31) M. S. Davis, A. Forman, and J. Fajer, Proc. Nat'l Acad. Sci. USA 1979,76,4170-4174.

(32) S. Schichman and H. B. Gray, to be published.

CHAPTER 1

QUANTUM EFFECTS IN ELECTRON-TRANSFER REACTIONS

Introduction

An outer-sphere electron transfer reaction in a polar solvent is characterized by changes in the force constants and bond lengths and bond angles of the reactants and by fluctuations in the surrounding solvent. In many systems the inner-sphere changes are very small, so that the reaction is controlled by fluctuations in the solvent polarization (e.g., $Ru(NH_3)_6^{3+/2+}$ [1,2] and $Cr(2,2'\text{-bipyridyl})_3^{3+/2+}$ [3]). On the other hand, some redox systems involve substantial internal reorganization (e.g., $Fe(H_2O)_6^{3+/2+}$ [2] and $Co(NH_3)_6^{3+/2+}$ [4]). In such systems inner-sphere effects are important.

In this paper we briefly describe classical, semiclassical and quantum theories of electron transfer. It has been suggested that reactions in which inner-sphere reorganization is important are not adequately described by classical theory, but require a quantum mechanical treatment.[5,6] A quantum mechanical treatment is available for nonadiabatic electron transfers, and was developed at first for the solvent modes[7] and later for the bond vibrations.[6,8,9]

We discuss the nature and magnitude of quantum effects in the particular cases of the very slow hexaamminecobalt self-exchange reaction, the hexaaquoiron self-exchange reaction, the hexaammine ruthenium self-exchange reaction, and the Fe^{2+}-$Ru(bpy)_3^{3+}$ cross reaction.

It is expected that if nuclear tunneling is to be important, it will be so for systems in which a high-frequency mode undergoes a

significant displacement. For example, in the hexaamminecobalt self-exchange reaction the equilibrium position of the symmetric stretching mode, $\hbar\omega \sim 431$ cm^{-1}, is displaced by 0.18 Å (cf. Table I), and in electron transfer reactions in which an electronically excited bipyridyl complex is quenched, a ring mode, $\hbar\omega \sim 1300$ cm^{-1}, undergoes a substantial equilibrium displacement.

Nuclear tunneling will, other things being equal, be more important for high, rather than for low-frequency modes as one can see from the nature of harmonic oscillator eigenstates. We consider for illustration purposes the one-dimensional model surface sketched in Fig. 1. Nuclear tunneling depends on the overlap of reactant and product wave functions in the classically nonallowed region, and therefore is directly related to the amplitude of the reactants' wave function in the region $q > b$. This wave function extends further into the classically forbidden region, for any given energy, the higher the vibration frequency. It follows that tunneling from a state of given energy is more probable for a high-frequency mode than for a low-frequency mode, at a given energy.

In the present paper it is found that for the reaction rate constant a reasonable order of magnitude estimate for the contribution of configurational changes of high-frequency quantum modes in the first coordination layer, for typical metal-ligand frequencies, can be provided by a classical expression.[9]

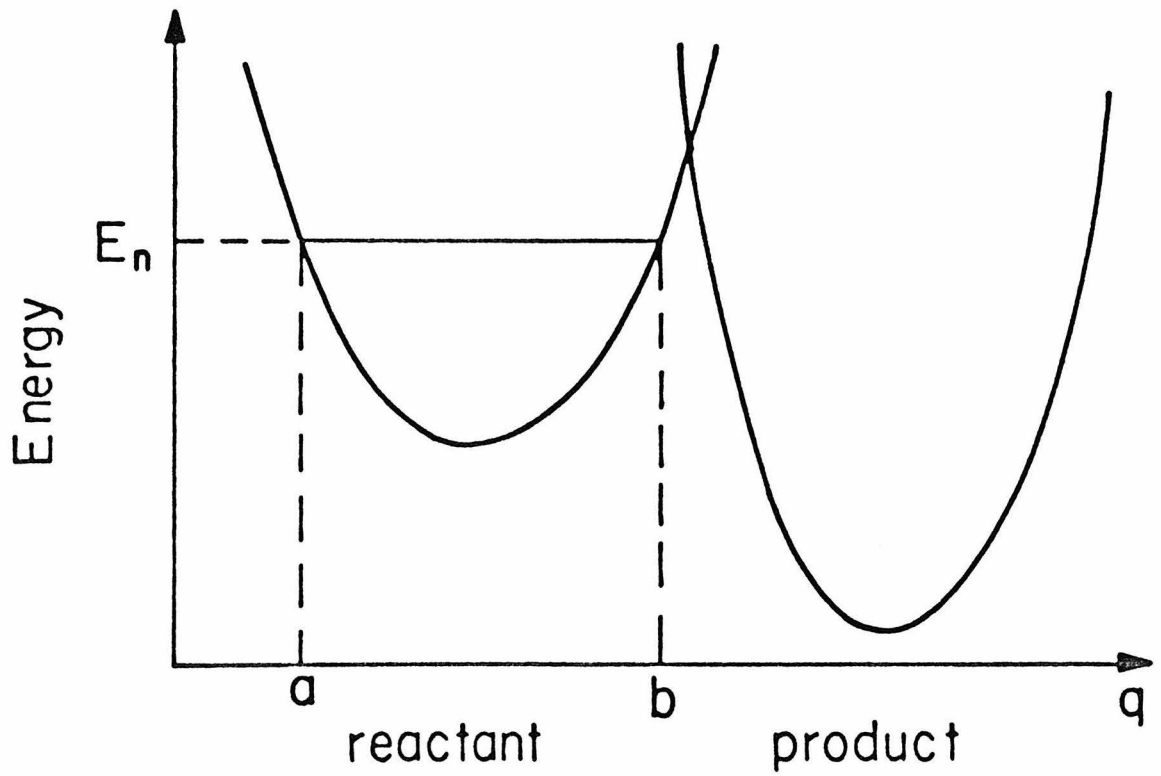

Figure 1 Model harmonic potentials for electron transfer versus a generalized configuration coordinate q. (Ref. 9.)

Quantum Treatment

Franck-Condon Factor. An approximate quantum-mechanical rate expression based on the golden-rule transition probability has been derived for electron transfer systems in the nonadiabatic limit.[6-8,10] Within the Condon approximation the transition probability in this expression involves the product of the square of an electron exchange integral, and a thermally-weighted sum, G of vibrational Franck-Condon factors:

$$G = \frac{1}{Q}\sum_n\sum_m e^{-E_n^{vib}/kT} \; |\langle n \,|\, m \rangle|^2 \; \delta(E_n - E_m) \qquad (1)$$

where Q is the reactants' (vibrational) partition function, and n and m designate initial and final vibronic states, respectively. E_n and E_m are initial- and final-state energies. E_n^{vib} is the initial-state vibrational energy; $|n\rangle$ and $|m\rangle$ are treated as harmonic oscillator eigenfunctions, equal to a product over the system's degrees of freedom of single-mode harmonic oscillator functions.

The single-mode harmonic oscillator overlap integrals required for evaluating G directly by the sum of eq 1 have been known for many years.[11-15] The expressions used in this work for these integrals are presented in the Appendix (eqs A1-A2) in terms of $f = \omega'/\omega$, ω' and ω being the frequencies associated with $|m\rangle$ and $|n\rangle$, respectively, and in terms of the dimensionless change $\sqrt{X}$ in equilibrium coordinate value from $|m\rangle$ to $|n\rangle$. For a normal mode $X = F(\Delta Q)^2/2\hbar\omega$, where ΔQ is the change in the normal coordinate, $\omega/2\pi$ is the vibration frequency, and F is the force constant for the mode. ($\omega^2 = F$).

In the case of $X \neq 0$ but $\omega' = \omega$, one obtains the well-known limiting form[14]

$$\langle n|m \rangle = X^{(n-m)/2} (m!/n!)^{\frac{1}{2}} e^{-X/2} L_m^{n-m}(X) \qquad (2)$$

where L is an associated Laguerre polynomial.

An approximate simple formula for the multimode case has also been derived elsewhere, together with limitations on its validity.[16] This relation was applied there to the hexaaquoiron self-exchange reaction and to the Fe^{2+} - $Ru(bpy)_3^{3+}$ cross-reaction and shown to give good agreement with the exact quantum values.[26]

Quantum Treatment of the Solvent. The interaction of the solvent with the reactant ions is implicitly included in eq 1 as a set of one or more harmonic modes. Usually only a single frequency, $\hbar\omega_1 = 1\ cm^{-1}$, is used in calculations.[6a,8e,17] However, in view of the significant decrease in the real part of the dielectric constant of water at 170 cm^{-1} (and the corresponding peak in the imaginary part)[18,19] we have chosen to use a two-frequency quantum description of the solvent interaction: $\hbar\omega_1 = 1\ cm^{-1}$ and $\hbar\omega_2 = 170\ cm^{-1}$. A dielectric dispersion in the solvent was first treated for electron transfer by Ovchinnikov and Ovchinnikova.[20]

As a first approximation for this two-frequency description we divide the outer-sphere reorganization energy into two parts, writing λ_{out}, which is four times the solvent reorganization energy,[21] as

$$\lambda_{out} = \lambda_1 + \lambda_2 \tag{3}$$

where

$$\lambda_1 = \lambda_{out} \left(\frac{1}{\varepsilon_s} - \frac{1}{\varepsilon_{ir}}\right) / \left(\frac{1}{\varepsilon_s} - \frac{1}{\varepsilon_{op}}\right)$$

$$\lambda_2 = \lambda_{out} \left(\frac{1}{\varepsilon_{ir}} - \frac{1}{\varepsilon_{op}}\right) / \left(\frac{1}{\varepsilon_s} - \frac{1}{\varepsilon_{op}}\right) \tag{4}$$

$\varepsilon_{ir} = 5.0$[19] = real part of the dielectric constant on the 'plateau' between 1 cm^{-1} and 170 cm^{-1}.

$\varepsilon_s = 78.3$[19] = static dielectric constant

$\varepsilon_{op} = 1.78$[22] = n_D^2

Thus, the quantum treatment of the solvent interaction (the solvent is taken to be aqueous in this paper) involves two harmonic modes included in the degrees of freedom of the system. In performing the quantum mechanical calculation for the solvent eq 2 was again used but X was obtained in the following manner. It is first recalled that for an internal normal mode i of the reactants X_i, which equals $F_i(\Delta Q_i)^2/2\hbar\omega_i$, can be rewritten as $\lambda_i/\hbar\omega_i$, since[9] $\lambda_i = F_i(\Delta Q_i)^2/2$. By analogy, we use for X for the solvent $\lambda_1/\hbar\omega_1$ and $\lambda_2/\hbar\omega_2$ where λ_1 and λ_2 have been defined in eqs 3 and 4. The numerical values employed for $\lambda_{1,2}$ are given later in the paper, while $\hbar\omega_{1,2}$ are given above.

Saddle-point Method. For a system having several vibrational normal modes of different frequencies, the direct evaluation of eq 1 can require considerable computing time. However, G can easily be evaluated approximately by replacing the delta function in eq 1 by its Fourier integral representation, and then using the saddle-point method. After some manipulations[23,24] one obtains

$$G = (2\pi Q)^{-1} \int_{-\infty}^{\infty} e^{-i\Delta E t + f(t)} dt \qquad (5)$$

and, after using the saddle-point method to approximate the integral,

$$G \sim |2\pi f''(t_0)|^{-\frac{1}{2}} Q^{-1} e^{-i\Delta E t_0 + f(t_0)}, \qquad (6)$$

where ΔE is the energy (endoergicity) of the transition; t_0 is the stationary phase value of t in the integrand in eq 5; f, f'' and t_0 are given in the Appendix.

In the case of a self-exchange reaction, product modes in the oxidized species are equivalent to reactant modes in the reduced species so that the formulae simplify considerably.[5] In a thermoneutral self-exchange reaction, $t_0 = -i/2kT$. For other cases eq A6 of the Appendix may be solved numerically, e.g., by iterating from the approximate root.

$$t_0 \sim -i(\Delta E + \lambda)/2kT\,\lambda \qquad (7)$$

where $\lambda = \sum_{j=1}^{N} \lambda_j$, and each $\lambda_j = \frac{1}{2} F_j (\Delta Q_j)^2$. Eq 7 gives the exact saddle point in the high temperature limit, when frequency changes are neglected, and provides a reasonable starting point for iteration in other cases.

Classical Treatment

When all the degrees of freedom of the system are treated in the classical limit, $\hbar\omega/2kT \rightarrow 0$, and when frequency changes are neglected, eq 5 reduces to

$$G = (4\pi kT\lambda)^{-\frac{1}{2}} \exp[-(\Delta E + \lambda)^2/4kT\lambda] \qquad (8)$$

This equation is similar in form to the classical expression for G,[2,4] but contains energies rather than free energies. This difference arises because eq 5 tacitly assumes zero entropy of reaction, and indeed the initial equation, (eq 1), with its assumption of harmonic oscillators, does not contain any important $\Delta S°$ term,[25] whereas the actual $\Delta S°$ can be quite large.[25] The classically derived expression is more general in this respect, since it doesn't assume harmonic oscillations for all motions.[26] As defined earlier, $\lambda_j = \frac{1}{2} F_j(\Delta Q_j)^2$ and $\lambda = \sum_{j=1}^{N} \lambda_j$. It has been shown[27] that frequency changes may be included in an approximate manner by using an average force constant to calculate λ_j, rather than using the initial force constant. F_j above is an averaged force constant.

$$F_{av} = 2FF'/(F + F') \qquad (9)$$

where F and F' are the force constants in the reactant and product states, respectively. The classical value of the Franck-Condon sum (eq 8) is computed using λ's calculated with average force constants given by eq 9.

'Semiclassical' Treatment[28]

Consider first a one-dimensional case with a coordinate Q. The $\delta(E_m-E_n)$ of eq 1 can be introduced into $|\langle n|m\rangle|^2$. When the commutator of the initial and final Hamiltonians, H_n and H_m, is neglected, $\delta(E_n-E_m)$ in the integral becomes $\delta(H_n-H_m)$, which in turn is $\delta(V_n-V_m)$ since the kinetic energy terms in H_n and H_m cancel; V_n and V_m are the potential energies of the reactants and products, respectively. By using the identity $\sum_m |m\rangle\langle m| = 1$, the thermally-weighted double sum of squared overlap integrals in eq 1 may be reduced to a single sum over n of $\langle n|\delta(V_n-V_m)|n\rangle$ (e.g., see analogous procedure for other problems in refs. 29). These integrals are readily evaluated, yielding a sum of factors proportional to $|\chi_n(Q)|^2$, where Q is that value of the coordinate for which the reactant and product potential energies are equal, and χ_n is the wavefunction of the reactants. The remaining sum over n in eq 1 is then readily evaluated to yield[29]

$$G = (2\pi\lambda\hbar\omega\coth\gamma)^{-\frac{1}{2}} \exp[-(\Delta E + \lambda)^2/(2\lambda\hbar\omega\coth\gamma)] \quad (10)$$

where $\gamma = \hbar\omega/2kT$, and E and λ are defined as in eq 7, but λ is for the single mode being considered. Equation 10 is the same as that obtained in ref. 28 by a different procedure. A detailed derivation of eq 10 is given in the appendix.

For systems having two or more frequencies, one obtains a convolution of Gaussians of the form of eq 10. The convolution is itself of the form of eq 10, but $\lambda\hbar\omega\coth\gamma$ must be replaced with $\sum_j \lambda_j \hbar\omega_j \coth\gamma_j$, and λ by $\sum_j \lambda_j$.[26,29]

This method of obtaining G's, which originated in the theory of optical spectra of solids,[29] is sometimes termed 'semiclassical' because of neglect of commutators of H_n and H_m, although the term 'semiclassical' has a variety of other meanings (corresponding to other approximations) in the literature.

Calculations and Discussion

We now proceed to consider quantum effects in four particular cases of chemical interest: the hexaamminecobalt and hexaammineruthenium self-exchange reactions, the $Fe^{2+/3+}$ (aq) self-exchange reaction, and the Fe^{2+} - $Ru(bpy)_3^{3+}$ cross reaction.

Hexaamminecobalt Self-exchange Reaction. The large difference between the rates of self-exchange reactions 11 and 12 has long been a matter of interest in the theory of electron transfer rates.

$$Co(NH_3)_6^{2+} + Co(NH_3)_6^{3+} \overset{k_1}{\rightarrow} Co(NH_3)_6^{3+} + Co(NH_3)_6^{2+}$$

$$k_1 \leq 10^{-12}\ M^{-1}s^{-1} \text{ at } 25°^{4} \qquad (11)$$

$$Ru(NH_3)_6^{2+} + Ru(NH_3)_6^{3+} \overset{k_2}{\rightarrow} Ru(NH_3)_6^{3+} + Ru(NH_3)_6^{2+}$$

$$k_2 = 10^{3}\ M^{-1}s^{-1} \text{ at } 25°^{30,31} \qquad (12)$$

In the quantum theory described earlier, the rate constant involves the product of the square of an electronic exchange integral and a sum of Franck-Condon factors. It has been suggested that the electronic factor for reaction 11 may be small because of spin multiplicity restrictions.[1,5] Further, the Franck-Condon term is much smaller for the Co reaction than for the Ru reaction because of the larger change in geometry from $Co(NH_3)_6^{2+}$ to $Co(NH_3)_6^{3+}$ (cf. Table I).

Buhks, et al.[5] evaluated the Franck-Condon sums, G, for reactions 11 and 12, using the saddle-point method described earlier. They found $G(Co) \sim 7 \times 10^{-18}$ cm and $G(Ru) = 1.5 \times 10^{-10}$ cm so that the ratio of Franck-Condon sums contributes a factor of ca 10^{-8} to the ratio k_1/k_2. But they also found that the classical value of $G(Co)/G(Ru)$ was $\sim 10^{-5}$. The gross discrepancy between the classical and quantum values, a factor of 1000, led them to suggest that G(Co) is heavily dependent on quantum effects. There is clearly some error in either the classical or the quantum Franck-Condon factors of ref. 5 since tunneling effects should cause G(Co)/G(Ru) to be larger in the quantum case than in the classical one, yet a smaller value was found for the quantum case in ref. 5.

Actually, we have found that the large classical value of ref. 5 for G(Co)/G(Ru) is the result of using the inaccurate estimate (28.5 kJ/mol) of Stynes and Ibers[1] for the hexaamminecobalt internal reorganization energy. The latter seem to have treated the bond length reorganization energy in the hexaamminecobalt ions as containing

TABLE I: Structural and Spectroscopic Data [a]

	$Co(NH_3)_6^{2+}$	$Co(NH_3)_6^{3+}$	$Ru(NH_3)_6^{2+}$	$Ru(NH_3)_6^{3+}$
M-N bond length, Å	2.114	1.936	2.144	2.104
$\hbar\omega$ (A_{1g}), cm^{-1}	357	494	350	500
$\hbar\omega$ (E_g)	255	442		
$\hbar\omega$ (F)	325	475		
$\hbar\omega$ (F)	192	331		
$\hbar\omega$ (F)	187	322		
$\hbar\omega$ (F)	143	246		
λ_{outer} (kJ/mol)	117		113	

[a]Ref. 5. Symmetries are for an effective octahedral geometry.

only diagonal terms $\frac{1}{2}\sum_{i=1}^{6} f_r(\Delta q_i)^2$, where Δq_i is the displacement in the ith Co-N bond length, and f_r is the Co-N bond force constant. But the reaction coordinate is actually the symmetric stretching normal mode, and when expressed in terms of bond modes cross-terms are obtained. The totally symmetric F-matrix force constant $F_{A_{1g}}$ is given in terms of generalized-valence-force field (GVFF) constants f by [32]

$$F_{A_{1g}} = f_r + 4f_{rr}' + f_{rr} \qquad (13)$$

where f_r is the diagonal force constant, and f_{rr} and f_{rr}' are off-diagonal force constants. f_{rr}' denotes interaction between displacements perpendicular to each other. f_{rr} denotes interaction between displacements on the same line. The symmetric stretching normal mode force constant F_1 involves both the F- and G-matrix elements and equals $F_{A_{1g}}/m_L$,[32] where m_L is the mass of one ligand. The bond length reorganization energy is[33] $\frac{1}{4} F_1(\Delta Q_1)^2$ where ΔQ_1, the normal-mode displacement, is $\sqrt{6m_L}\,\Delta q_i$[32] (all six Δq_i's are equal). Thus, this reorganization energy equals $\frac{1}{4}(f_r + 4f_{rr}' + f_{rr})\,6(\Delta q_i)^2$. It thereby involves both diagonal (f_r) and off-diagonal (f_{rr} and $f_{rr'}$) GVFF force constants, and the latter are almost as important as the former.[34] Accordingly, we have made a comparison of the more correct classical value with the quantum sum, as well as with the semiclassical sum for G.

In the high-temperature (classical) limit, the Franck-Condon factors usually depend mainly on modes in which the product potential is displaced in coordinate space relative to the reactant potential (i.e., $\lambda \neq 0$). In the Co- and Ru-hexaammine self-exchange reactions only the solvent modes and the totally symmetric A_{1g} internal modes have nonzero λ's. Changes of frequency in the other modes would also make some contribution to G, of course, and as

an example we include the modes of E_g and F symmetry later in quantum calculations of G. The approximate classical expression for G (eq 8) cannot treat modes for which $\lambda = 0$.

Using the known A_{1g} stretching frequencies (cf. Table I) for Co(II/III) - hexaammine, the A_{1g} symmetry force constants F_{III} and F_{II} (i.e., the $F_{A_{1g}}$ for oxidation states III and II) are calculated to be 2.45×10^3 N/m and 1.28×10^3 N/m, respectively. Using the average force constant of eq 9 and the Co-N bond lengths in Table I, the internal reorganization energy is found to be about 48 kJ/mol[35] (instead of the 28.5 kJ/mol calculated in ref. 1). By analogous calculation, the Ru(II/III) hexaammine internal reorganization energy is found to be 2.5 kJ/mol. The total outer-sphere λ's for the cobalt and ruthenium reactions have recently been estimated as 117 kJ/mol and 113 kJ/mol, respectively.[5]

Using these energy parameters, eq 8 yields as a classical result $G(Co)/G(Ru) \sim 5 \times 10^{-9}$ which is in reasonable agreement with the quantum result, both as given by Buhks, et al., and as calculated below.

In order to assess the accuracy of the saddle-point method for the hexaamminecobalt system, the values of G obtained by direct sum are compared with those obtained by saddle-point integration. For simplified models consisting of only the A_{1g} internal mode, or of both the A_{1g} and one of the two degenerate E_g internal modes, both the direct and saddle-point calculations have been performed. (For the E_g modes ΔQ_i is zero, if in the transition state each reactant has octahedral symmetry, but $\Delta\omega_i$ is nonzero.) The results are given in Table II. At least for the models in this Table the saddle-point evaluation is a very good approximation.

For the complete hexaamminecobalt system consisting of all the

TABLE II: Franck-Condon Sums, G

System[a]	Direct Sum	Saddle-Point
$Ru(NH_3)_6^{2+/3+}$ (All values for G have been multiplied by 10^9 cm^{-1}.)		
quantum solvent, quantum internal	1.04	1.08
classical solvent, quantum internal	0.93	0.97
effective force constant[b]		
classical solvent, quantum internal	1.02	1.02
classical solvent, classical internal[c]	0.82	
$Co(NH_3)_6^{2+/3+}$ (All values for G have been multiplied by 10^{18} cm^{-1}.)		
A_{1g} internal modes		
quantum solvent, quantum internal	20.0	20.0
classical solvent, quantum internal	17.9	17.8
effective force constant[b]		
classical solvent, quantum internal	19.1	19.1
effective force constant[b];		
classical solvent, classical		
internal[c]	4.4	
A_{1g} and E_g internal modes		
classical solvent, quantum internal	15.6	15.6
All internal modes		
classical solvent, quantum internal		3.3

"internal" refers to intramolecular degrees of freedom of reactants.

[a]Frequencies and displacements from Table I.

[b]Effective internal frequency used (see eq 9). The saddle-point approximation is exact in this case.

[c]Eq 8.

frequencies listed in Table I ($\Delta Q_i = 0$ for the E_g and F modes), the direct sum was found to require excessive computation time, so only the saddle-point value of the Franck-Condon sum was calculated. Assuming that it is reliable, we find (cf. Table II) $G(Co)/G(Ru) \sim 10^{-8}$, in agreement with the saddle-point-method-value in ref. 5.

Also listed in Table II are values of G calculated using the two-frequency quantum solvent model described earlier and analogous values calculated assuming wholly classical solvent interaction. As expected, the classical solvent model yields a slightly smaller value of G (less nuclear tunneling). The effect is small, about 10% in the systems considered.

Hexaaquoiron (II/III) Self-exchange Reaction. Like the hexaamminecobalt self-exchange reaction, the hexaaquoiron self-exchange reaction proceeds with a large internal reorganization energy involving the metal-ligand internal modes. Using metal-oxygen symmetric stretching frequencies in the ferric and ferrous ions of roughly 490 cm^{-1} and 389 cm^{-1} respectively,[2] and a change in equilibrium bond length of 0.14 Å,[36] the internal reorganization energy is calculated to be 35 kJ/mol, when an effective single frequency of 431 cm^{-1}, based on eq 9, is used. The outer-sphere reorganization energy has been estimated as 27 kJ/mol.[2]

It has been suggested that in a system like this one, in which a high-frequency mode undergoes a significant bond length change, quantum effects should be large. But calculation of the sum over Franck-Condon factors yields a quantum value of about 3.5 times the classical value (cf. Table III). Thus, as in the hexaammine-

TABLE III: Franck-Condon Sums For Hexaaquoiron and Tris-bipyridyl-ruthenium Self-Exchange and Cross-Reactions

Reaction	Quantum	Classical	Semiclassical
Fe^{2+} - Fe^{3+}	8.5[a]	2.4[a]	145.[a]
$Ru(bpy)_3^{2+}$ - $Ru(bpy)_3^{3+}$	1.4[b]	1.4[b]	1.6[b]
Fe^{2+} - $Ru(bpy)_3^{3+}$	2.5[c]	1.5[c]	3.8[c]
$k_{12}/(k_{11}k_{22}K_{12}f_{12})^{\frac{1}{2}}$ [d]	0.94	1.00	0.40

[a] Multiplied by 10^{15} cm^{-1}.

[b] Multiplied by 10^{6} cm^{-1}.

[c] Multiplied by 10^{7} cm^{-1}.

[d] cf. eq 17. Rate constants are from Table IV. k_{11}, k_{22}, and k_{12} are the rate constants for the preceding three reactions, in the order listed.

cobalt self-exchange reaction, no very large quantum effect on the Franck-Condon sum is observed. Indeed, the discrepancy is smaller than the other uncertainties in the overall calculation of the reaction rates, and the quantum expression is more complex (cf. the cancellation of terms in the classical expression, leading to the simple cross-relation expression[21] given below).

The 'semiclassical' result in Table III is seen to be in large error. It was shown in ref. 26 that the semiclassical method corresponds, tacitly, to assuming that the nuclear tunneling distance along the abscissa is ac in Fig. 2, whereas it is actually ab. This assumption is valid only when the products' curve at the intersection is very steep, for then point b $\cong$ point c, and so is valid when ΔE is quite negative. Identical remarks apply to the reverse reaction when $-\Delta E$ is quite negative and hence, by microscopic reversibility, to the forward reaction when ΔE for the forward reaction is quite positive. For $\Delta E \cong 0$ one concludes, since ac $\ll$ ab, that the "semiclassical" tunneling rate will exceed the quantum one,[26] a result confirmed in Table III (Fe^{2+} - Fe^{3+}). Related remarks apply to use of the semiclassical result in the so-called inverted region ($|\Delta E| \gg \lambda$), only now the semiclassical answer is too low, for now it was shown,[26] the actual nuclear tunneling distance is less than the tacitly assumed one.[26]

Cross Reactions. Quantum effects on the classical cross-relation[37] are found below to be relatively small, in the 'normal' ΔG° regime. In this relation, the rate constant k_{12} of

$$A_1(ox) + A_2(red) \rightarrow A_1(red) + A_2(ox) \qquad (14)$$

is related to those (k_{11}, k_{22}) of the self-exchange reactions

$$A_1(ox) + A_1(red) \rightarrow A_1(red) + A_1(ox) \qquad (15)$$

$$A_2(ox) + A_2(red) \rightarrow A_2(red) + A_2(ox) \qquad (16)$$

when the work terms are either small or nearly cancel, via[21]

$$k_{12} \cong (k_{11}k_{22}\, K_{12}f_{12})^{\frac{1}{2}} \qquad (17)$$

where K_{12} is the equilibrium constant of reaction 14 and f_{12} is given by

$$\ln f_{12} = (\ln K_{12})^2/[4 \ln(k_{11}k_{22}/Z^2)] \qquad (18)$$

where Z is the collision frequency in solution. Expressed in terms of of the classical G's, this expression can be rewritten as

$$\bar{G}_{12} = (\bar{G}_{11}\, \bar{G}_{22}\, K_{12}\, \bar{f}_{12})^{\frac{1}{2}} \qquad (19)$$

where

$$\ln \bar{f}_{12} = (\ln K_{12})^2/[4 \ln(\bar{G}_{11} \bar{G}_{22})] \quad (20)$$

and

$$\bar{G}_{ij} = (4\pi\lambda_{ij}kT)^{\frac{1}{2}} G_{ij} \quad (21)$$

The classical results in Tables III and IV are those for a classical adiabatic result,

$$k_{ij} = Z \bar{G}_{ij} \quad (22)$$

where Z is defined above (and is taken to be 10^{11} $M^{-1}s^{-1}$ [21,27]). Eq 22 is valid when work terms for formation of the precursor and successor complexes are neglected and when nonadiabaticity is negligible. To assess a quantum correction, the "quantum results" in Tables III and IV were obtained using eqs 21-22 but with the G_{ij} in eq 21 replaced by its quantum value. The 'semiclassical' values in Table III were calculated by introducing the semiclassical value of G_{ij} into eqs 21-22. From the results of Table III for the cross-reaction

$$Fe^{2+} + Ru(bpy)_3^{3+} \rightarrow Fe^{3+} + Ru(bpy)_3^{2+} \quad (23)$$

one can see that the quantum effect on the calculated cross-reaction rate (eq 17) is only a factor of 2 for reaction 23. The quantum effect on the cross-relation, i.e., on the ratio of the left to the right hand side in eq 17, is calculated to be a factor of 0.94.

In obtaining these results, the inner-and outer-sphere reorganization energies for the $Ru(bpy)_3^{2+/3+}$ self-exchange reaction were taken from ref. 2: $\lambda_{inner} \cong 0$ and $\frac{1}{4}\lambda_{out} \cong 13.4$ kJ/mol. The reorganization energies for the $Fe^{2+/3+}$ self-exchange are given above. The inner- and outer-sphere reorganization energies for reaction 23 were then estimated from the additivity rule[27] to be 17.6 kJ/mol and 20.1 kJ/mol, respectively. To allow direct comparison between the quantum and classical results, the effective frequency 431 cm^{-1} was employed for the $Fe^{2+/3+}$ symmetric stretch, according to the rule for effective force constants given by eq 9. The free energy of reaction for reaction 23 is readily calculated to be -47.3 kJ/mol from the reduction potentials of $Ru(bpy)_3^{3+}$ (1.26 eV[38-40]) and $Fe(aq)^{3+}$ (0.770 eV[22]).

The calculated self-exchange rate constants in Table IV agree reasonably well with the measured rate constants. However, the calculated values of the rate constant for the cross reaction differ from the experimental value by two to three orders of magnitude. Several explanations for the apparent failure of the theory to predict this particular cross reaction rate, when it predicts many others so well, have been offered:[2,44,45] (1) large differences in

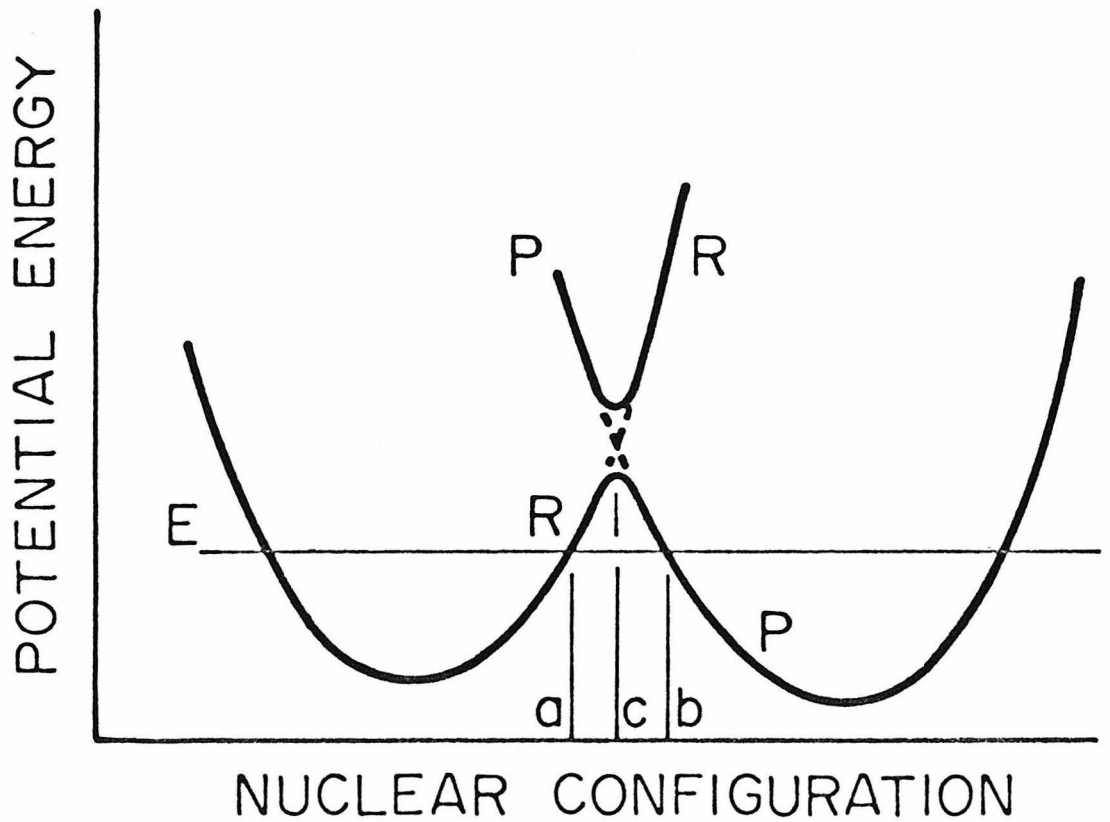

Figure 2 Curve similar to Figure 1, but for a nearly thermoneutral reaction ($\Delta E \sim 0$). Points a and b here are classical 'turning points' of motion on the reactants' and products' potential energy curves, for the given energy E. Point c is at the intersection of the two potential energy surfaces. The actual nuclear tunneling distance is ab. Cf. Ref. 26.

TABLE IV: Rate Constants For Hexaaquoiron and Tris-bipyridyl-ruthenium Self-Exchange and Cross-Reactions [a]

Reaction	k_{calc}(quantum)	k_{calc}(classical)	k_{obs}
Fe^{2+} - Fe^{3+}	6.3	1.7	4.2 [41]
$Ru(bpy)_3^{2+}$ - $Ru(bpy)_3^{3+}$	4.9×10^8	4.6×10^8	1.2×10^9 [42]
Fe^{2+} - $Ru(bpy)_3^{3+}$	1.4×10^8	8.4×10^7	7×10^5 [43,44]

[a] Units are $M^{-1}s^{-1}$.

the stability of the precursor and successor complexes, (2) non-adiabaticity, and (3) nuclear tunneling. Since the quantum and classical calculated rate constants are in good agreement, the third suggestion, nuclear tunneling, can now be eliminated, so that the discrepancy is probably due to (1) or (2).

Conclusion

We have shown that the Franck-Condon contributions to the rates of the hexaamminecobalt, hexaammineruthenium, and hexaaquoiron self-exchange reactions at 300 K can be reasonably well approximated by the classical expression (factors of 4.3, 1.2 and 3.5, respectively). These corrections are relatively minor, in view of the uncertainties in the various quantities involved in the rate expression. A non-adiabatic model was assumed, but analogous results would be expected for an adiabatic model.

Also for these systems, we have seen by direct comparison with the exactly evaluated quantum sum of Franck-Condon terms that the saddle-point approximation is a very good approximation to the exact sum. The 'semiclassical' approximation (eq 10) is a poor one for self-exchange reactions such as Fe^{2+} - Fe^{3+}.

The quantum effect on the cross-reaction relation (eq 17) for hexaaquoiron(II) with tris-bipyridylruthenium(III) is negligible (a factor of 0.94), since some cancellation of quantum effects occurs in the calculation of cross-reaction rates.

We conclude that a reasonable order of magnitude estimate for the contribution of configurational changes of high frequency quantum modes in the first coordination layer, for typical metal-ligand frequencies, to the rate constant can be provided by a classical expression. Pre-exponential factors and activation energies are expected to be more sensitive to use of the classical approximation (they are to other approximations also), and will be discussed in a subsequent paper.

Appendix

Harmonic-oscillator overlap integrals. The overlap integral $\langle n|m\rangle$ is given by

$$\langle n|m\rangle = (-1)^{m+n}[2\sqrt{f}/(1+f)]^{\frac{1}{2}}(2^{m+n}m!n!)^{-\frac{1}{2}} e^{-Xf/(1+f)}$$

$$\times[(1-f)/(1+f)]^{(m+n)/2} \sum_{\ell=0}^{\infty} \frac{m!n!}{\ell!(m-\ell)!(n-\ell)!} [4\sqrt{f}/(1-f)]^{\ell} \qquad \text{(A1)}$$

$$\times F_{n-\ell}\left(f\sqrt{\frac{2X}{1-f^2}}\right) H_{m-\ell}\left(\sqrt{\frac{2Xf}{1-f^2}}\right)$$

where f and X are described in the text. H_n is the Hermite polynomial of order n, and $F_n(x) = i^n H_n(ix)$. (Eq A1 is given, for example, in refs. 14 and 15 although with a few misprints.)

For the case X = 0 and f ≠ 1, eq A1 reduces to:[13]

$$\langle 2n|2m\rangle = \left[\frac{4f}{(1+f)^2}\right]^{\frac{1}{4}} \left(\frac{2n!\ 2m!}{2^{2n+2m}}\right)^{\frac{1}{2}} (-1)^n \left(\frac{f-1}{f+1}\right)^{n+m}$$

$$\times \sum_{\ell=0}^{\infty} \frac{(-1)^\ell}{2\ell!(n-\ell)!(m-\ell)!} \left[\frac{16f}{(f-1)^2}\right]^\ell \tag{A2}$$

$$\langle 2n+1|2m+1\rangle = \left[\frac{4f}{(1+f)^2}\right]^{\frac{3}{4}} \left[\frac{(2n+1)!(2m+1)!}{2^{2n+2m}}\right]^{\frac{1}{2}} (-1)^n \left(\frac{f-1}{f+1}\right)^{n+m}$$

$$\times \sum_{\ell=0}^{\infty} \frac{(-1)^\ell}{(2\ell+1)!(n-\ell)!(m-\ell)!} \left[\frac{16f}{(f-1)^2}\right]^\ell$$

$$\langle 2n|2m+1\rangle = \langle 2n+1|2m\rangle = 0$$

The sums in eq A1 and A2 are only formally infinite; they are actually terminated by the factorials in the denominators of the terms of the sums when ℓ exceeds either m or n.

Generating function for the saddle-point approximation. f(t) (eqs 5 and 6) is found (using methods in refs. 23 and 24) to be given by

$$f(t) = -\sum_{j=1}^{N} \left\{ \frac{1}{2} \ln[\sinh 2\beta_j \sinh 2\alpha_j (\omega_j \tanh \beta_j + \omega_j' \tanh \alpha_j) \right.$$

$$\times (\omega_j \coth \beta_j + \omega_j' \coth \alpha_j)/(\omega_j \omega_j')] \tag{A3}$$

$$\left. + 2\lambda_j \omega_j'/(\hbar\omega_j)/(\omega_j \coth \alpha_j + \omega_j' \coth \beta_j) \right\}$$

The second derivative of f(t) is

$$f''(t) = -\frac{1}{2}\hbar^2 \sum_{j=1}^{N} \Big\{ \omega_j^2 \operatorname{csch}^2 2\beta_j + \omega_j'^2 \operatorname{csch}^2 2\alpha_j$$

$$+ \frac{\omega_j'^3 \operatorname{sech}^3\alpha_j \sinh \alpha_j + \omega_j^3 \operatorname{sech}^3 \beta_j \sinh \beta_j}{2(\omega_j \tanh \beta_j + \omega_j' \tanh \alpha_j)}$$

$$+ \frac{(\omega_j^2 \operatorname{sech}^2 \beta_j - \omega_j'^2 \operatorname{sech}^2 \alpha_j)^2}{4(\omega_j \tanh \beta_j + \omega_j' \tanh \alpha_j)^2} + \frac{(\omega_j'^2 \operatorname{csch}^2 \alpha_j - \omega_j^2 \operatorname{csch}^2 \beta_j)^2}{4(\omega_j \coth \beta_j + \omega_j' \coth \alpha_j)^2}$$

$$- \frac{\omega_j'^3 \operatorname{csch}^3 \alpha_j \cosh \alpha_j + \omega_j^3 \operatorname{csch}^3 \beta_j \cosh \beta_j}{2(\omega_j \coth \beta_j + \omega_j' \coth \alpha_j)} \qquad \text{(A4)}$$

$$+ \frac{2\lambda_j \omega_j'^2 (\omega_j' \operatorname{csch}^3 \alpha_j \cosh \alpha_j + \omega_j \operatorname{csch}^3 \beta_j \cosh \beta_j)}{\hbar(\omega_j \coth \alpha_j + \omega_j' \coth \beta_j)^2}$$

$$- \frac{2\lambda_j \omega_j'^3 \omega_j (\operatorname{csch}^2 \alpha_j - \operatorname{csch}^2 \beta_j)^2}{\hbar(\omega_j \coth \alpha_j + \omega_j' \coth \beta_j)^3} \Big\}$$

where N is the number of harmonic modes in the system,

$$\beta_j = \frac{1}{2}\hbar\omega_j\left(\frac{1}{kt} - it\right), \quad \alpha_j = \frac{1}{2} i\hbar\omega_j' t, \quad \lambda_j = \frac{1}{2}\omega_j^2 (\Delta Q_j)^2, \qquad \text{(A5)}$$

and ω_j, ω_j' and ΔQ_j are defined in the text. t_0 is the saddle-point value of t, i.e. t such that

$$0 = f'(t) = \frac{1}{2} i\hbar \sum_{j=1}^{N} \Bigg\{ \omega_j \coth 2\beta_j - \omega_j' \coth 2\alpha_j + \frac{\omega_j^2 \operatorname{sech}^2 \beta_j - \omega_j'^2 \operatorname{sech}^2 \alpha_j}{2(\omega_j \tanh \beta_j + \omega_j' \tanh \alpha_j)} + \frac{\omega_j'^2 \operatorname{csch}^2 \alpha_j - \omega_j^2 \operatorname{csch}^2 \beta_j}{2(\omega_j \coth \beta_j + \omega_j' \coth \alpha_j)} - \frac{2\lambda_j \omega_j'^2 (\operatorname{csch}^2 \alpha_j - \operatorname{csch}^2 \beta_j)}{\hbar(\omega_j \coth \alpha_j + \omega_j' \coth \beta_j)^2} \Bigg\} \tag{A6}$$

'Semiclassical' Franck-Condon sum. The 'semiclassical' Franck-Condon sum, eq 10, may be derived from eq 1, the Golden-Rule expression for the Franck-Condon sum, using techniques originally applied to other problems.[29] Consider first the case in which a single normal vibrational mode, of frequency ω, normal mode force constant $k = \omega^2$, and normal coordinate q, characterizes both the reactants and the products. The reactant Hamiltonian is

$$H_r = p^2/2 + kq^2/2 \tag{A7}$$

The products' Hamiltonian, in which the equilibrium value of q is displaced by an amount a, is

$$H_p = p^2/2 + \frac{1}{2} k(q-a)^2 + \Delta E \tag{A8}$$

where ΔE is the reaction endoergicity. Eq 1 gives

$$G = (hQ)^{-1} \sum_n e^{-(n+\frac{1}{2})\hbar\omega/kT} \int_{-\infty}^{\infty} \sum_m \langle n|m\rangle \langle m|n\rangle e^{i(E_m - E_n)t/\hbar} dt \tag{A9}$$

where the Fourier-integral representation of the delta function has been introduced. Inserting the exponential in the coordinate integral and noting that the wavefunctions corresponding to $|n\rangle$ and $|m\rangle$, χ_n and χ_m, are eigenfunctions of H_r and H_p, respectively, one obtains

$$G = (hQ)^{-1} \sum_n e^{-(n+\frac{1}{2})\hbar\omega/kT} \int_{-\infty}^{\infty} \sum_m \langle n|m\rangle \langle m|e^{iH_p t/\hbar} e^{-iH_r t/\hbar}|n\rangle \, dt \quad (A10)$$

If all commutators of H_r and H_p are neglected, which is the semi-classical approximation in this approach, then[29a]

$$e^{iH_p t/\hbar} e^{-iH_r t/\hbar} = e^{it(H_p - H_r)t/\hbar} \quad (A11)$$

From eqs A7 and A8 it is found that $H_p - H_r = -ka(q - \frac{1}{2} a - \Delta E/ka)$, so eq A10 becomes

$$G = (hQ)^{-1} \sum_n e^{-(n+\frac{1}{2})\hbar\omega/kT} \int_{-\infty}^{\infty} \langle n|e^{-itka(q-\frac{1}{2}a-\Delta E/ka)}|n\rangle \, dt \quad (A12)$$

where use has been made of the identity $\sum_m |m\rangle\langle m| = 1$. Eq A12 may be rewritten as

$$G = (ka\hbar Q)^{-1} \sum_n e^{-(n+\frac{1}{2})\hbar\omega/kT} \langle n|\delta(q - \tfrac{1}{2} a - \Delta E/ka)|n\rangle \quad (A13)$$

or simply

$$G = (ka\hbar Q)^{-1} \sum_n e^{-(n+\frac{1}{2})\hbar\omega/kT} |\chi_n(q^{\neq})|^2 \quad (A14)$$

where $q^{\ddagger} = \frac{1}{2} a + \Delta E/ka$ is the value of q for which the reactant and product potential energies are equal. According to Mehler's formula,[23] the sum in eq A14 may be reduced to the single term

$$G = (2\pi\lambda\hbar\omega\coth\gamma)^{-\frac{1}{2}} \exp[-(\Delta E+\lambda)^2/2\lambda\hbar\omega\coth\gamma] \qquad \text{(A15)}$$

where $\gamma \equiv \hbar\omega/2kT$, $\lambda \equiv \frac{1}{2} ka^2$, and we have used $Q = [2 \sinh(\hbar\omega/2kT)]^{-1}$.[45]

Consider now a system having N normal vibrational modes, each characterized by a frequency ω_j and normal mode force constant $k_j = \omega_j^2$. Let a_j be the difference between the equilibrium values of the jth normal coordinate in the product and reactant. Define $\lambda_j = \frac{1}{2} k_j a_j^2$ and $\gamma_j = \hbar\omega_j/2kT$. $G_j(\Delta E)$ is given by eq A15 for each mode individually. $G(\Delta E)$ for the N-mode system, where ΔE is again the reaction endoergicity, is a convolution of the G_j's (j = 1, 2,..., N). That is

$$G(\Delta E) = \int_{-\infty}^{\infty} \cdots \int_{-\infty}^{\infty} G_1(y_1) \cdots G_{N-1}(y_{N-1})\, G_N(\Delta E - \sum_{j=1}^{N-1} y_j)\, dy_1 \cdots dy_{N-1} \,. \qquad \text{(A16)}$$

Since each $G_j(E)$ is a gaussian distribution in E, $G(\Delta E)$ is a convolution of the gaussians G_j. Therefore $G(\Delta E)$ is itself a gaussian distribution, and has a mean equal to the sum of the means of the G_j, and variance equal to the sum of the variances of the G_j.[47]

Thus $G(\Delta E)$ for an N-mode system is given by eq A15, but with

$\lambda = \sum_{j=1}^{N} \lambda_j$ and $\lambda\hbar\omega\coth\gamma = \sum_{j=1}^{N} \lambda_j \hbar\omega_j \coth\gamma_j$. Explicitly,

$$G = (2\pi \sum_{j=1}^{N} \lambda_j \hbar\omega_j \coth \gamma_j)^{-\frac{1}{2}} \exp[-(\Delta E + \sum_{j=1}^{N} \lambda_j)^2 / (2 \sum_{j=1}^{N} \lambda_j \hbar\omega_j \coth \gamma_j)] \qquad \text{(A17)}$$

References and Notes

(1) H. Stynes and J. Ibers, Inorg. Chem. 1971,10,2304.

(2) N. Sutin in "Tunneling in Biological Systems," B. Chance, D.C. DeVault, H. Frauenfelder, J. R. Schrieffer and N. Sutin, Eds. (Academic, New York, 1979).

(3) C. Creutz and N. Sutin, J. Am. Chem. Soc. 1977, 99,241.

(4) D. Stranks, Disc. Far. Soc. 1960,29,116.

(5) E. Buhks, M. Bixon, J. Jortner, and G. Navon, Inorg. Chem. 1979,18,2014.

(6) (a) N. Kestner, J. Logan, and J. Jortner, J. Phys. Chem. 1974,78,2148; and

(b) J. Ulstrup and J. Jortner, J. Chem. Phys. 1975, 63,4358.

(7) (a) V. G. Levich and R. R. Dogonadze, Coll. Czech. Chem. Comm. 1961,26,1934; Transl., O. Bosko, Univ. of Ottawa, Ontario, Canada; and

(b) V. Levich in "Physical Chemistry: An Advanced Treatise," Vol. 9B, H. Eyring, D. Henderson and W. Jost, Eds., (Academic,New York,1970).

(8) (a) R. R. Dogonadze and A. M. Kuznetsov, Elektrokhimiya 1967,3,1324, Engl. transl. Sov. Electrochem. 1967,3,1189; and

(b) R. R. Dogonadze, A. M. Kuznetsov, and M. A. Vorotyntsev, Phys. Status Solidi (Ger.) 1972,54,125,425; and

(c) R. Van Duyne and S. Fischer, Chem. Phys. 1974, 5,183; and

(d) S. Efrima and M. Bixon, Chem. Phys. 1976,13,447; and

(e) J. Jortner, J. Chem. Phys. 1976,64,4860.

(9) (a) R. A. Marcus, Disc. Faraday Soc. 1960,29,21; and

(b) R. A. Marcus, Ann. Rev. Phys. Chem. 1964,15,155.

(10) (a) P. P. Schmidt, Spec. Per. Rep. Electrochem. 1975,5,21; and

(b) J. Ulstrup, "Charge Transfer Processes in Condensed Media," Lecture Notes in Chemistry, No. 10 (Springer, New York,1979).

(11) E. Hutchisson, Phys. Rev. 1951,36,410.

(12) C. Manneback, Physica 1951,17,1001.

(13) T. Keil, Phys. Rev. 1965,140(2A),601. Equation A3 contains a misprint: the value it gives for $\langle 2n+1 \mid 2m+1 \rangle$ is too small by a factor of 2.

(14) D. Heller, K. Freed, and W. Gelbart, J. Chem. Phys. 1972,56,2309.

(15) M. Prais, D. Heller, and K. Freed, Chem. Phys. 1974,6,331.

(16) Eq 19 of ref. 26. The condition for the validity of this eq 19 is given by eq 21 there.

(17) R. R. Dogonadze, Usp. Chimi. 1965,34,1779.

(18) D. Draegert, N. Stone, B. Curnutte, and D. Williams, J. Opt. Soc. Am. 1966,56,64.

(19) "Water: A Comprehensive Treatise," Vol. 1, F. Franks, Ed. (Plenum, New York.1972).

(20) A. A. Ovchinnikov and M. Ya. Ovchinnikova, Zh. Eksp. Teor. Fiz. 1969,56,1278, English trans. Sov. Phys. JETP 1969,29,688.

(21) R. A. Marcus, J. Phys. Chem. 1968,72,891.

(22) "Handbook of Chemistry and Physics" (C.R.C., Cleveland, 1975).

(23) J. Markham, Rev. Mod. Phys. 1959,31,956.

(24) (a) S. H. Lin, J. Chem. Phys. 1968,44,3759; and

(b) S. H. Lin, Theor. Chim. Acta 1968,10,301.

(25) The only entropy change present in eq 1 (and hence in eq 5) is the minor contribution from inner-sphere frequency changes, wheras the actual ΔS^{o} can be much larger. For reactions in which the set of reactants' vibration frequencies equals the set of products' vibration frequencies $\Delta S^{o}_{vib} = 0$, where ΔS^{o}_{vib} is the contribution to ΔS^{o} from inner-sphere vibration frequency changes. ΔS^{o} for the Fe^{2+}-$Ru(bpy)_3^{3+}$ cross-reaction (eq 23) is -180 J mol^{-1} K^{-1}.[2] ΔS^{o}_{vib} for this reaction may be estimated as follows: Symmetric stretching frequencies for Fe^{2+}_{aq} and Fe^{3+}_{aq} are given in the text (389 cm^{-1} and 490 cm^{-1}, respectively). For simplicity we will assume that the ratio of a frequency in the reduced state to that in the oxidized state is the same for each of the 15 (octahedral) normal modes. Vibration frequencies in the 2+ and 3+ oxidation states of $Ru(bpy)_3$ are unknown. If by analogy with $Fe(bpy)_3^{2+}$ (for which at least the symmetric stretching frequency is unchanged upon oxidation [32b]) it is assumed that the vibration frequencies in the 2+ and 3+ oxidation states of $Ru(bpy)_3$ are the same, then the $Ru(bpy)_3^{2+/3+}$ couple's vibrations contribute nothing to ΔS^{o}_{vib}. Using standard equations [45] for the quantum-mechanical vibrational partition functions and for ΔS^{o}, one

obtains $\Delta S^{o}_{vib} = -20$ J mol^{-1} K^{-1} at 300 K, which is only about 10% of the total ΔS^{o} for the reaction.

(26) R. A. Marcus, in "Third Int. Symp. on Oxidases," T. E. King, H. S. Mason, and M. Morrison, Eds., (Pergamon, New York, 1981).

(27) R. A. Marcus, J. Chem. Phys. 1965,43,679.

(28) (a) J. J. Hopfield, Proc. Nat'l Acad. Sci. USA 1974,71,3640; and

(b) J. J. Hopfield, in "Electrical Phenomena at the Biological Membrane Level," E. Roux, Ed., (Elsevier, Amsterdam, 1977) p.471.

(29) (a) M. Lax, J. Chem. Phys. 1952,20,1752; and

(b) R. Kubo and Y. Toyazawa, Prog. Theor. Phys. 1955,13,160; and

(c) K. Maeda, Phys. Chem. Solids 1959,9,335; and

(d) D. Curie, "Luminescence in Crystals" (Wiley, New York, 1963), p.47 ff.; and

(e) T. F. Soules and C. B. Duke, Phys. Rev. B 1971,3,262.

(30) T. Meyer and H. Taube, Inorg. Chem. 1971,10,2304.

(31) G. Brown and N. Sutin, J. Am. Chem. Soc. 1979,101,883.

(32) (a) C. W. F. T. Pistorius, J. Chem. Phys. 1958,29,1328; and

(b) K. Nakamoto, "Infrared and Raman Spectra of Inorganic and Coordination Compounds," 3rd Ed. (Wiley, New York, 1978).

(33) R. A. Marcus, Ref. 9a. See eq 4.3.8 (taking $m = \frac{1}{2}$ and $K_s^p = K_i^{\ddagger}$) and the discussion in appendix 2. Note that the internal reorganization energy $\Delta E_i^{\ddagger}$ involves a sum over both reactants, in the case of the present self-exchange reaction.

(34) K. Schmidt, W. Hauswirth, and A. Müller, J. Chem. Soc., Dalton Trans. 1975,2199.

(35) The actual value calculated and used was 47.7 kJ/mol.

(36) N. Hair and J. Beattie, Inorg. Chem. 1977,16,245.

(37) R. A. Marcus, J. Phys. Chem. 1963,67,853,2889.

(38) J. Miller and R. Prince, J. Chem. Soc. 1966,A,1048.

(39) F. Lytle and D. Hercules, Photochem. Photobiol. 1971,13,123.

(40) T. J. Meyer, Isr. J. Chem. 1977,15,200.

(41) J. Silverman and R. W. Dodson, J. Phys. Chem. 1952,56,846.

(42) R. C. Young, F. R. Keene, and T. J. Meyer, J. Am. Chem. Soc. 1977,99,2468.

(43) B. M. Gordon, L. L. Williams, and N. Sutin,J. Am. Chem. Soc. 1961,83,2061.

(44) J. N. Braddock and T. J. Meyer, J. Am. Chem. Soc. 1973,95,3158.

(45) R. A. Marcus and N. Sutin, Inorg. Chem. 1975,14,213.

(46) E. A. Moelwynn-Hughes, "Physical Chemistry," Second Ed., (Pergamon, New York, 1961). Pages 347 and 352.

(47) A. Renyi, "Foundations of Probability" (Holden-Day, San Francisco, 1970). Pages 125 and 208.

CHAPTER 2

QUANTUM EFFECTS FOR ELECTRON-TRANSFER REACTIONS IN THE "INVERTED REGION"

Introduction

In the usual range of standard free energies of reaction ΔG°, outer-sphere homogeneous electron transfer reactions have rates which increase with increasingly negative ΔG°. However, when $-\Delta G^\circ$ is very large both classical[1,2] and quantum[3,4] theories predict that the electron transfer rate will ultimately decrease with increasingly negative ΔG° (inverted region), namely when $-\Delta G^\circ$ is greater than λ, four times the total reorganization energy of the reaction. Experimental studies have shown little or no decrease of the rate constant in this 'inverted' region.[5-8] There have been suggestions that quantum effects are responsible,[3,4,9-12] suggestions that electronically-excited products may be responsible[5] (they correspond to reactions with a smaller $-\Delta G^\circ$), and suggestions that where the rate of electron transfer is inferred from and, in fact, equated to the rate of fluorescence quenching, the fluorescence quenching in the inverted region may be due instead to a faster alternate non-electron transfer initial step, exciplex formation.[13]

In the present paper we consider the importance of nuclear tunneling first for a model system and then for an actual system using realistic vibration frequencies and bond length changes for the data of Creutz and Sutin.[6] The discrepancy is found to remain very large, some quantum effects notwithstanding. An alternate pathway of forming an electronically-excited product is explored; it reduces the discrepancy considerably. Another possible alternate pathway is an atom transfer. Still another possibility (longer range electron transfer) is also considered.

Theory

Quantum Treatment. An approximate quantum-mechanical rate expression based on the golden-rule transition probability is applicable to electron transfer systems in the nonadiabatic limit.[14] Within the Condon approximation the transition probability involves the product of the square of an electron exchange integral and a thermally weighted sum, G, over Franck-Condon factors:

$$G = \frac{1}{Q} \sum_n \sum_m e^{-E_n^{vib}/kT} \left| \langle \chi_n | \chi_m \rangle \right|^2 \delta(E_n - E_m) \qquad (1)$$

where Q is the reactants' vibrational partition function, and n and m designate initial and final vibronic states, respectively. E_n and E_m are initial- and final-state energies. E_n^{vib} is the initial-state vibrational energy, and $|\chi\rangle$ is treated as a harmonic oscillator eigenfunction assumed equal to a product over the system's degrees of freedom of single-mode haromonic oscillator functions.

The overlap integrals required for evaluating G directly by the sum of eq 1 are well known (Ref. 15, for example). The solvent interaction is included in eq 1 via two harmonic modes that have frequencies $\hbar\omega_1 = 1\ cm^{-1}$ and $\hbar\omega_2 = 170\ cm^{-1}$. Details are given in Ref. 15.

Classical Treatment. When all the degrees of freedom of the system are treated in the classical limit, $\hbar\omega/2kT \to 0$, and when frequency changes are neglected, eq 1 reduces to

$$G = (4\pi kT\lambda)^{-\frac{1}{2}} \exp[-(\Delta E + \lambda)^2/4kT\lambda] \qquad (2)$$

where λ equals $\sum_{j=1}^{N} \lambda_j$, ΔE is the energy of reaction, and λ_j is four times the reorganization energy for the jth mode. For a vibrational normal coordinate, $\lambda_j = \frac{1}{2} F_j (\Delta Q_j)^2$, where F_j is the force constant and ΔQ_j is the equilibrium displacement from reactant state to product state, of the jth normal coordinate. Eq 2 is similar in form to a classical expression[1,2] which allowed for large entropies of reaction when they occurred. However unlike this classical expression it contains energies rather than free energies, since eq 1 does not include any large entropy terms.[15] The other classical expression[1,2] is more general in this respect.[16]

It has been shown[17] that frequency changes may be included in an approximate manner by using average force constants to calculate λ, rather than using the actual force constants. The average force constant is

$$F_{av} = 2FF'/(F + F') \qquad (3)$$

where F and F′ are the force constants in the reactant and product states, respectively. We use F_{av} when evaluating the classical value of the Franck-Condon sum (eq 2). Arguments were given in Appendix IV of ref. 17 based on a perturbation expansion suggesting that the approximation in eq 3 is adequate.

Semiclassical Treatment. A 'semiclassical' treatment of electron transfer has been given[18] and discussed in detail elsewhere.[15,16] The semiclassical expression for the thermally weighted Franck-Condon sum is

$$G = (2\pi\lambda\hbar\omega \coth\gamma)^{-\frac{1}{2}} \exp[-(\Delta E + \lambda)^2/(2\lambda\hbar\omega \coth\gamma)] \qquad (4)$$

The variables of eq 4 are defined as for eq 2 and $\lambda\hbar\omega \coth\gamma$ is an abbreviation for $\sum_{j=1}^{N} \lambda_j \hbar\omega_j \coth\gamma_j$, where γ_j is $\hbar\omega_j/2kT$. 'Semiclassical' has come to denote a variety of different methods in the dynamics literature, one of which yields eq 4.

Comparison of the Three Treatments

Fig. 1 is a plot of G, the Franck-Condon sum, calculated classically and quantum mechanically, versus $\Delta G°$, the standard free energy of reaction for a model system. $\Delta G°$ is the same as ΔE in eqs 1 and 2, since eq 1 tacitly assumes zero for $\Delta S°$ when $F_i = F_i'$. The model system represents metal-bipyridyl systems (e.g., $Ru(bpy)_3^{2+}$ + $Os(bpy)_3^{3+}$). The internal reorganization in such systems is negligible ($\lambda_{inner} = 0$) and the outer-sphere reorganization energy $\frac{1}{4}\lambda_{out}$ is ≈ 13.4 kJ/mol.[19] The ordinate is a plot of $\log_{10}(Ge^{\Delta G°/2kT})$ vs $\Delta G°$. As shown in a

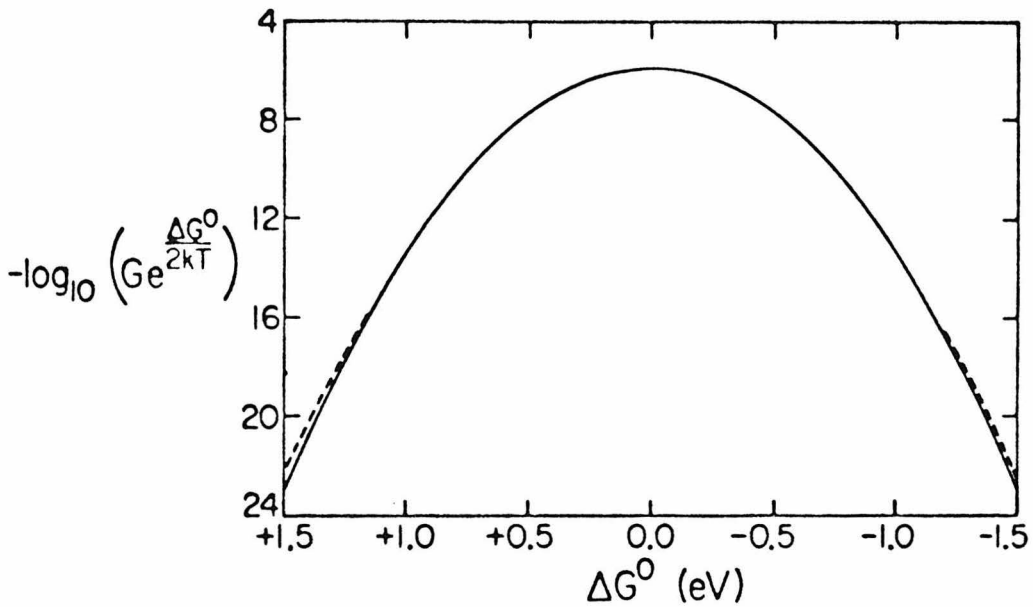

Figure 1. Model $M(bpy)_3^{3+/2+}$

—— Classical Franck-Condon Sum.

-- Quantum Franck-Condon Sum.

λ_{out} = 54 kJ/mol. λ_{inner} = 0. Temp. = 300 K.

recent paper,[16] both the classical and quantum values of the ordinate are symmetric in $\Delta G°$, when plotted in this manner.

Fig. 2 is a plot similar to Fig. 1. The λ's and frequencies used are for the hypothetical system described in Table I. This system differs from that of Fig. 1 by including two high-frequency internal modes and having both a larger inner-sphere and a larger outer-sphere reorganization energy. (The frequencies of the internal modes are comparable to those in the cobalt hexaammine system.) In Fig. 2 the ordinate is a log plot of the Franck-Condon sum, G, versus $\Delta G°$, and so Fig. 2, unlike Fig. 1, is not symmetrical about $\Delta G° = 0$.

The two plots are qualitatively alike. The classical value for the ordinates in each plot is generally less than the quantum value, as expected since the classical theory does not include vibrational tunneling. In the normal region (i.e., $-\Delta G° < \lambda$) the classical and quantum values agree very well. But as the free energy decreases into the inverted region, the quantum value decays less rapdily than the classical. Because of the high-frequency internal modes included in the second system, the discrepancy between the classical and quantum values only becomes appreciable in Fig. 2. Similar results were observed earlier by Jortner et al. using other model systems.[4]

The 'semiclassical' values are compared with the quantum for selected values of $\Delta G°$ in Table II. They are smaller when the system is in the inverted region and high otherwise. This effect is due to an approximation to vibrational tunneling inherent in the 'semiclassical'

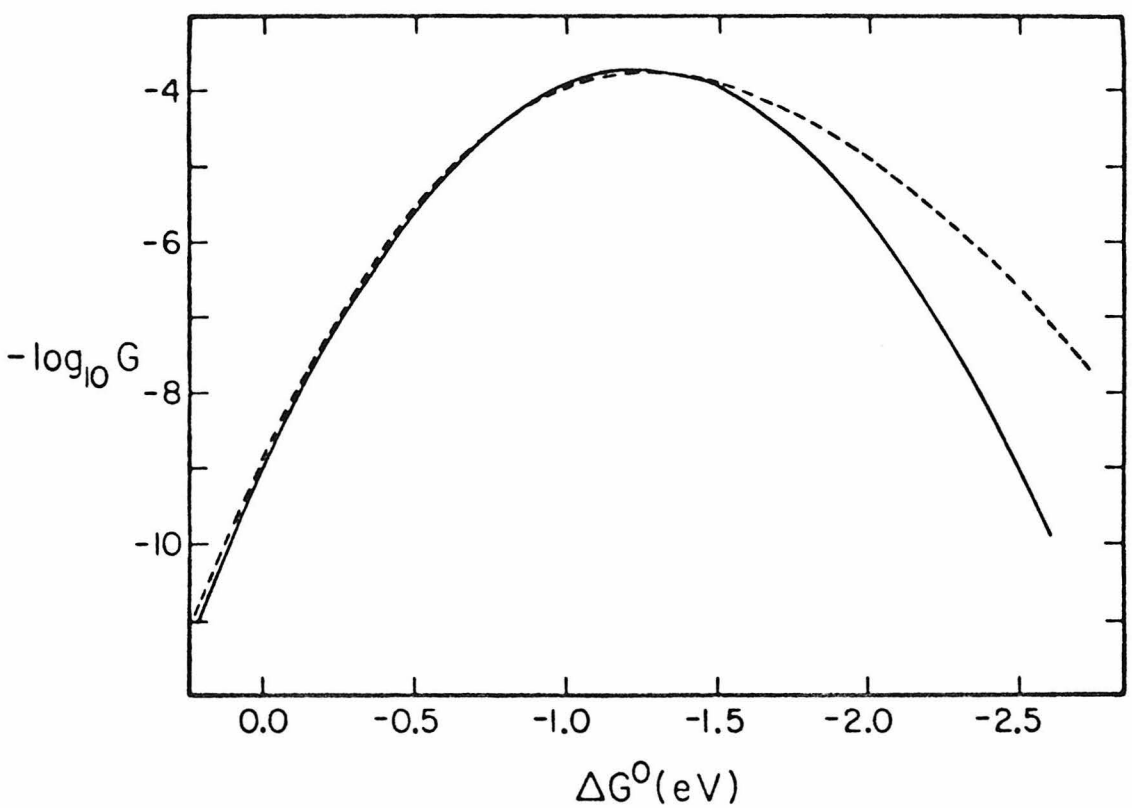

Figure 2. Hypothetical Systems (λ's and frequencies in Table I).

— Classical Franck-Condon Sum, assuming also eq. 3.

-- Quantum Franck-Condon Sum.

Table I: Hypothetical System (Temp. = 300 K)

	$\hbar\omega_{react.}(cm^{-1})$	$\hbar\omega_{prod.}(cm^{-1})$	λ(kJ/mol)
internal modes	494	357	35
	357	494	18
solvent modes	170	170	48
	1	1	25

Table II: Comparison of Quantum and Semiclassical Franck-Condon Sums, [a] - $\log_{10}$ G.

System	$\Delta G°$(eV)	Quantum	Semiclassical
Model [b] $M(bpy)_3^{3+/2+}$	0.5	12.2	9.4
	0.0	6.3	5.7
	-0.5	3.8	3.9
	-1.0	3.0	4.0
	-1.5	5.6	6.1
	-2.0	8.0	10.1
Hypothetical [c]	0.5	13.9	12.7
	0.0	8.8	8.3
	-0.5	5.5	5.4
	-1.0	4.0	3.9
	-1.5	3.9	3.9
	-2.0	4.9	5.4

[a] G is in cm.

[b] λ_{inner} = 0. λ_{out} = 35.3 kJ/mol at $\hbar\omega_1$ = 170 cm^{-1}, and 18.2 kJ/mol at $\hbar\omega_2$ = 1 cm^{-1}. Temp. = 300 K.

[c] λ's and ω's used are those in Table I.

method which, as discussed in recent papers,[15,16] is valid only when the slope of the products' potential energy curve is extremely steep near its intersection with the reactants' potential energy curve. (Only then is the semiclassical nuclear tunneling distance ac in Figs. 3 and 4 of ref. 16 or Fig. 2 of ref. 15 equal to the effective nuclear tunneling distance ab there.)

The quantum values plotted in Figs. 1 and 2 were calculated both by the direct evaluation of eq 1 and by the saddle-point method described elsewhere.[15,20] The results of the two computations were found to be superimposable, so that the saddle-point approximation is a very good approximation in these common electron-transfer systems. Another approximation - an equivalent single mode approximation - is also available (eq 19 of ref. 16) and has yielded excellent agreement with the quantum results when used within its region of validity (given in eq 21 of ref. 16).

Reactions Having Large Negative Free Energies

Both the classical and the quantum theories described earlier predict that the electron transfer rate will ultimately decrease when ΔG° becomes increasingly negative, i.e., when $-\Delta G^\circ$ exceeds the total λ for the system. The classical theory predicts quadratic dependence in the very negative ΔG° region (cf. Refs. 3 and 4, and also as seen in Figs. 2 and 3). But experimental studies of highly exothermic reactions have shown little or no decrease of the rate constant in the inverted region,[5-8] due to a variety of possible reasons discussed earlier.

We first explore the kinetic effect of formation of products in their lowest electronic state, for reactions of excited $Ru(bpy)_3^{2+}$

with tris-bipyridyl Ru, Os and Cr quenchers, studied experimentally by Creutz and Sutin.[6] The reactions are listed in Table III. Given there are the standard free energies of reaction calculated from the known reduction potentials in Table IV. The reactions consist of electron-transfer quenching of the lowest luminescent excited state of $Ru(bpy)_3^{2+}$ or $Ru(Mebpy)_3^{2+}$, where bpy = 2,2'-bipyridyl , and Mebpy = 4,4' -dimethyl-2,2'-bipyridyl.

The nature of the ruthenium (II) complex excitation - metal to ligand charge transfer[27,28] - contributes a significant internal reorganization energy to the electron transfer reaction. From vibrational progressions in the low-temperature luminescence and absorption spectra of $Ru(bpy)_3^{2+}$, it appears that a high-frequency mode, $\hbar\omega$ = 1300 cm^{-1}, is excited in the luminescing state.[29,30] We have found the associated λ_{inner} to be 1300 $\pm$ 100 cm^{-1} (15.5 $\pm$ 1 kJ/mol) by fitting the following line-shape function to the emission spectrum:

$$\text{Intensity} \propto e^{-x} \frac{x^n}{n!} \qquad (5)$$

where n is the vibrational quantum number in the ground electronic state, and $x = \lambda/\hbar\omega$; $\hbar\omega$ is the frequency of the vibrational mode ($\hbar\omega$ = 1300 cm^{-1} in the present case). Eq 5 gives the square-overlap of the lowest single-mode harmonic oscillator state of the electronically excited state with the nth vibrational state of the lowest electronic state of the ruthenium (II) complex, when both states

Table III: Creutz and Sutin Reactions[6]

$$*RuL_3^{2+} + ML'_3{}^{3+} \xrightarrow{k_{obs}} RuL_3^{3+} + ML'_3{}^{2+}$$

Reaction[a]	M	L	L'	$\Delta G°$ (eV)	$\Delta G°*$[b] (eV)
1	Cr	bpy	bpy	-0.57	1.19
2	Cr	Mebpy	bpy	-0.83	0.93
3	Os	bpy	bpy	-1.66	0.1
4	Os	Mebpy	bpy	-1.78	-0.02
5	Ru	bpy	Mebpy	-1.96	-0.20
6	Ru	Mebpy	Mebpy	-2.07	-0.31
7	Ru	bpy	bpy	-2.09	-0.33

[a] The numbers correspond to the numbered points in Fig. 3

[b] $\Delta G°*$ is the $\Delta G°$ to form the electronically excited state of the RuL_3^{3+}.

Table IV: Reduction Potentials

	Reduction Potential (eV)	Ref.
$Cr(bpy)_3^{3+}$	-0.26	21,22
$Os(bpy)_3^{3+}$	0.82	8
$Ru(Mebpy)_3^{3+}$	1.10	23
$Ru(bpy)_3^{3+}$	1.26	24,25,26

have the same frequency but the equilibrium position of the nth state is displaced relative to that of the zeroth state.[31] Because the vibrational quantum is so large relative to kT (kT = 208.5 cm^{-1} = 2.494 kJ/mol at 300 K) transitions from vibrational states higher than the zeroth need not be considered in the emission equation, eq 5.

In the appendix it is shown that when the emission and absorption line shapes are due to a high-frequency vibration ($\hbar\omega \gg kT$) the Stokes shift is approximately twice λ_{inner} for the transition from electronic ground state to electronic excited state. Using the average of the singlet-triplet absorption maxima at 77 K reported in refs. 27, 28, 30 and 32 (18,300 cm^{-1} with some uncertainty) and the average of the emission maxima at 298 K reported in refs. 7, 23 and 27 (16,200 cm^{-1} with some uncertainty) one obtains $\lambda_{inner} = \frac{1}{2}$ (18,300 - 16,200) cm^{-1} = 1050 cm^{-1} = 12.5 kJ/mol for the ruthenium charge transfer transition. This estimate for λ_{inner} is in fair agreement with the value λ_{inner} = 15.5 kJ/mol obtained above by fitting eq 5 to emission spectra. λ_{inner} = 15.5 kJ/mol will be assumed for the contribution of the $*Ru(bpy)_3^{2+}$ $Ru(bpy)_3^{3+}$ subsystem to the electron transfer reactions in Table III.

The reactant $Ru(bpy)_3^{2+}$ may be in one of three triplet states, but the splitting of these states is small and may be neglected. (In the ruthenium and osmium complexes the lowest excited states are formed by metal A_{1g} to ligand $^3\pi^*$ excitations.) The triplet states have a total splitting of 0.73 kJ/mol in $Ru(bpy)_3^{2+}$, and 0.77 kJ/mol in $Ru(Mebpy)_3^{2+}$.[33] Both of these splittings are small relative to the ΔG^o's of the electron transfer reactions being considered, so that each triplet state may be regarded as essentially a single triply degenerate state. The

splitting of the $Os(bpy)_3^{2+}$ excited state (needed later) is not known, but will be assumed to be negligible when calculating electron transfer rates to form excited products. It has been postulated to be similar to the splitting in $Ru(bpy)_3^{2+}$ excited state.[34]

Except for the high-frequency mode discussed above, the bipyridyl systems undergo negligible internal reorganization during electron transfer.[19,22,35] The outer-sphere reorganization energy is roughly constant throughout the series of reactions. λ_{out} has been estimated as λ_{out} = 54 kJ/mol.[19,35]

The spacing of the lines in the low-temperature (77 K) emission and absorption spectra of $Ru(Mebpy)_3^{2+}$ [29] indicates that a mode for which $\hbar\omega$ = 1300 cm^{-1} is excited in the luminescing state. Fitting the emission intensities to eq 5 yields λ_{inner} = 15.5 kJ/mol for this ruthenium charge transfer transition.

Using λ_{inner} = 15.5 kJ/mol, λ_{out} = 54 kJ/mol, and the $\Delta G°$'s in Table III, we calculated rate constants for the reactions to form ground-state products. In the adiabatic limit the classical rate constant is given by[17] eq 6 when work terms are negligible,

$$k_{et} = Z(4\pi kT\,\lambda)^{\frac{1}{2}}\ G, \qquad (6)$$

where G is the classical Franck-Condon sum given by eq 2, with ΔE replaced by $\Delta G°$, and $\lambda = \sum_j \lambda_j$ is the sum over inner- and outer-sphere λ's. Z is the collision frequency in solution: $\sim 10^{11}$ $M^{-1}s^{-1}$.[2,17,36] For simplicity, the quantum rate constant was assumed to be given by

the same expression (eq 6) but with the quantum Franck-Condon sum (eq 1) used for G. In this way, the quantum expression reduces to the classical in the limit $\hbar \to 0$. Strictly speaking eqs 1 and 2 for the G's (classical and quantum) were derived for nonadiabatic electron transfers.

The classical and quantum rates and the observed rates are plotted in Fig. 3 (solid line for classical, dashed line for quantum). The plotted values are not the electron-transfer rate constants themselves, but rather the rate constants corrected for diffusion[36] k_{obs},

$$k_{obs} = \left(\frac{1}{k_{et}} + \frac{1}{k_d}\right)^{-1} \qquad (7)$$

where k_d is the diffusion limit: $\sim 3.5 \times 10^9$ $M^{-1}s^{-1}$.[6]

The difference between the quantum and the classical calculations in the very negative $\Delta G°$ region is again not negligible, because of the high-frequency internal mode involved in the present reactions, $\hbar\omega = 1300$ cm^{-1}, and the fact that its contribution to λ_{inner} is not negligible. Still, the classical and quantum calculations are in qualitative agreement and <u>neither</u> explains the observed rates in the inverted region, as Fig. 3 demonstrates. The discrepancy would be even greater if a nonadiabaticity factor[2] κ were introduced.

In order to assess the possibility of the electron transfer products being formed in excited electronic states we have calculated quantum mechanically the rates of electron transfer to excited product states. The calculation requires a λ_{inner} for formation

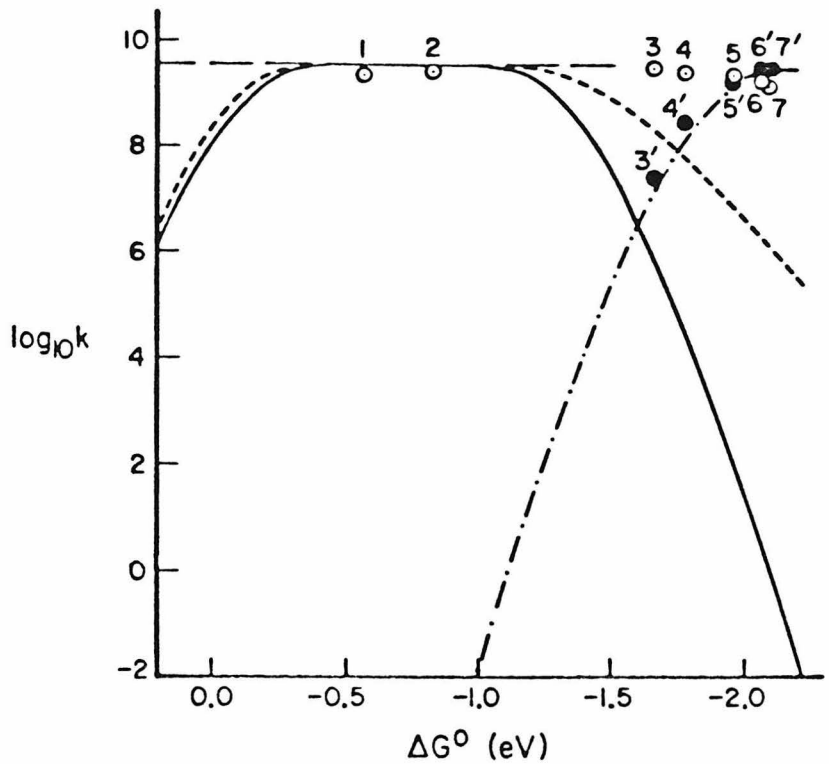

Figure 3. k (calculated and experimental) for bipyridyl systems. $k = (k_{et}^{-1} + k_d^{-1})^{-1}$ with $k_d \simeq 3.5 \times 10^9$ $M^{-1}s^{-1}$. $\Delta G°$ is for formation of ground-state products.

— Classical to ground-state products.

-- Quantum to ground-state products.

-·- Calculated classical rate to *Ru(III) products.

● Calculated quantum rate to *Ru(III) products.

⊙ Experimental rate constant.

The numbers correspond to the numbers in Table III. Primes indicate calculated rates to excited-state products. λ_{out} = 54 kJ/mol. λ_{inner} = 15.5 kJ/mol. Temp. = 300 K. Ru(III) excitation energy = 1.76 eV.

of these products. The emission and absorption spectra of $Os(bpy)_3^{2+}$ [37] indicate that a 1300 cm^{-1} mode is involved in the transition to its luminescing state, with λ_{inner} = 9.0 kJ/mol ($\hbar\omega$ was obtained from the spacing of the lines in the emission spectrum, λ_{inner} was obtained by fitting the intensities to eq 5). Quantum mechanical calculations for the reactions involving quenching by $Os(bpy)_3^{3+}$ indicate that formation of electronically-excited $Os(bpy)_3^{2+}$ product is less favorable than formation of excited ruthenium (III) products, so formation of electronically-excited $Os(bpy)_3^{2+}$ is not considered further. The effect on λ_{inner} of forming electronically-excited rutheinium (III) in the reactions of Table III is not known, so λ_{inner} for reactions to form excited-state ruthenium (III) products is taken to be the same as the λ_{inner} for formation of electronic-ground-state products; λ_{inner} = 15.5 kJ/mol.

The excitation energies in Table V were used, together with the reduction potentials of Table IV, to yield the $\Delta G°$'s (Table III) for formation of electronically-excited ruthenium (III) products. The three reactions involving quenching of excited ruthenium (II) by ruthenium (III) appear to proceed more favorably to an excited ruthenium (III) product than to the ground-state. The quantum mechanically calculated rates to excited ruthenium (III) are indicated by solid circles in Fig. 3, and are in good agreement with experiment (open circles) for the three reactions involving ruthenium (III) quenchers (points labelled 5, 6, 7 and 5′, 6′, 7′).

Table V: Excitation Energies

	$E_{0 \leftarrow 0}$ (eV)	Ref.
$Cr(bpy)_3^{2+}$	1.05 ± 0.1[a]	38,39
$Os(bpy)_3^{2+}$	1.78 ± 0.01	27,32,37
$Ru(bpy)_3^{2+}$	2.12 ± 0.02	22,23,27,29,30,32,40
$Ru(Mebpy)_3^{2+}$	2.06 ± 0.02	23,29
$Ru(bpy)_3^{3+}$	1.76 ± 0.07[b]	6
$Ru(Mebpy)_3^{3+}$	1.76[c]	

[a]The large uncertainty is due to estimating $E_{0 \leftarrow 0}$ from the absorption spectrum alone.

[b]The large uncertainty is due to estimating $E_{0 \leftarrow 0}$ from the absorption spectrum alone (maximum at 1.83 eV[6]), assuming a Stokes shift $\leq$ 2300 cm^{-1} = 0.07 eV.

[c]Estimated from $E_{0 \leftarrow 0}$ for $Ru(bpy)_3^{3+}$.

In the case of quenching of excited ruthenium (II) by the chromium (III) complex there is good agreement between the quantum mechanically calculated values and the experimental values if the electronic ground state of the ruthenium (III) complex is the product (points 1 and 2 in Fig. 3). Thus, the alternate pathway of forming an electronically-excited ruthenium (III) complex would not be expected to be important and indeed is calculated to be slower than formation of ground-state ruthenium (III) by 22 and 16 orders of magnitude for reactions 1 and 2, respectively.

In the case of the two reactions involving quenching by the osmium (III) complex, the quantum mechanically calculated rate for formation of excited ruthenium (III) products was found to be little or no faster than for the formation of ground-state products (cf. points 3′ and 4′ in Fig. 3 with the dashed line). The calculated (quantum) rate constants for formation of ground-state products are two and three orders of magnitude below the observed rate constants. In view of the approximations in the theory, this discrepancy may not be a conclusive one.

Alternatively, unless some not yet known low-lying electronically-excited product state exists, quenching by the osmium complex may proceed via another mechanism. For example, H-atom transfer followed by proton exchange with the solvent is a possibility. A third possibility is described later in this section.

To allow comparison, we have also calculated classically the rate constants for electron transfer to form electronically-excited ruthenium (III) products. The same λ's and ΔG°'s were used as for the quantum calculations discussed above. The classical

rates to excited products are shown in Fig. 3 by the 'dash-dot' line and agree well with the quantum (solid circles) values. We note that excited-state formation corresponds to the normal free energy region, while ground-state product formation lies in the inverted region.

There is a third possible explanation for the large rate constants observed for reactions 3 and 4 in Fig. 3 (reaction of two electronically-excited ruthenium (II) complexes with the osmium (III) complex). The distance between the centers of the reactants in the activated complex, r, may, in this case of an electronically-excited reactant, be greater than the distance of closest approach. The distance of closest approach equals $a_1 + a_2$ where a_1 and a_2 are the radii of the two reactants. The value of the outer-sphere reorganization energy used in the rate-constant calculations above ($\frac{1}{4}\lambda_{out}$ = 13.4 kJ/mol) was calculated using the classical expression[1] for λ_{out} (eq 8) and assuming $r = a_1 + a_2$.[6]

$$\lambda_{out} = (\Delta e)^2 \left(\frac{1}{\epsilon_{op}} - \frac{1}{\epsilon_s}\right)\left(\frac{1}{2a_1} + \frac{1}{2a_2} - \frac{1}{r}\right) \qquad (8)$$

In eq 8, Δe is the change in charge of a reactant, ϵ_{op} is the optical dielectric constant, and ϵ_s is the static dielectric constant of the solvent. If r were greater than $a_1 + a_2$, then the outer-sphere reorganization energy would be calculated to be greater than 13.4 kJ/mol, as may be seen from eq 8: The reactions in which $Os(bpy)_3^{3+}$ quenches electronically excited ruthenium (II) complexes to form ground-electronic-state ruthenium (III) (reactions 3 and 4 of Table III) have large negative free energies, and they lie in the 'inverted region'. In this case increasing r and hence increasing λ_{out} has, as is seen from eq 2, the effect of

increasing the calculated electron transfer rate. At least, it has this effect of rate enhancement if the reactions do not become too nonadiabatic at the larger r.

Indeed, if $r = 1.3(a_1 + a_2)$ and $a_1 \simeq a_2$, then the quantum-mechanically calculated rate constants (corrected for diffusion according to eq 7) for the electron-transfer reaction between $^*Ru(bpy)_3^{2+}$ and $^*Ru(Mebpy)_3^{2+}$ and $Os(bpy)_3^{3+}$ (reactions 3 and 4 of Table III), are $k_3 = 8 \times 10^8\ M^{-1}s^{-1}$ and $k_4 = 3 \times 10^8\ M^{-1}s^{-1}$, respectively. These values are within an order of magnitude of the experimental values obtained by Creutz and Sutin;[6] $k_3 \simeq 3.2 \times 10^9\ M^{-1}s^{-1}$ and $k_4 \simeq 2.6 \times 10^9\ M^{-1}s^{-1}$. If $r = 2(a_1 + a_2)$ and $a_1 \simeq a_2$, the quantum-mechanically calculated values of the rate contants are $k_3 = 2 \times 10^9\ M^{-1}s^{-1}$ and $k_4 = 1 \times 10^9\ M^{-1}s^{-1}$; essentially in agreement with the experimental values. These calculations were performed using the same numerical values for the quantities other than λ_{out} as were used in the calculations described above that yielded the (dashed line) quantum values in Fig. 3. However, electron transfer at too large an r makes the reaction increasingly nonadiabatic and then reduces the reaction rate. The appropriate r is the one which achieves a maximum rate.

At least in the Creutz and Sutin systems, it appears that the lack of significant inverted behavior is indicative either (a) of the third possibility above or (b) of alternate reaction pathways becoming competitive at large negative ΔG^o's, rather than (c) of nuclear tunneling. Nuclear tunneling due to the very high-

frequency modes involved in transitions from the electronically excited reactants is a significant effect at very large negative ΔG^{o}'s, but does not explain the lack of inverted behavior, as one sees from the dashed line in Fig. 3.

Conclusion

Rate calculations for a hypothetical system and for the bipyridyl systems studied by Creutz and Sutin suggest that quantum effects are expected to be small in the normal region (i.e., for small to moderate ΔG^{o}'s) even for systems having fairly large internal frequencies. At large negative ΔG^{o}'s, quantum effects may frequently be significant. For most of the reactions considered in the 'inverted' region, the calculated and experimental results agree within an order of magnitude, provided that electronically-excited products are formed. An alternate atom transfer pathway may occur in reactions where the calculated rate constant for an electron transfer is appreciably less than the experimental one in this 'inverted' region. A third possibility of electron transfer at a larger distance is also considered.

Appendix. Relation between λ and the Stokes shift.

We consider the case where excitation of a single harmonic vibrational mode is responsible for the emission and absorption line-shapes. We define $X \equiv \lambda/h\nu$, where $\frac{1}{4}\lambda$ is the inner-sphere reorganization energy for the transition from the electronic ground-state to the

luminescing state, and ν is the frequency of the mode. (ν is assumed to be the same in both electronic states.)

We assume for brevity that $h\nu \gg kT$, and then luminescence will occur from essentially only the lowest vibrational level in the electronically-excited state. Eq 5 gives the emission line-shape as

$$I_e(\ell) \propto e^{-X} X^{\ell}/\ell! \qquad \text{(A1)}$$

where ℓ is the quantum number of the vibrational level in the ground electronic state to which luminescence occurs. The energy of the corresponding quantum emitted is $E_{o\leftarrow o} - \ell h\nu$, where $E_{o\leftarrow o}$ is the electronic-excitation-energy of the luminescing state relative to the ground state. The energy E_e of this quantum at the emission maximum is

$$E_e = E_{o\leftarrow o} - \ell^* h\nu \qquad \text{(A2)}$$

where ℓ^* is the value of ℓ which maximizes (A1), $\ell^* = X$.

Similarly, since $h\nu >> kT$, absorption occurs essentially only from the lowest vibrational level in the electronic ground state, so the absorption intensity is

$$I_a(m) \propto e^{-X} X^{m}/m! \qquad \text{(A3)}$$

where m is the vibrational quantum number of an electronically-excited vibronic level to which absorption occurs. $I_a(m)$ is maximized with respect to m, and the energy E_a of the absorption maximum is

$$E_a = E_{0\leftarrow 0} + m^*h\nu \qquad (A4)$$

where m^* is found by maximization of (A3) to equal X.

The Stokes shift is $E_s = E_a - E_e$.[41] From eqs A2 and A4 we have

$$E_s = (m^* + \ell^*)h\nu = 2Xh\nu \qquad (A5)$$

But $X = \lambda/h\nu$, so

$$E_s = 2\lambda \qquad (A6)$$

Eq A6 is a well-known approximate formula (e.g., ref. 4b). A simple classical derivation is given in ref. 42. Eq A6 can also be obtained from the quantum mechanical theory of optical spectra in solids given in ref. 43.

References

(1) R. A. Marcus, Discussions Faraday Soc. 1960,29,21.

(2) R. A. Marcus, J. Chem. Phys. 1965,43,2654.

(3) R. P. Van Duyne and S. F. Fischer, Chem. Phys. 1974,5,183.

(4) (a) J. Ulstrup and J. Jortner, J. Chem. Phys. 1975, 63,4358.

(b) N. Kestner, J. Logan, and J. Jortner, J. Phys. Chem. 1974,78,2148.

(5) D. Rehm and A. Weller, Israel J. Chem. 1970,8,259.

(6) C. Creutz and N. Sutin, J. Am. Chem. Soc. 1977,99,241.

(7) B. Ballardini, G. Varani, M. T. Indelli, F. Scandola, and V. Balzani, J. Am. Chem. Soc. 1978,100,7219.

(8) V. Balzani, F. Bolletta, M. T. Gandolfi, and M. Maestri, Topics Current Chem. 1978,75,1.

(9) S. Efrima and M. Bixon, Chem. Phys. Letters 1974,25,34 and Chem. Phys. 1976,13,447.

(10) R. A. Marcus and N. Sutin, Inorg. Chem. 1975,14,213.

(11) W. Schmickler, J. Chem. Soc. Faraday Trans. 2 1975, 72,307.

(12) R. R. Dogonadze, A. M. Kuznetsov, and M. A. Vorotyntsev, Z. Phys. Chem. N. F. 1976,100,1.

(13) (a) A. Weller and K. Zachariasse, Chem. Phys. Letters 1971,10,590.

(b) J. Joussot-Dubien, A. C. Albrecht, H. Gerischer, R. S. Knox, R. A. Marcus, M. Schott, A. Weller, and F. Willig, "Light-Induced Charge Separation in Biology and Chemistry," H. Gerischer and J. J. Katz, Eds., Berlin: Dahlem Konferenzen, October 16-20,1978 (Verlag Chemie, New York, 1979) pp. 129-149.

(14) P. P. Schmidt, Spec. Per. Rep. Electrochem. 1975,5,21

and; J. Ulstrup, "Charge Transfer Processes in Condensed Media," Lecture Notes in Chemistry, No. 10 (Springer, New York, 1979); and many references cited in these reviews.

(15) P. Siders and R. A. Marcus, J. Am. Chem. Soc. 1981,103,741.

(16) R. A. Marcus in "Oxidases and Related Redox Systems," T. E. King, M. Morrison, and H. S. Mason, Eds., (Pergamon, Oxford, 1982) pp. 3-19.

(17) R. A. Marcus, J. Chem. Phys. 1965,43,679.

(18) (a) J. J. Hopfield, Proc. Nat. Acad. Sci. USA 1974,71,3640;

(b) J. J. Hopfield in "Tunneling in Biological Systems," B. Chance, D. C. DeVault, H. Frauenfelder, J. R. Schrieffer, and N. Sutin, Eds., (Academic, New York, 1979);

(c) J. J. Hopfield in "Electrical Phenomena at the Biological Membrane Level," E. Roux, Ed., (Elsevier, Amsterdam, 1977) p.471;

(d) This method was originally designed for spectral line-shape problems, e.g., M. Lax, J. Chem. Phys. 1952,20,1752; and D. Curie, "Luminescence in Crystals," (Wiley, New York, 1963) pp. 47 ff.

(19) N. Sutin in "Tunneling in Biological Systems," B. Chance, D. C. DeVault, H. Frauenfelder, J. R. Schrieffer, and N. Sutin, Eds., (Academic, New York, 1979).

(20) E. Buhks, M. Bixon, J. Jortner, and G. Navon, Inorg. Chem. 1979,18,2014.

(21) B. Baker and D. Mehta, Inorg. Chem. 1965,4,848.

(22) B. Brunschwig and N. Sutin, J. Am. Chem. Soc. 1978,100,7568.

(23) C.-T. Lin, W. Bottcher, M. Chou, C. Creutz, and N. Sutin, J. Am. Chem. Soc. 1976,98,6536.

(24) J. Miller and R. Prince, J. Chem. Soc. 1966,A,1048.

(25) F. Lytle and D. Hercules, Photochem. Photobiology 1971,13,123.

(26) T. J. Meyer, Israel J. Chem. 1977,15,200.

(27) C.-T. Lin and N. Sutin, J. Phys. Chem. 1976,80,97.

(28) G. Navon and N. Sutin, Inorg. Chem. 1974,13,2159.

(29) G. Hager and G. Crosby, J. Am. Chem. Soc. 1975, 97,7031.

(30) D. Klassen and G. Crosby, J. Chem. Phys. 1968, 48,1853.

(31) D. Heller, K. Freed, and W. Gelbart, J. Chem. Phys. 1972,56,2309.

(32) F. Zuloago and M. Kasha, Photochem. Photobiology 1968,7,549.

(33) G. Hager, R. Watts, and G. Crosby, J. Am. Chem. Soc. 1975,97,7037.

(34) K. Hipps and G. Crosby, J. Am. Chem. Soc. 1975,97,7042.

(35) G. Brown and N. Sutin, J. Am. Chem. Soc. 1979,101,883.

(36) R. A. Marcus, J. Phys. Chem. 1968,72,891.

(37) G. Crosby, D. Klassen, and S. Sabath, Mol. Cryst. 1966,1,453.

(38) E. König and S. Herzog, J. Inorg. Nucl. Chem. 1970,32,585.

(39) I. Fujita, T. Yazaki, Y. Torii, and H. Kobayashi, Bull. Chem. Soc. Japan 1972,45,2156.

(40) J. Demas and G. Crosby, J. Am. Chem. Soc. 1971,93,2841.

(41) A. W. Adamson and P. D. Fleischauer, "Concepts of Inorganic Photochemistry," (Wiley, New York, 1975) p. 26.

(42) C. C. Klick and J. H. Schulman, Solid State Physics 1957,5,97.

(43) K. Maeda, Phys. Chem. Solids 1959,9,335.

CHAPTER 3

FURTHER DEVELOPMENTS IN ELECTRON TRANSFER

Some time ago it was predicted (1, 2) that, in a series of weak-overlap electron transfer reactions, the rate would first increase when ΔG^o was made more negative, and then, when ΔG^o became very negative, eventually decrease. Evidence for such an 'inverted effect' has been given in a number of papers (3-11), but in many other studies the reaction rate reaches a limiting value, rather than a decreasing value, when $-\Delta G^o$ becomes large (e.g., (12-18)). Possible explanations for the latter result have been suggested: (a) alternate pathways for the reaction when ΔG^o is very negative [such as H-atom transfer (19, 20), electronically-excited product states (11, 20), or, when the reaction was observed via quenching of fluorescense, exciplex formation (21, 22)], (b) quantum mechanical nuclear tunneling (20, 23-27), (c) masking by diffusion, and (d) reduction of the inverted effect [by electron transfer over a distance (19)].

Quantum mechanical tunneling reduces the magnitude of the predicted effect but does not eliminate it in weak-overlap systems, as one sees, for example, in some recent calculations for an actual experimental system (20). Moreover, there is a 1:1 correspondence between the quantum mechanically calculated charge transfer spectrum (emission or absorption vs hν) for a weak overlap redox system and the plot (eq 8 and 9 given later) of k_{act} versus the energy of reaction, ΔE (25), and hence in a series of reactions of given ΔS^o, versus $-\Delta G^o$. Here, k_{act} is the activation-controlled quantum mechanically calculated rate constant. Thus, the well-known existence of a maximum in the charge transfer vs wavelength spectrum implies that there will be a maximum in the $\ln k_{act}$ vs $-\Delta G^o$ plot when the electron transfer is a weak-overlap reaction. This correspondence removes any question that nuclear tunneling would eliminate the inversion, since that tunneling occurs to the same extent in both the charge transfer spectrum and the k_{act} vs $-\Delta G^o$ plots, and the former has a well-known maximum. It also removes any argument that large anharmonicities in practice eliminate the effect: the correspondence applies regardless of whether the vibrations are harmonic or anharmonic, as long as the electron transfer is a weak-overlap one. (The effects of having a very strong-overlap electron transfer remain to be investigated.)

In a recent paper, an approximate calculation was made of effects (b) to (d) above (19), using an approximate analytical solution for the diffusion problem, for the case where the reaction occurs readily over a short range of separation distances of the reactants. In the present report, we summarize the results of our recent calculations on a numerical solution of the same problem. A more complete description is given elsewhere (28). One additional modification made here to (19) is to ensure that the current available rate constant data at $\Delta G^o = 0$ (Appendix) are satisfied.

Theory

The diffusion-reaction equation for the pair distribution function g(r,t) of the reactants, which react with a rate constant which at any r is k(r), is given by (29-32)

$$\frac{\partial g(r,t)}{\partial t} = \frac{1}{r^2}\frac{\partial (r^2 J_r)}{\partial r} - k(r)g(r,t) \tag{1}$$

where J_r is the inward radial flux density (per unit concentration) due to diffusion and to any forced motion arising from an interaction potential energy, U(r), assumed to depend only on the separation distance r. The magnitude of J_r is given by

$$J_r = D\frac{\partial g}{\partial r} + \frac{Dg}{k_B T}\frac{dU}{dr}$$

$$\equiv De^{-U/k_B T}\frac{\partial}{\partial r}\left(ge^{U/k_B T}\right) \tag{2}$$

where D is the sum of the diffusion constants of the two reactants.

The observed rate constant, k_{obs}, at time t is then given by (31, 33)

$$k_{obs} = \int_0^\infty k(r)g(r,t)4\pi r^2\, dr \tag{3}$$

The steady-state solution to eq 1 satisfies $\partial g/\partial t = 0$, i.e., it satisfies

$$(1/r^2)d(r^2 J_r)/dr = k(r)g(r) \tag{4}$$

For the experimental conditions investigated thus far, the steady-state solution is an excellent approximation to the solution of eq 1 and we consider this case. However, in proposing some experiments in the picosecond regime to enhance the chance of observing the inverted effect, we consider the time-dependent equation 1.

The rate constant k(r) is typically assumed to depend exponentially on r, varying as $\exp(-\alpha r)$. Theoretical estimates have been made for α of 1.44 Å^{-1} when there is intervening material between the reactants (34), and 2.6 Å^{-1} when there is not (35). A recent calculation for the hexaaquoiron self-exchange reaction yielded α = 1.8 Å^{-1} (36). Experimentally, the value inferred indirectly for an electron transfer between aromatic systems in rigid media is about 1.1 Å^{-1} (37).

These values of α are sufficiently large that k(r) falls off rapidly with r. When this "reaction distance" is small relative to the distance over which the function $h(r) = g \exp(U/k_B T)$ changes significantly, i.e., over which $(h(r) - h(\sigma))/(h(\infty) - h(\sigma))$ becomes appreciable, one can introduce an approximate analytic solution to eq 4 (28, 38, 39):

$$\frac{1}{k_{obs}} = \frac{1}{k_{act}} + \frac{1}{k_{diff}} \tag{5}$$

where, in the present case, we have (from eq 3 with $g(r) \equiv 0$ for $r < \sigma$)

$$k_{act} = \int_{\sigma}^{\infty} k(r) e^{-U/k_B T} 4\pi r^2 \, dr \tag{6}$$

and where (40)

$$k_{diff} = 4\pi D / \int_{\sigma}^{\infty} \frac{e^{U/k_B T}}{r^2} dr \tag{7}$$

Equation 5 was actually derived for the case where reaction occurs at some contact distance $r = \sigma$. A derivation of eq 5 for the present case of a volume distributed rate constant $k(r)$ is approximate and is given elsewhere (28).

For $k(r)$ we shall assume at first, as in (19), that the reaction is adiabatic at the distance of closest approach, $r = \sigma$, and that it is joined there to the nonadiabatic solution which varies as $\exp(-\alpha r)$. The adiabatic and nonadiabatic solutions can be joined smoothly. For example, one could try to generalize to the present multi-dimensional potential energy surfaces, a Landau-Zener type treatment (41). For simplicity, however, we will join the adiabatic and nonadiabatic expressions at $r = \sigma$. We subsequently consider another approximation in which the reaction is treated as being nonadiabatic even at $r = \sigma$.

The well-known perturbation theory expression for the non-adiabatic rate constant is given by (25, 42-45)

$$k(r) \cong \frac{2\pi}{\hbar} |V(r)|^2 \, (F.C.) \tag{8}$$

where (F.C.) is the Franck-Condon factor and $V(r)$ is the electronic matrix element for the electron transfer. (F.C.) is given by

$$(F.C.) = \frac{1}{Q} \Sigma_{i,f} e^{-E_i/k_B T} |\langle i|f\rangle|^2 \delta(E_f - E_i + \Delta E) \tag{9}$$

where i and f denote initial and final (reactants' and products') nuclear configuration states, including those of the solvent; ΔE is the energy of reaction; and Q is $\Sigma_i \exp(-E_i/k_B T)$. The solvent will be treated classically (1) to avoid the quantum harmonic oscillator treatment of the polar solvent which is sometimes used. (The latter yields a large error for ΔS^o when ΔS^o is large (46)). The contribution of the polar solvent to the Franck-Condon factor is (42, cf. 1)

$$(F.C.)_{solvent} = (4\pi\lambda_{out} k_B T)^{-\frac{1}{2}} \exp[-(\Delta G^{o''} + \lambda_{out})^2 / 4\lambda_{out} k_B T] \tag{10}$$

where $\Delta G^{o''} = \Delta G^o + E_f^v - E_i^v$ and the superscript v denotes (inner shell) vibrational energy.

The matching of the adiabatic and nonadiabatic expressions for k(r) at r = σ yields a value for V(σ) given by (28)

$$\frac{2\pi}{\hbar} |V(\sigma)|^2 (4\pi\lambda k_B T)^{-\frac{1}{2}} \sim 10^{13}\ s^{-1} \qquad (11)$$

and, for a reorganization parameter λ of about 70 kJ/mol, yields $|V(\sigma)| \sim 0.023$ eV. This value and

$$|V(r)|^2 = |V(\sigma)|^2 \exp[-\alpha(r - \sigma)] \qquad (12)$$

were introduced into eq 8 as our first approximation to V(r).

The series of electron transfer reactions (14) for which we calculated rate constants involve quenching of the lowest excited electronic state of $Ru(bpy)_3^{2+}$. This *Ru(II) state is a metal-to-ligand charge-transfer state (47, 48) in which an excess electron appears to be localized on one of the bipyridyl ligands (49), and this electron may be transferred to a metal-centered orbital on the oxidant, at least when an unexcited oxidant is formed. A calculation of the distance dependence of V(r) for this particular transfer would be desirable, but lacking that the simple exponential form indicated in eq 12 has been used instead.

The actual numerical integration of eqs 2 and 4 was performed by converting eq 4 to a pair of ordinary differential equations, then using a standard integration routine (50) for integrating the latter, integrating outward from r = σ to large r until g(r) had its correct functional value at large r, $g(r) \sim 1 - c/r$ where c is a constant. (This functional form is the solution of eqs 2 and 4 at r large enough that k(r) = U(r) = 0 and for U vanishing more rapidly than 1/r.) Because g(σ) was unknown to a multiplicative constant initially, we actually performed the integration for a function $G(r) = g(r)c_1$, with c_1 unknown and with a preassigned value for G(r) at r = σ. The terms c_1 and c could be determined from the numerical values of G at large r, and then $g(r) = G(r)/c_1$. The value of k_{obs} was calculated from the total flux at r = ∞:

$$k_{obs} = 4\pi D \lim_{r\to\infty} \left(r^2 \frac{dg}{dr}\right) = 4\pi D c \qquad (13)$$

Results

Calculations were performed for the system studied by Creutz and Sutin (9)

$$*Ru(II)bpy_3 + M(III)bpy_3 \rightarrow Ru(III)bpy_3 + M(II)bpy_3 \qquad (14)$$

where the bpy's are various bipyridyls, M is one of several metals, and the asterisk denotes an electronically-excited molecule. The question we address is how, for a model which has the 'experimental' rate constant at $\Delta G^o = 0$ ($k_{obs} \sim 4 \times 10^8\ M^{-1}s^{-1}$) (Appendix) and the observed diffusion-limited rate constant ($k_{diff} \sim 3.5 \times 10^9\ M^{-1}s^{-1}$) (9), do the values predicted for k_{obs} at quite negative ΔG^o's compare with those calculated from eq 5 and with the experimental results? Is the effect of electron transfer over a range of distances sufficiently large to explain the observed results (i.e., very little fall-off of rate constant with increasing $-\Delta G^o$'s)?

We use a λ_{in} of 15.5 kJ/mol associated with a frequency of 1300 cm^{-1} (20), and λ_{out} of 54 kJ/mol at $r = \sigma$ (51). All calculations were performed with T = 298K. The dependence of λ_{out} on r (2) is incorporated in the calculation. An equilibrium Debye-Hückel expression for the ion-atmosphere-shielded Coulombic repulsion of the reactants is assumed (52, 53), given by

$$U(r) = \frac{z_1 z_2 e_o^2}{\varepsilon r} \frac{e^{\kappa a}}{(1 + \kappa a)} e^{-\kappa r} \qquad (15)$$

for the case where the two reactants have the same radius. Here, κ is the reciprocal of the Debye-Hückel screening length, ε is the static dielectric constant, the $z_i e_o$ values are the ionic charges of the reactants, and a is the distance of closest approach of the ions in the ion atmosphere to a reactant ion. The distance a is $r_i + r_a$, where r_i is the radius of a reactant ion and r_a is the radius of the principal ion of opposite sign in the ionic atmosphere. When $r_i \geq r_a$, a lies between $2r_i$ and r_i, being $2r_i$ when $r_i = r_a$ and being r_i when $r_a = 0$. Using the current approximate radii we shall, for concreteness, take $a = 3\sigma/4$. (In eq 15 the reactants are assumed to have the same radius. A more general expression than eq 15 is cited in ref. 28). At the prevailing ionic strength of about 0.52 M, κ^{-1} is about 4.2 Å. Because of this large ionic strength, U(r) is quite small, even at $r = \sigma$.

Using $\alpha = 1.5$ $Å^{-1}$ and, at first, $V(\sigma) = 0.023$ eV, k_{act} at $\Delta G^o = 0$ is found to be 1.2×10^{10} $M^{-1}s^{-1}$ which is substantially higher than the current experimental value (Appendix) of ca 4×10^8 $M^{-1}s^{-1}$. Assuming the validity of the latter, either $V(\sigma)$ is less than 0.023 eV, i.e., the reaction is not adiabatic at the contact distance $r = \sigma$, or λ is higher than estimated, or eq 15 underestimates U(r). We consider first using a different $V(\sigma)$, namely, 0.0045 eV, which yields the current "experimental" rate constant at $\Delta G^o = 0$. (The same final results for the ln k_{obs} vs ΔG^o plot would be obtained, essentially, if one used instead a different $U(\sigma)$, as long as there is agreement of k_{act} at $\Delta G^o = 0$.)

The numerical solution of eq 4 and the rate constant data of Figure 1 agree at the data's maximum (~3.5×10^9 $M^{-1}s^{-1}$) when one chooses 3.0×10^{-6} cm^2s^{-1} for the sum of the D's of the two reactants. This D is somewhat near those estimated rather indirectly (electrochemically) for the individual D's of ferric and ferrous phenanthroline complexes (~1.9×10^{-6} and 3.7×10^{-6} cm^2s^{-1}, respectively) (54).

Since reaction may also yield electronically-excited products when ΔG^o is sufficiently negative, we include this reaction, as we did in (20). The mean excitation energy used for the formation of the electronically-excited Ru(III) product is 1.76 eV (20). As has been explained elsewhere (20, 28), the formation of the other possible electronically excited products

is, in most cases at least, less probable. The same V(r) was used for formation of electronically excited $Ru(bpy)_3^{3+}$ as for formation of other products because the detailed information necessary to make a distinct estimate for V(r) was lacking.

We first compare the present numerical results for the solution of the steady-state eqs 3 and 4 with the approximate solution given by eqs 5, 6 and the experimental value for k_{diff}. The results agreed to about three percent when ΔG^o was varied from +0.6 to -3.0 eV. The experimental value for k_{diff} and eq 7 imply a value of $D = 3.5 \times 10^{-6}$ $cm^2 s^{-1}$, compared with the 3.0×10^{-6} $cm^2 s^{-1}$ found when eqs 3 and 4 were solved. Had the same D been used for both the exact (eqs 3, 4) and the approximate (eq 5) solutions, their agreement for the rate constants would have been about 10% instead of 3%, which is still very close.

The results of solving eqs 3 and 4 are next compared with the experimental data in Figure 1 (9), using $V(\sigma) = 0.0045$ eV. The solid line refers to the formation of ground state products, and the dotted line to the formation of an electronically-excited Ru(III) product. For further comparison with the solid line, a calculation was made with λ_{out} held fixed (54 kJ/ mol, the value at $r = \sigma$) and is given by the dash-dot line. In order to obtain agreement with the solid line at $\Delta G^o = 0$, $V(\sigma)$ was reduced to 0.0039 eV in calculating the dash-dot line. The dashed line is the result of a calculation (20) in which reaction was treated as occurring adiabatically, but only at some contact distance σ, and in which eq 5 was used, together with the experimental value for k_{diff}. The λ_{out} value used for this last curve was again 54 kJ/mol, the present $\lambda_{out}(\sigma)$.

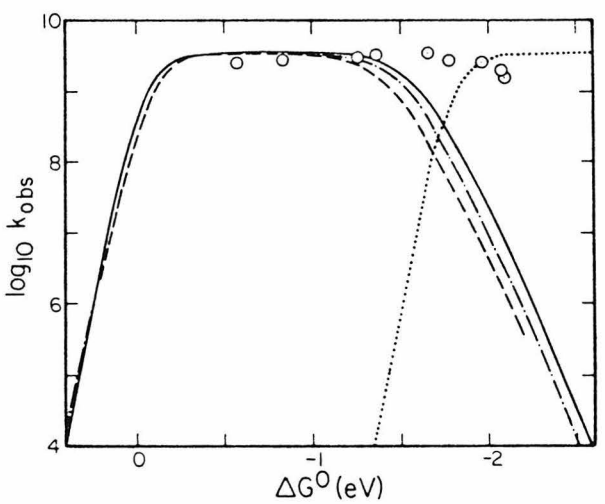

Figure 1. Calculated and experimental rate constants for Reaction 14 vs. ΔG°. Key: ——, r-dependent λ_{out}; — · —, fixed λ_{out}; – – –, from Ref. 1 in which reaction occurred only at $r = \sigma$; and · · ·, current result (r-dependent λ_{out}) for formation of an electronically excited product.

In Figure 2 we give a comparison of the solid line of Figure 1 with that obtained using $V(\sigma)$ = 0.023 eV and a larger λ ($\lambda_{out}(\sigma)$ = 83 kJ/mol). A slightly smaller D (2.7 x 10^{-6} cm^2s^{-1}) was required to make the latter calculation yield the experimental value of the maximum observed rate constant, 3.5 x 10^9 $M^{-1}s^{-1}$. Both curves have the same k_{obs} at ΔG^o = 0.

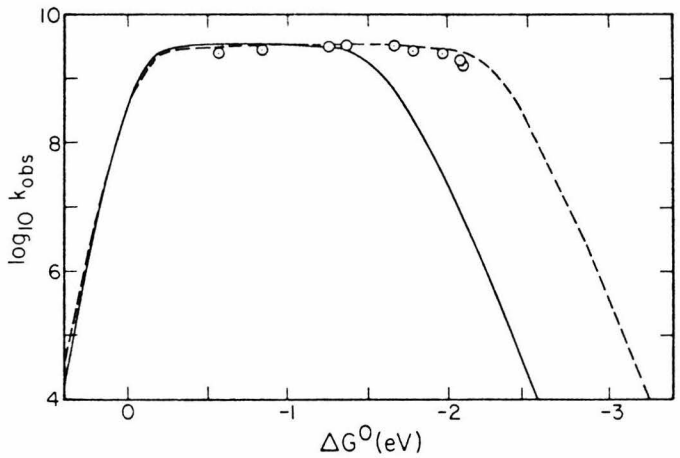

Figure 2. Calculated rate constants for Reaction 14 vs. $\Delta G°$. Key: ——, taken from solid line in Figure 1, $V(\sigma) = 0.0045$ eV, $\lambda_{out}(\sigma) = 54$ kJ/mol; and – – –, $V(\sigma) = 0.023$ eV and $\lambda_{out}(\sigma) = 83$ kJ/mol.

Discussion

The results comparing the exact eqs 3 and 4 with the approximate eqs 5 and 6 show that the latter provide a good approximation for the present conditions, at least. The results in Figure 1 show that, to account for the experimental results at very negative ΔG^o's using the present value of λ_{out} (54 kJ/mol), it is necessary to postulate the formation of electronically-excited products. This was also the case in an earlier result (20). The sum of the two rate constants in Figure 1 yields agreement with the data in Figure 1 to a factor of about 2. If, as for the dashed line in Figure 2, the value of λ were actually appreciably larger, the formation of ground state products alone would suffice to obtain agreement. (Classically, the maximum in the k_{act} versus ΔG^o curve occurs at $\Delta G^o = -\lambda$ and so is shifted to more negative ΔG^o's when λ_{out} is increased.)

Returning to Figure 1, one sees that holding λ_{out} fixed at its value at $r = \sigma$ (dash-dot line) does not cause a large deviation from the more correct result (r-dependent λ_{out}, solid line) in the inverted region. A similar approximation was used, of course, for the dashed line, where a $k(\sigma)$ was used instead of a $k(r)$.

We also have explored the solution of the time-dependent eq 1 to study the plot corresponding to Figure 1 when the observation of fluorescence quenching in reaction 14 is made at short times. In these short-time calculations we have assumed, for simplicity, that reaction occurs only at $r = \sigma$. (Calculations are planned for the case in which electron transfer occurs over a range of distance.) Results for $k_{obs}(t)$ are given for several times in Figure 3, and curves are also given for the formation of electronically-excited products. The value of $k_{obs}(t)$ is obtained as the slope at time t of a plot of $[M(III)bpy_3^{+2}]^{-1}$ $\ln[^*Ru(II)bpy_3]$ vs t. The results show the enhancement of the predicted inversion effect at small times, and an experimental study of this or related systems at such times would be desirable, and may, in fact, distinguish between the possibilities cited earlier that $V(\sigma) < 0.023$ eV or that $\lambda > (15.5 + 54)$ kJ/mol; at short times there would be a double maximum in the total rate constant versus ΔG^o plot in the first case and a single maximum in the second.

The details of these short-time calculations, made for the case that $U(r) \cong 0$, are given elsewhere (28). Searching for the inverted effect in unimolecular systems (reactants linked to each other) would also be very desirable since their rates would not be diffusion limited.

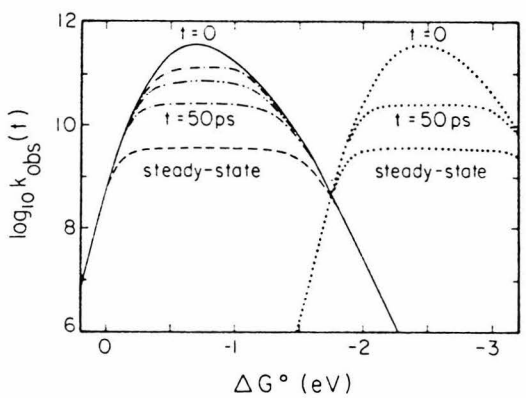

Figure 3. Time-dependent calculations of $k_{obs}(t)$ vs. $\Delta G°$ for various observation times. Key: – · –, 1 ps; – · · –, 5 ps; and · · ·, $k_{obs}(t)$ for formation of an excited-state Ru(III).

Literature Cited

1. Marcus, R. A. Discuss. Faraday Soc. 1960, 29, 21.
2. Marcus, R. A. J. Chem. Phys. 1965, 43, 2654.
3. Allen, A. O.; Gangwer, T. E.; Holroyd, R. A. J. Phys. Chem. 1975, 79, 25.
4. Henglein, A. Can. J. Chem. 1977, 55, 2112.
5. Lipsky, S. J. Chem. Ed. 1981, 58, 93.
6. Frank, A. J.; Grätzel, M.; Henglein, A.; Janata, E. Ber. Bunsenges. Phys. Chem. 1976, 80, 294.
7. Frank, A. J.; Grätzel, M.; Henglein, A.; Janata, E. Ber. Bunsenges. Phys. Chem. 1976, 80, 547.
8. Ulstrup, J. "Charge Transfer Processes in Condensed Media, Lecture Notes in Chemistry, No. 10"; Springer-Verlag: New York, 1979; pp. 163-4.
9. Creutz, C.; Sutin, N. J. Am. Chem. Soc. 1977, 99, 241.
10. Brunschwig, B.; Sutin, N. J. Am. Chem. Soc. 1978, 100, 7568.
11. Beitz, J. V.; Miller, J. R. J. Chem. Phys. 1979, 71, 4579.
12. Rehm, D.; Weller, A. Israel J. Chem. 1970, 8, 259.
13. Romashov, L. V.; Kiryukhin, Yu. I.; Bagdasar'yan, Kh. S. Doklady Phys. Chem. (Engl. Transl.) 1976, 230, 961.
14. Scheerer, R.; Grätzel, M. J. Am. Chem. Soc. 1977, 99, 865.
15. Ballardini, R.; Varani, G.; Indelli, M. T.; Scandola, F.; Balzani, V. J. Am. Chem. Soc. 1978, 100, 7219.
16. Balzani, V.; Bolletta, F.; Gandolfi, M. T.; Maestri, M. Top. Curr. Chem. 1978, 75, 1.
17. Eriksen, J.; Foote, C. S. J. Phys Chem. 1978, 82, 2659.
18. Vogelmann, E.; Schreiner, S.; Rauscher, W.; Kramer, H. E. A. Z. Phys. Chem. N. F. 1976, 101, 321.
19. Marcus, R. A. Int. J. Chem. Kin. 1981, 13, 865.
20. Siders, P.; Marcus, R. A. J. Am. Chem. Soc. 1981, 103, 748.
21. Weller, A.; Zachariasse, K. Chem. Phys. Lett. 1971, 10, 590.
22. Joussot-Dubien, J.; Albrecht, A. C.; Gerischer, H.; Knox, R. S.; Marcus, R. A.; Schott, M.; Weller, A.; Willig, F. Life Sci. Res. Rep. 1979, 12, 129.
23. Efrima, S.; Bixon, M. Chem. Phys. Lett. 1974, 25, 34; Chem. Phys. 1976, 13, 447.
24. Van Duyne, R. P.; Fischer, S. F. Chem. Phys. 1974, 5, 183.
25. Ulstrup, J.; Jortner, J. J. J. Chem. Phys. 1975, 63, 4358.
26. Marcus, R. A.; Sutin, N. Inorg. Chem. 1975, 14, 213.
27. Schmickler, W. J. Chem. Soc., Faraday Trans. 2 1976, 72, 307.
28. Marcus, R. A.; Siders, P. J. Phys. Chem. 1982, 86, 622.
29. Waite, T. R. J. Chem. Phys. 1958, 28, 103.
30. Pilling, M. J.; Rice, S. A. J. Chem. Soc., Faraday Trans. 2 1975, 71, 1563.
31. Butler, P. R.; Pilling, M. J.; Rice, S. A.; Stone, T. J. Can. J. Chem. 1977, 55, 2124.
32. Wilemski, G.; Fixman, M. J. Chem. Phys. 1973, 58, 4009.
33. Keizer, J. J. Phys. Chem. 1981, 85, 940.
34. Hopfield, J. J. Proc. Nat. Acad. Sci., USA 1974, 71, 3640.
35. Jortner, J. J. Chem. Phys. 1976, 64, 4860.
36. Newton, M. D. Int. J. Quant. Chem.: Quant. Chem. Symp. 1980, 14, 363.
37. Alexandrov, I. V.; Khairutdinov, R. F.; Zamaraev, K. I. Chem. Phys. 1978, 32, 123.

38. Noyes, R. M. Progr. Reaction Kinetics 1961, 1, 129.
39. Marcus, R. A. Discuss. Faraday Soc. 1960, 29, 129.
40. Debye, P. Trans. Electrochem. Soc. 1942, 82, 265.
41. Brunschwig, B. S.; Logan, J.; Newton, M. D.; Sutin, N. J. Am. Chem. Soc. 1980, 102, 5798.
42. Kestner, N.; Logan, J.; Jortner, J. J. Phys. Chem. 1974, 78, 2148.
43. Levich, V. G.; Dogonadze, R. R. Collect. Czech. Chem. Commun. 1961, 26, 193.
44. Levich, V. G. "Physical Chemistry: An Advanced Treatise"; Eyring, H.; Henderson, D.; Jost, W., Editors; Academic Press: New York, 1970; Vol. 9B.
45. Dogonadze, R. R.; Kuznetsov, A. M.; Vorotyntsev, M. A. Phys. Status Solidi B 1972, 54, 125, 425.
46. Siders, P.; Marcus, R. A. J. Am. Chem. Soc. 1981, 103, 741.
47. Palmer, R. A.; Piper, T. S. Inorg. Chem. 1966, 5, 864.
48. Lytle, F. E.; Hercules, D. M. J. Am. Chem. Soc. 1969, 91, 253.
49. Sutin, N.; Creutz, C. Adv. Chem. Ser. 1978, No. 168, 1.
50. Gordon, M. K. Sandia Laboratories Report, SAND75-0211. For a discussion of the algorithm, see Shampine, L. F.; Gordon, M. K. "Computer Solution of Ordinary Differential Equations"; Freeman: San Francisco, 1975.
51. Sutin, N. in "Tunneling in Biological Systems"; Chance, B.; DeVault, D. C.; Frauenfelder, H.; Schrieffer, J. R.; Sutin, N.; Eds., Academic Press: New York, 1979; p. 201.
52. Debye, P.; Hückel, E. Physikal Z. 1923, 24, 185.
53. Moore, W. J. "Physical Chemistry"; 4th ed.; Prentice-Hall: Englewood Cliffs, N. J., 1972; eq 10.58.
54. Ruff, I.; Zimonyi, M. Electrochimica Acta 1973, 18, 515.
55. Lin, C-T.; Bottcher, W.; Chou, M.; Creutz, C.; Sutin, N. J. Am. Chem. Soc. 1976, 98, 6536.
56. Young, R. C.; Keene, F. R.; Meyer, T. J. J. Am. Chem. Soc. 1977, 99, 2468.
57. Sutin, N. Acc. Chem. Res. 1968, 1, 225.

CHAPTER 4

THEORY OF HIGHLY EXOTHERMIC ELECTRON-TRANSFER REACTIONS

Introduction

It has been predicted that the rate constant of a series of homogeneous electron transfer reactions,

$$ox_1 + red_2 \rightarrow red_1 + ox_2 \quad , \tag{1}$$

in which ox_1 or red_2 is varied (at constant intrinsic reorganization energy λ) should first increase with increasingly negative standard free energy of reaction ΔG^0 at small ΔG^0. It should then achieve a maximum at some value of ΔG^0 and thereafter decline as ΔG^0 continues to become still more negative. The region of decline was termed the 'inverted' region.[1] The existence of an inverted region was first predicted on the basis of a classical theory.[1, 2] The quantum-mechanical correction given by quantum-mechanical perturbation theories predicts a smaller but nevertheless finite inversion.[3-7] The difference arises from nuclear tunneling.

The experimental evidence for the existence of an inverted region is sparse: Some evidence for the effect is available for the reactions of electrons with different solutes, where the ΔG^0 for a given solute was varied by varying the hydrocarbon solvent and, thereby, the electron-solvent binding energy.[8-10] Supporting data appears in the reactions of micelle-trapped pyrene with various anion radicals,[11, 12] in reactions of hydrated electrons with organic molecules trapped in micelles[12, 13] and (a small decrease) in the reduction of electronically-excited bipyridyl complexes of Ru(II) by various metal bipyridyl complexes.[14, 15] In the two micellar examples, the ΔG^0's are uncertain, however. Evidence has also been offered in studies[16] of the rate of fluorescence quenching of trapped electrons in a glass at 77K by various aromatic acceptors. (To see the effect, it has been suggested,[17]

it is necessary to divide the acceptors studied in ref. 16 into subgroups.)

Again, according to the theoretical expressions there is a 1:1 correspondence[4] between the optical lineshape and the activation rate constant k_{act} vs the energy of reaction ΔE plot (for a weak overlap system). Thus, for a given ΔS^0, there should be a correspondence with a k_{act} versus ΔG^0 plot for an electron transfer reaction. We then conclude that the existence of a well-known maximum in a charge transfer absorption versus wavelength plot implies that there should be a maximum in the ln k_{act} vs ΔG^0 plot, a point discussed in greater detail in a concluding section.

On the other hand, many studies of highly exothermic reactions have found a diffusion-limited rate constant which extends to quite negative ΔG^0's, rather than the predicted declining rate constant, e.g.,[18-24]. (Many other studies that are sometimes cited have not been studied at sufficiently negative ΔG^0 to draw any conclusions.) These studies frequently involve measuring the rate of quenching of fluorescence by a series of reactants, where quenching was presumed or demonstrated to proceed by electron transfer. In most cases, the reason for the absence of decrease in the rate is unknown, although several possibilities have been suggested. They include (i) competing mechanisms at large $-\Delta G^0$, such as H-atom transfer,[7, 25] formation of products in excited electronic states,[7, 16] or, when reaction is observed by quenching of fluorescence, exciplex formation,[26, 27] (ii) quantum effects[3-7, 28-31] (nuclear tunneling), (iii) the modifying effect of electron transfer occurring over a range of distances r,[25] and (iv) the increase of the reorganization parameter λ with r in (iii), thereby reducing the extent of inversion.

In the present paper we report calculations which incorporate effects (ii) to (iv) and, in part, (i), and compare with the experimental results of Creutz and Sutin and with a simple approximation[25] to the problem. It is also proposed that experiments conducted at very short times following the onset of reaction will enhance the chances of observing inverted behavior that, in bimolecular systems, is masked by diffusion in conventional steady-state rate measurements. Unimolecular systems, in which the reactants are linked to each other should be even better in this respect, since they are unaffected by diffusion. A brief summary of the present study has been given elsewhere.[32]

Theory

Diffusion. In extracting the "activation rate constant" from an observed rate constant that is near the diffusion limit, it can be shown that the observed rate equals the harmonic mean of the activated rate and the diffusion-limited rate, when reaction occurs at some specified encounter distance σ,[33,34]

$$k_{obs} = 1/\left(\frac{1}{k_{act}} + \frac{1}{k_{diff}}\right) \tag{2}$$

where the diffusion rate constant k_{diff} is given by[33-35]

$$k_{diff} = 4\pi D/\int_{\sigma}^{\infty} \exp(U/k_B T)\, r^{-2}\, dr \quad . \tag{3}$$

In eq 3 D is the sum of the reactants' diffusion coefficients, U(r) is the intermolecular potential of the reactants, and k_B is Boltzmann's constant.

Electron transfers can occur over a range of reactant separation distances, rather than only at a specified distance. In such cases the observed bimolecular rate constant k_{obs} is related to the unimolecular

rate constant k(r), the rate of reaction of pairs of reactants having fixed internuclear, center-to-center, separation distance r, via a pair distribution function g(r):

$$k_{obs} = 4\pi \int_0^\infty g(r)k(r)r^2\, dr \qquad (4)$$

(cf use of eq 4 for related processes[36, 37]). In eq 4 we have assumed that k and g are radially symmetric. When the system has a k(r) instead of only a k at $r = \sigma$, k_{act} is defined by using eq 4 with g(r) replaced by its equilibrium value, $\exp[-U(r)/k_BT]$, for $r > \sigma$ and, in the present model, by zero for $r < \sigma$, since k_{act} would be the observed rate constant if diffusion were infinitely fast. Thus,

$$k_{act} = 4\pi \int_\sigma^\infty k(r)r^2 \exp(-U/k_BT)\, dr \quad . \qquad (5)$$

We shall wish to compare eq 4 with the use of eqs 2, 3 and 5, for reactions occurring over a range of separation distances. To this end we solve eq 6 below.

In the present case the reactants are substantially larger than the solvent molecules and so we shall assume that short-range intermolecular contributions to g(r) can be neglected. Then g(r) in eq 4 may be obtained as the solution to a diffusion equation,[37-39] which is given by eq 6 for the case of radial symmetry.

$$\frac{\partial}{\partial t} g(r, t) = \frac{D}{r^2} \frac{\partial}{\partial r} \left(r^2 \frac{\partial g}{\partial r}\right) + \frac{D}{k_BTr^2} \frac{\partial}{\partial r} \left(r^2 g \frac{dU}{dr}\right) - g\, k(r) \qquad (6)$$

The first term on the right arises from the diffusive flux, the second term from the conductive flux due to the long-range intermolecular potential U(r) between the reactants, and the third term from the loss of reactants due to reaction. A discussion of shortcomings of eq 6 at higher concentrations of reactants is given in refs. 34 and 36.

For two reactants having charges z_1e and z_2e, e being the electronic charge, U in the Debye-Hückel approximation is given by eq 7,[35, 40-43] where a is the distance of closest approach and r is the separation distance of the two centers.

$$U(r) = \frac{z_1 z_2 e^2}{2\epsilon r}\left[\frac{\exp \kappa a_1}{1 + \kappa a_1} + \frac{\exp \kappa a_2}{1 + \kappa a_2}\right] \exp(-\kappa r) \quad . \tag{7}$$

In eq 7, ϵ is the static dielectric constant of the solvent, and κ is the inverse of the Debye-Hückel screening length, and a_i is the radius of ion i, r_i, plus that of the principal ions of opposite sign in the ion atmosphere, r_i^a.

$$a_i = r_i + r_i^a \tag{8}$$

We comment briefly in Appendix A on some assumptions underlying eq 7. Examples of eq 7 in the literature are many and include the case[41] where $r_1 = r_2 = r_1^a = r_2^a$, the case[35,42a] (tacitly) where $r_i^a \cong 0$, and the case where $z_1 = \pm z_2$ and higher order corrections to (7) are included.[42b] The related case of colloid particles, also including additional terms, has been treated by Levine and Dube.[43] In the present paper the two reacting ions are of the same size and are both positively charged, and so $a_1 = a_2 \equiv a$, i. e.,

$$U(r) = \frac{z_1 z_2 e^2}{\epsilon r}\,\frac{\exp \kappa a}{1 + \kappa a}\,\exp(-\kappa r) \tag{9}$$

and a is the distance of closest approach between a reacting ion and the principal ion of opposite sign in the ion atmosphere.

At large internuclear separations, the concentration of reactants must equal the bulk (no reaction) concentration. Thus, one of the boundary conditions on eq 6 is lim g(r, t) = 1 as $r \to \infty$. When a volume distributed rate constant k(r) is used instead of the usual surface one k(σ),

the boundary condition at the distance of closest approach $r = \sigma$ is obtained by requiring total flux (diffusive plus conductive) across $r = \sigma$ to be zero. This inward-directed flux (per unit concentration) is given by $4\pi r^2 D$ times the lelf-hand side of

$$\frac{\partial}{\partial r} g(r, t) + g \frac{dU}{dr} / (k_B T) = 0 \text{ at } r = \sigma \quad (t \geq 0) , \tag{10}$$

and so eq 10 provides the second boundary condition.

A derivation of eqs 2, 3 and 5, as an approximate solution to eqs 6 and 10 at steady-state is given in Appendix B.

Unimolecular Rate. The electron transfer reaction may be adiabatic, nonadiabatic or somewhere in between.[44-46] A first-order quantum perturbation treatment of nonadiabatic electron transfer reactions yields the familiar result[3-5,47-49]

$$k(r) = \frac{2\pi}{\hbar} |V(r)|^2 (\text{F. C.}) \quad . \tag{11}$$

In eq 11 V(r) is the matrix element between the reactant and product electronic states of the perturbation that gives rise to electron transfer. The quantity (F. C.) is a thermally weighted sum of Franck-Condon factors given by (12), and has dimensions of $(\text{energy})^{-1}$.

$$\text{F. C.} = \frac{1}{Q} \sum_{i,f} e^{-E_i/k_B T} |\langle i|f\rangle|^2 \delta(E_f - E_i + \Delta E) \tag{12}$$

In (12) i and f designate initial and final (reactants' and products') nuclear configuration states. The reactant state includes the pair of reactant molecules and the solvent surrounding them. Q is the nuclear partition function of the initial state. The functions $|i\rangle$ and $|f\rangle$ will be treated,

for simplicity, in the harmonic oscillator approximation in the case of the intramolecular vibrations.

In the classical limit $\hbar\omega/k_BT \rightarrow 0$, and when frequency changes in individual vibrational modes are neglected, the F. C. given in (12) reduces to the expression in (13).[4, 5, 48]

$$\text{F. C.} = (4\pi\lambda k_BT)^{-1/2} \exp\left[-(\Delta E + \lambda)^2/(4\lambda k_BT)\right] \tag{13}$$

As has been discussed elsewhere, e. g., ref. 50, the quantum nonadiabatic result (11)-(12) plus a dynamical (harmonic oscillator)[47, 51] assumption for the motion of the solvent does not allow for any large entropies of reaction.[52] To avoid this difficulty one can use, instead, a more correct treatment of the polar solvent, one which is classical but in which no harmonic oscillations for the solvent are assumed.[44] In this case the Franck-Condon factor for the solvent is (cf ref. 5)

$$(\text{F.C.})_{\text{solv}} = (4\pi\lambda_{\text{out}}k_BT)^{-\frac{1}{2}} \exp[-(\Delta G^0 + E_f^v - E_i^v + \lambda_{\text{out}})^2/(4\lambda_{\text{out}}k_BT)] \tag{14}$$

where the v superscripts denote vibrational energy. Equation 14 may be compared with the quantum results we obtained in ref. 50, where a quantum treatment of the solvent water, was used, described by two modes which have frequencies of 1 cm^{-1} and 170 cm^{-1}. The latter correspond to significant declines in the real part of the dielectric constant of water at those frequencies.[53, 54] The 1 cm^{-1} mode was treated classically and the 170 cm^{-1} quantum mechanically.[50] The quantum $(\text{F. C.})_{\text{solv}}$ at room temperature was only 20% different from the classical value given by eq 14, and so in the present paper we shall use eq 14 for the solvent contribution.

We turn next to the estimate of V(r). An adiabatic model corresponding to the nonadiabatic model of (13) yields

$$k_{ad} = \nu \exp\left[-(\Delta E + \lambda)^2 / (4 \lambda k_B T)\right] \qquad (15).$$

(cf ref. 44 with ΔG^0 replaced by ΔE). In (15) ν is a typical frequency for nuclear rearrangement, $\nu \sim 10^{13}\ s^{-1}$. If one assumes at first that at some distance, e.g., at van der Waals' contact ($r = \sigma$), the reaction is adiabatic and that it becomes nonadiabatic for larger r's,[25] one can then evaluate the pre-exponential factor in (11)-(13) approximately by matching (11)-(13) with (15) at $r = \sigma$. Thereby (16) is obtained when this joining is made at $r = \sigma$.

$$\frac{2\pi}{\hbar} \left| V(\sigma) \right|^2 (4 \pi \lambda k_B T)^{-1/2} \sim 10^{13}\ s^{-1} \qquad (16)$$

For a reaction for which the nuclear reorganization energy term λ is 70 kJ/mol, the $V(\sigma)$ calculated from (16) is about 0.023 eV. If instead of (16) the reaction is nonadiabatic at $r = \sigma$, the actual value of $V(\sigma)$ is less than this. (In a more elaborate calculation a Landau-Zener type theory for the adiabatic-nonadiabatic aspect could be adopted, but this elaboration is hardly warranted in view of the approximate value of the function $V(r)$).

For an exponential dependence of the matrix element on r, $V(r)$ is given by

$$\left| V(r) \right|^2 = \left| V(\sigma) \right|^2 \exp\left[-\alpha(r - \sigma)\right] \qquad (17)$$

where $r-\sigma$ is on the average (and, for spherically symmetric reactants, exactly) the edge-to-edge distance between the reactants. The theoretically estimated[55, 56] or experimentally inferred[57] values of α range from 2.6 to 1.1 Å^{-1}. The value of 2.6 refers to a theoretical calculation where the electron tunnels from one reactant to the other <u>via</u> a vacuum.[55] When medium is present a value of 1.44 Å^{-1} was roughly estimated,[56] using a calculation based on an electron tunneling through a square barrier of about

2 eV.[58] More recent but ab initio calculations have been given for the hexaaquairon (II/III) self-exchange reaction ($\alpha \sim 1.8$ Å^{-1}).[59] [See also ref. 60.] The 1.1 Å^{-1} was estimated indirectly from experiments on electron transfer between aromatic anions and aromatic molecules in frozen media.[57] (For a quite different system, reactions of solvated electrons in frozen media, values of α have also been estimated indirectly in the same manner.[16, 61]) We shall use a value of 1.5 Å^{-1}. The results given later in Figures 1 and 2 are not very sensitive to the value of α. All calculations were performed with T = 298 K.

Method of calculation. The equilibrium (no-reaction) steady-state solution to (6) is $g(r) = \exp(-U(r)/k_BT)$, when the two boundary conditions (i) lim $g(r) = 1$ as $r \to \infty$ and (ii) eq 10 at $r = \sigma$ are employed. Reaction will cause deviation from this solution. If we rewrite the diffusion equation in terms of $h(r) = g(r) \exp(U/k_BT)$ then, at steady state ($\partial g/\partial t = 0$), eq 6 becomes

$$\frac{d}{dr}\left(r^2 e^{-U/k_BT} \frac{dh}{dr}\right) - \frac{r^2}{D} k(r)h(r) e^{-U/k_BT} = 0 \quad . \tag{18}$$

The asymptotic solution to (18) at large r is obtained (for the case that U and k decrease more rapidly than 1/r at large r) by setting U and k equal to their values at large r, namely, zero, and then solving (18). This asymptotic solution is

$$h(r) \underset{r\to\infty}{\sim} 1 - c_2/r \quad , \tag{19}$$

where c_2 is a constant and where we have satisfied the boundary condition that $h(r) \to 1$ as $r \to \infty$. We wish to construct the exact solution for h(r) by numerical integration from $r = \sigma$ outward. Since $h(\sigma)$ is not known a priori, we first solve numerically for a function related to h(r) by an unknown multiplicative constant c_1, $H(r) = c_1 h(r)$, and choose $H(\sigma)$ arbitrarily. ($H(\sigma) = 0.01$ was found to be convenient.) Equation 18 is

first rewritten, in terms of H(r), as an equivalent pair of coupled first-order differential equations 20 to facilitate the numerical integration by a standard routine.

$$\left.\begin{aligned} \frac{d\theta}{dr} &= \frac{r^2}{D}\, k(r)\, e^{-U/k_B T}\, H \\ \frac{dH}{dr} &= r^{-2}\, e^{U/k_B T}\, \theta \quad , \end{aligned}\right\} \tag{20}$$

where θ is defined by (21) and is $1/4\pi D$ times the flux at r.

$$\theta = r^2 \exp(-U/k_B T)\,(dH/dr) \quad . \tag{21}$$

The boundary conditions at $r = \sigma$ are $H(\sigma) = 0.01$ and, from eqs 10 and 21, $\theta(\sigma) = 0$. The numerical integration was begun at $r = \sigma$, and a standard program[62] for integration of a system of ordinary differential equations was used. H(r) was calculated at successively larger values of r, using k(r) as described in the preceding section, until it was found that H(r) displayed its asymptotic behavior, that is, until H(r) behaved as $c_1(1 - c_2/r)$ to within a small tolerance (constancy of c_1 and c_2 to 10^{-8}). At that point the calculation was stopped. The values of c_1 and c_2 were obtained from these parameters in H(r) at large r, and g(r) was computed using

$$g(r) = H(r) \exp(-U(r)/k_B T)/c_1 \quad . \tag{22}$$

Finally, k_{obs} was calculated from the net flux at large r

$$k_{obs} = 4\pi D \lim_{r \to \infty} \left(r^2 \frac{dg}{dr}\right) = 4\pi D c_2 \tag{23}$$

(An alternative way of calculating k_{obs} is by integration of eq 4 using the numerically-calculated g(r), but this second method required smaller step-sizes and tolerances to obtain convergence.)

Had U(r) decreased as $1/r$ at large r, as for example for an unshielded Coulombic interaction potential, a related functional form for the asymptotic solution (19) and for the flux in eq 23 would have been used, $g(r) \sim c[\exp(-U(r)/k_BT) - 1] + 1$.

Steady-State Results

With k(r) determined as described previously we are in a position to examine numerically the effect on k_{obs} of a reaction rate constant contributed from a range of internuclear separation distances. The steady-state (long-time) solutions of (4) and (6) will be examined first, since they are more easily found and correspond to existing experimental measurements.

The detailed calculations presented in this section are for the quenching of bipyridyl complexes of Ru(II) by various metal (III) bipyridyl complexes, studied experimentally by Creutz and Sutin.[14] The inner-sphere λ is estimated to be 15.5 kJ/mol, and is associated with a frequency of 1300 cm^{-1}.[7] The outer-sphere λ has been estimated to be 54 kJ/mol.[63] If we calculate k(r) as described in the preceding section (with $\alpha = 1.5$ Å^{-1} and $V(\sigma) = 0.023$ eV) we find that the k_{act} calculated from (5) at $\Delta G^0 = 0$ is 1.2×10^{10} $M^{-1}s^{-1}$, much higher than the currently estimated experimental value, $\sim 4 \times 10^8$ $M^{-1}s^{-1}$, for k_{obs} (Appendix C). To obtain a k_{obs} at $\Delta G^0 = 0$ in agreement with this value one requires either a smaller $V(\sigma)$, a larger λ, or a less shielded repulsive potential U(r). Use of $V(\sigma) \sim 0.0045$ eV gives a $k_{obs}^{calc} \sim 4 \times 10^8$ $M^{-1}s^{-1}$ at $\Delta G^0 = 0$ and we report calculations with this $V(\sigma)$. Use, instead, of a larger $U(\sigma)$ but a $V(\sigma) = 0.023$ eV would have given similar results. For comparison we also report results obtained using a larger λ and $V(\sigma) = 0.023$ eV.

The encounter distance, σ, has been estimated to be 14 Å,[63] and the experimental diffusion-limited rate constant is 3.5×10^9 $M^{-1} s^{-1}$ at 298 K.[14] The quenching experiments were performed in 0.5 M sulfuric acid. Using the acid dissociation constant of 0.012 M for HSO_4^-,[64] the ionic strength is estimated to be 0.52 M. This large ionic strength implies a short Debye length, 4.2 Å, which in view of the large size of the reactants is expected to make the effect of Coulombic repulsion between the reactants small.

Numerical solution of eq 6 and comparison of these calculated k_{obs} with the maximum experimental value for k_{obs} for the present system shows that with $\alpha = 1.5$ $Å^{-1}$ and $V(\sigma) = 0.0045$ eV, $D = 3.0 \times 10^{-6}$ $cm^2 s^{-1}$. For ferric and ferrous tris-phenanthroline complexes indirect approximate experimental (electrochemical) diffusion coefficients have been reported as 1.9 and 3.7×10^{-6} $cm^2 s^{-1}$,[65] respectively, and so the value of D used in this paper (the sum of D's of the two tris-bipyridyl complexes) is more or less consistent with these.

Calculations were made for the formation of ground state products and of an electronically-excited Ru(III)bpy_3 product, using the excitation energy, 1.76 eV, employed in ref. 7.[66] The formation of alternative excited products is discussed in Appendix D. We have neglected any possible spin-restriction effects.

With the parameters discussed above and the k(r) discussed in the preceding section, we have calculated the reactant pair distribution function g(r) and the observed rate constant k_{obs} as a function of ΔG^0. We first test the approximate eqs 2 and 5, using for k_{diff} the maximum value observed for k_{obs} (which we will call the "experimental" k_{diff},

since $k_{act}^{max} \gg k_{diff}$). In Table I the results from eqs 2 and 5 are compared with those using the numerical steady-state solution of eqs 4 and 6. The agreement is about 5% over the entire range of ΔG^0's studied, + 0.6 to - 3.0 eV. The D inferred from k_{obs}^{max} ($\cong k_{diff}$) when eq 3 is used was 3.5×10^{-6} $cm^2 s^{-1}$, which is close to the value (3.0×10^{-6}) inferred by using, instead, eqs 4 and 6. Had the latter value been used instead of 3.5×10^{-6}, the agreement in Table I would have been about 10% instead of 5%.

The results for k_{obs} versus ΔG^0 are plotted in Figure 1, where the experimental points are indicated by circles. The solid line in this figure is the result of the present calculation using eqs 4 and 6, and the dotted curve is for formation of an electronically excited Ru(III) product. For the dash-dot line the solvent reorganization energy was held constant at the value it has when $r = \sigma$, rather than being allowed to vary with r as it should. The dashed line in Figure 1 is a result taken from ref. 7, based on eq 2, and assumes that reaction occurs at the contact distance only. There, λ_{out} was taken to be $\lambda_{out}(\sigma)$ = 54 kJ/mol, and the experimental value of k_{diff} was introduced into eq 2.

The closeness of the solid and dash-dot curves in Figure 1 shows that the effect of having an r-dependent λ_{out} instead of a λ_{out} fixed at $r = \sigma$ is small. The approximation used in ref. 1 of treating the reaction as occurring at $r = \sigma$ and as being adiabatic there, agrees well with the present results (cf solid and dash-dot curves in Figure 1), because of compensation. (The nonadiabaticity for the solid curve decreases the rate but the reaction-over-a distance causes an enhanced rate, compared with the rate for the dash-dot curve.)

To be consistent with the experimental data in Figure 1, if one uses the above λ's, it is necessary to introduce the formation of an electronically-excited Ru(III) product, namely the dotted curve there.

Table I. Comparison of the Approximate and the More Rigorous Treatments of Diffusion.

	k_{obs} ($M^{-1} s^{-1}$)	
ΔG^0 (eV)	Exact[a]	Approximate[b]
0.0	4.1×10^8	4.1×10^8
-0.5	3.3×10^9	3.4×10^9
-1.0	3.4×10^9	3.4×10^9
-1.5	1.9×10^9	1.9×10^9
-2.0	2.1×10^7	2.1×10^7

[a]Calculated using eqs 4 and 6 with k(r) the same as that for the solid line in Figure 1.

[b]Calculated using eqs 2 and 5 with $k_{diff} = 3.5 \times 10^9 M^{-1} s^{-1}$, and k(r) the same as that for the solid line in Figure 1.

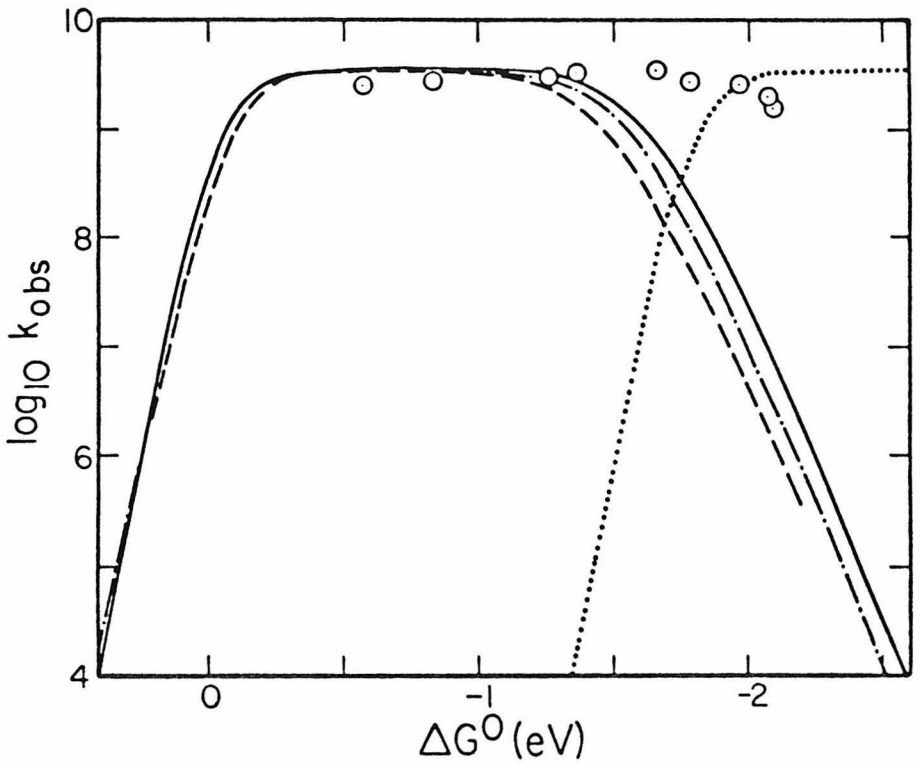

Figure 1. Calculated and experimental rates of electron-transfer quenching of Ru(II) bipyridyls vs ΔG^0. The experimental points (circles) are due to Creutz and Sutin.[14, 15] The solid line and dotted curves are for formation of ground state products and an electronically-excited product, respectively, using an r-dependent λ_{out}, with $\lambda_{out}(\sigma)$ = 54 kJ/mol and $V(\sigma)$ = 0.0045 eV. The dash-dot curve is for formation of ground state products with λ_{out} fixed at $\lambda_{out}(\sigma)$. The dashed curve is the calculation reported in ref. 7 in which reaction occurred only at $r = \sigma$.

The calculated total k_{obs}, which is the sum of the calculated rate constants for forming ground- and excited-state products, then agrees with the experimental points to a factor of about four.

If a larger value of λ_{out} or of λ_{in} were used this remaining discrepancy could be reduced significantly.[15] For example, with $\lambda = \lambda_{out} + \lambda_{in}$ increased by only 5%, to 73 kJ/mol, (and $V(\sigma)$ accordingly increased to 0.0054 eV to maintain agreement with the "experimental" rate constant at $\Delta G^0 = 0$) we find that the calculated total k_{obs} agrees with the experimental points to within a factor of about two.

In Figure 2 calculations having a larger but still r-dependent λ_{out} [$\lambda_{out}(\sigma)$ = 83 kJ/mol, $V(\sigma)$ = 0.023 eV] are given (dashed line) and compared with the solid line [$\lambda_{out}(\sigma)$ = 54 kJ/mol, $V(\sigma)$ = 0.0045 eV] of Figure 2. A slightly smaller D(2.6×10^{-6} $cm^2 s^{-1}$) was required to make the larger λ_{out} calculation yield the experimental value of the maximum k_{obs}, 3.5×10^9 $M^{-1} s^{-1}$.

The position of the dashed curve in Figure 2 in the inverted region relative to the other curve reflects the large value for λ_{out} in that case ($\geq$ 83 kJ/mol). The value of λ_{out} for the solid curve was $\geq$ 54 kJ/mol. As is evident from the approximate eq 14, the greater λ_{out} the less the tendency to inversion, other things being equal. Indeed, one sees from Figure 2 that if $\lambda_{out}(\sigma)$ equalled 83 kJ/mol, it would not be necessary to invoke the excited electronic state of Ru(III).

Short-Time Experiments

Reactions that are fast relative to diffusion are controlled by the rate of diffusion rather than by their 'activated' rates, and so diffusion can mask interesting rate behavior. In the case of reactions that can be induced in a very short time, for example, by a pulse of light, such as reaction (24), followed by reaction (25), this masking effect may be reduced.

$$red_2 + h\nu \rightarrow red_2^* \qquad (24)$$

$$ox_1 + red_2^* \rightarrow red_1 + ox_2 \qquad (25)$$

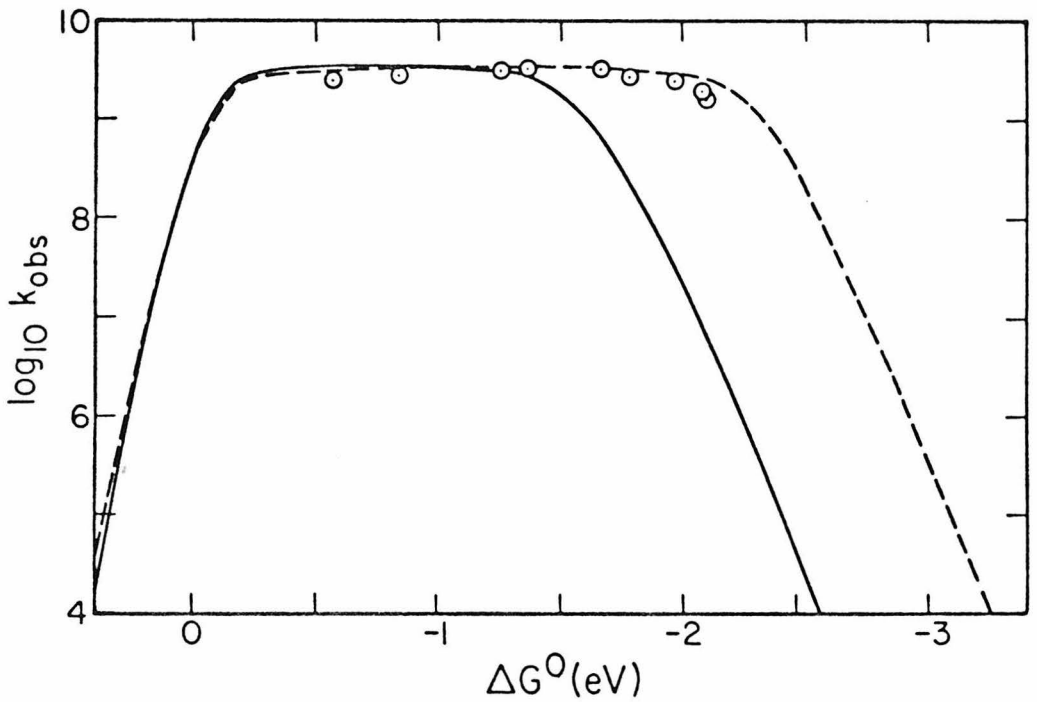

Figure 2. Calculated and experimental rates of electron-transfer quenching of Ru(II) bipyridyls vs ΔG^0. The solid curve is taken from Figure 1. The dashed-curve is with an r-dependent λ_{out}, $\lambda_{out}(\sigma)$ = 83 kJ/mol and V(σ) = 0.023 eV. The experimental points (circles) are those of Creutz and Sutin.[14, 15]

In a fast bimolecular reaction (25) in which the reactants ox_1 and red_2^* are initially randomly distributed, reaction causes the reactant pair distribution function, $g(r, t)$, to depart from its equilibrium value. Since the reactants closest together tend to react first, $g(r, t)$ becomes increasingly depleted near $r = \sigma$ as time increases. At long time $g(r, t)$ approaches the steady-state distribution function discussed previously. However, at small t, the distribution of reactants is closer to the equilibrium one, even for quite fast reactions, and the observed rate constant is then nearer the value it would have in the limit of infinitely rapid diffusion. That is, as $t \rightarrow 0$ k_{obs} approaches the activated rate constant k_{act} given by (5). Thus, if the rates of fast reactions such as (25) can be measured at sufficiently short times, the masking effect of diffusion can be circumvented.

For simplicity of presentation, we shall consider first the time-dependent problem for the case that $U = 0$, a realistic case at the present high ionic strength. The following time-dependent solution to (4) and (6) with $U = 0$ is well-known, and will suffice to provide order-of-magnitude estimates for the rate enhancement to be expected at short times. When reaction occurs only at a fixed internuclear separation σ, with bimolecular rate constant k_{act}, and in the absence of long-range forces between the reactants, k_{obs} is given by[34, 67]

$$k_{obs}(t) = \frac{1}{1/k_{act} + 1/k_{diff}} \left[1 + \frac{k_{act}}{k_{diff}} e^{x^2} \operatorname{erfc}(x) \right] , \qquad (26)$$

where erfc(x) is the well-known complementary error function

$$\mathrm{erfc}(x) = \frac{2}{\sqrt{\pi}} \int_x^\infty e^{-u^2}\, du \quad , \tag{27}$$

$$x = \sqrt{Dt}\,(1 + k_{act}/k_{diff})/\sigma \quad , \tag{28}$$

and k_{act} is for reaction occurring at $r = \sigma$, but we shall use (cf Appendix B for the steady-state case)

$$k_{act} = 4\pi \int_\sigma^\infty k(r) r^2\, dr \quad . \tag{29}$$

D is again the sum of the reactants' diffusion coefficients. k_{diff} is the diffusion-limited rate constant, and is the same as in eq 3, but with U = 0, i. e.,

$$k_{diff} = 4\pi D\sigma \quad . \tag{30}$$

In obtaining (26) the usual boundary condition,[67] eq 31, on the flux at $r = \sigma$, was satisfied.

$$4\pi D\sigma \, \frac{\partial g(\sigma)}{\partial \sigma} = k_{act}\, g(\sigma) \tag{31}$$

At large t the second term in the brackets in (26) vanishes, so that (26) reduces to the steady-state expression, (2). As $t \rightarrow 0$, on the other hand, k_{obs} as given by (26) approaches k_{act}. The rate behavior for large values of k_{act} at sufficiently short times is, thus, not masked by diffusion.

Figure 3 shows the behavior of k_{obs} predicted by (26) at various times from t = 0 to t = 1 μs. The time t = 1 μs is sufficiently long that a steady-state has been reached. In making the calculation for Figure 3, k_{act} was calculated with (29), using k(r) as described in the preceding

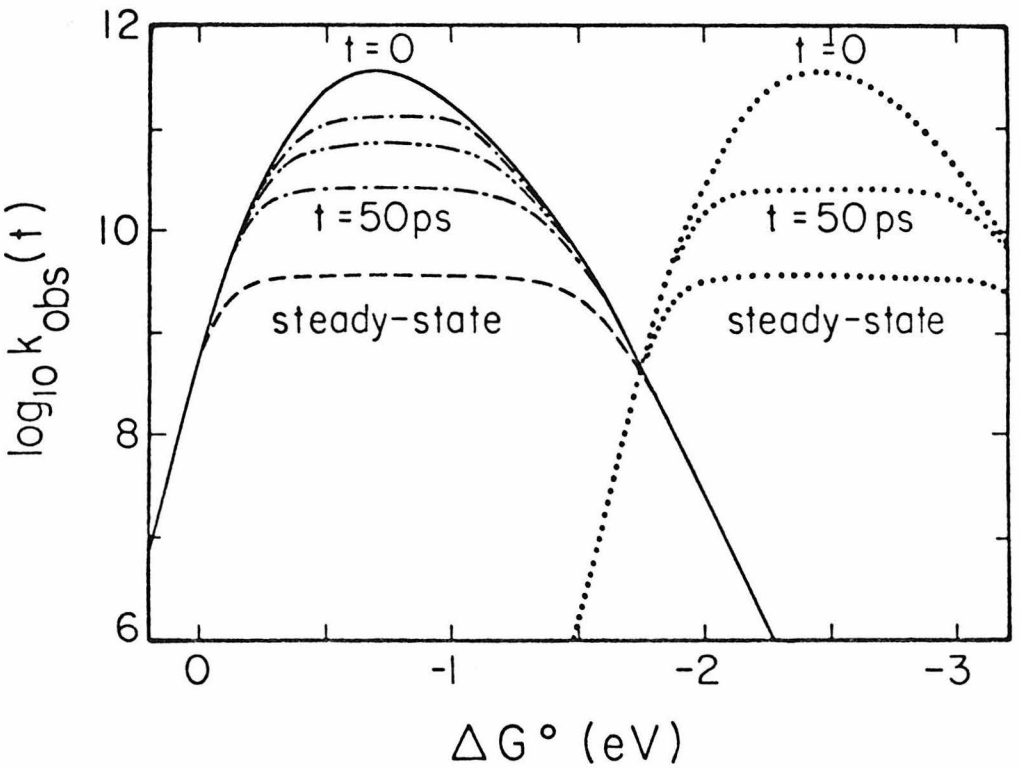

Figure 3. Observed rate constant at various times following the onset of reaction. The values of k_{obs} are calculated from eq 26. The observation time for –· – was 1 ps and for –· · · – was 5 ps. The $k_{obs}(t)$ for formation of an excited-state Ru(III) is depicted by the dotted lines.

section. The experimental value of k_{diff}, $3.5 \times 10^9\ M^{-1}s^{-1}$, was used. At observation times on the order of 0.5 ps, which may be accessible using present subpicosecond techniques, the rate constants are greatly enhanced, and there is a pronounced double maximum in the plot in Figure 3, and also, indeed, for the 5 and 50 ps curves. An experimental study at small times would be desirable, and may in fact distinguish the behavior in Figure 2 from that in Figure 3. Calculations using the time-dependent counterpart of the present treatment would be somewhat more accurate than the results given in Figure 3.

A solution analogous to (26) but which allows for a general nonzero U(r) is also available.[68] With U(r) as described in a preceding section, k_{act} as defined in (5), and $k_{diff} = 3.5 \times 10^9\ M^{-1}s^{-1}$, the rate constants were calculated using the equation given in ref. 68. As expected at the present high ionic strength, the recalculated values differ little from those presented in Figure 3.

It may, of course, be equally useful or more useful to look experimentally for inverted behavior in electron transfer reactions between redox centers that are linked chemically (cf [69]). Having the reactants linked together would entirely circumvent the problem of slow diffusion. Also, if the chemical link were rigid, the reaction would be forced to occur at a single, well-defined reactant separation distance.

We consider the first-order reaction shown in (32) and (33)

$$ox_1 \sim\sim red_2 + h\nu \rightarrow ox_1 \sim\sim red_2^* \qquad (32)$$

$$ox_1 \sim\sim red_2^* \rightarrow red_1 \sim\sim ox_2 \qquad (33)$$

Reaction (33) would be followed by the reverse electron transfer to reform ox_1 and red_2. In (32) and (33) the oxidized and reduced species have been linked by some bridging group(s). For the case of a $\lambda_{out}(\sigma)$ = 54 kJ/mol, i. e., for two reactants virtually in contact, the results for the rate constant k are given by the t = 0 plot in Figure 3, apart from absolute scale.

Finally, it remains to consider the relationship mentioned earlier between the charge transfer absorption spectrum versus frequency plot and the ln k_{act} vs ΔG^0 plot. We do so in the next section.

Analogy Between Charge-Transfer Spectrum and Plot of k_{act} vs. ΔG^0.

The probability of the optical dipole-induced transition from the i'th vibrational level of electronic state $|a\rangle$ to the f'th vibrational level of electronic state $|b\rangle$ is given by[4]

$$\Gamma(\Delta E_1 \pm h\nu) = C \sum_{i,f} e^{-E_i/k_B T} \; |\langle i|f\rangle|^2 \delta[E_f - E_i + (\Delta E_1 \pm h\nu)] \qquad (34)$$

using the Golden Rule and the Condon approximations. In (34), C is a proportionality constant $[2\pi |\langle a|\mu|b\rangle|^2/Q\hbar]$, ΔE_1 is the difference in energy of the zero point vibrational levels of electronic states $|b\rangle$ and $|a\rangle$ for a particular system, and $h\nu$ is the energy of the radiation emitted (+) or absorbed (-). E_f and E_i are the vibrational energies associated with $|f\rangle$ and $|i\rangle$.

Comparing eq 34 with eqs 11-12 we see that Γ/C is the same function of $\Delta E_1 \pm h\nu$ that k_{act}/C' is of ΔE, where $C' = 2\pi |V(r)|^2/Q\hbar$. Thus, since Γ, and hence Γ/C, has a maximum as a function of $\Delta E_1 \pm h\nu$ (where this argument is varied by varying $h\nu$) in the absorption plot, k_{act} must have

a maximum as a function of ΔE. In the k_{act} vs ΔE plot, ΔE is varied by studying a series of reactants, by varying one of the reactants, in which (ideally) the vibration frequencies and bond lengths of this series of reactants are fixed, as are those of the corresponding products, and so the ψ_i's, ψ_f's, E_i's and E_f's are the same for each member of the series. ΔE is the only variable in this series. Because of the constancy of the ψ_i's, etc. the ΔS^0 is also a constant, and so a plot of k_{act} vs ΔE is merely a displacement of the plot of k_{act} vs ΔG^0. In summary, the maximum in the absorption coefficient vs absorption frequency plot, well-known in charge transfer (and other) absorption spectra, implies a maximum in the plot of k_{act} vs ΔG^0. The condition on the argument is that eq 34 provide a suitable description of the former and that eqs 11-12 adequately describe the latter.

Conclusion

We have seen that the r-dependence of the solvent reorganization energy increases the predicted rate constant in the inverted region, as expected. For the particular system for which calculations were performed the increase was relatively small.

In the calculation of steady-state rate constants we found it adequate to use a simple analytical approximation to the problem, eq 2, in which one calculates an activated rate constant and then obtains the observed rate constant as the harmonic mean of the activated and diffusion-limited rate constants.

It is suggested that experiments measuring the rate of electron transfer at very short times following the onset of reaction can improve the chances of observing inverted behavior that may be masked by the slowness of diffusion in typical steady-state measurements. It may also be fruitful to seek inverted behavior in electron transfer reactions between chemically linked redox centers.

Appendix A. Comment on Equation 7

The approximations contained in eq 7 include the following: (1) replacing the discrete molecular environment of the ion, namely the solvent and the counter ions, by a dielectric continuum and a continuous charge distribution, (2) use of the linearized form of this continuum (Poisson-Boltzmann) equation, eq A1 below, (3) treating the reactants as spherical even in cases where they are not, and (4) neglecting dielectric image effects arising from the presence of a low dielectric constant sphere (the second ion) in the presence of the first, e. g., by using as a solution eq A2 below.

The linearized Poisson-Boltzmann equation for the electrostatic potential ψ is

$$\nabla^2\psi = \kappa^2\psi \quad . \tag{A1}$$

When there are two central ions of charges $\gamma z_1 e$ and $\gamma z_2 e$ (γ is a charging parameter which will later be increased from 0 to 1), eq A1 has the approximate solution at any point in the medium

$$\psi = \frac{\gamma z_1 e e^{\kappa a_1} e^{-\kappa R_1}}{(1 + \kappa a_1)\epsilon R_1} + \frac{\gamma z_2 e e^{\kappa a_2} e^{-\kappa R_2}}{(1 + \kappa a_2)\epsilon R_2} \tag{A2}$$

where a_i is given by (8) and R_i is the distance from the point to the center of ion i. Equation A2 is the sum of potentials that one would have if only one of the two central ions were present, individual solutions which are well-known.[42a] Equation A2 ignores the fact that when one brings ion 2 up to ion 1 one is changing the boundary in the vicinity of ion 1 (a new boundary is introduced). Accordingly, the first term, which formerly was an exact solution to eq A1, is now only approximate; analogous remarks apply to the second term.

The potential energy of interaction of the two central ions, U(r) in eq 7, is obtained by multiplying the second term in (A2) by the infinitesimal element of charge $z_1 e d\gamma$, replacing R_2 by its average value r at the center of ion 1, (an approximation, which we shall eliminate in a later paper) and multiplying the first term in (A2) by $z_2 e dr$, replacing R_1 by its average value r at the center of ion 2, and integrating γ from 0 to 1. The missing terms, e. g., the first term in eq A2 times $z_1 e d\gamma$, contribute to the interaction of ion 1 with its environment and so are present at $r = \infty$. Therefore, they do not contribute to the mutual interaction energy of ions 1 and 2. The integration yields eq 7.

Another expression for U(r) which has sometimes been used, for the case of a large ion (ion 1) interacting with a small one, is[70a] (cf [70b])

$$U(r) = \psi(r, \text{ ion 1 only present})\, z_2 e \quad . \tag{A3}$$

(For the case of a spherical charge distribution on ion 1 this U(r) is $z_1 z_2 e^2 \exp[\kappa(a_1 - r)]/\epsilon r(1 + \kappa a_1)$.) This expression and eq 7 yield the same answer in several limiting cases: (a) $a_1 = 0$, $a_2 = 0$, (b) $a_1 = a_2$, and (c) $\kappa = 0$. Equation A3 is commonly also tacitly used for the interaction of an ion (ion 2) with an electrode (ion 1 is allowed to become extremely large, and hence ultimately a plane). In the present case, the two radii a_1 and a_2 are equal, and so eqs 7 and A3 both yield the same result, namely eq 9.

Appendix B. Derivation of Equation 2 for Reactions Over a Range of r's

We obtain eq 5 first: If diffusion is sufficiently fast the steady-state solution to (6) is given by the equilibrium expression,

$$g(r) = \exp(-U(r)/k_BT) \quad \text{(fast diffusion)} \tag{B1}$$

for $r \geq \sigma$, and $g(r < \sigma) = 0$. The activated bimolecular rate constant may be obtained by substituting this equilibrium g into eq 4, yielding eq 5.

To obtain an approximate steady-state solution[25] of eq 6 under other conditions the equation is first rewritten as

$$\frac{D}{r^2}\frac{d}{dr}\left[e^{-U/k_BT} r^2 \frac{d}{dr}\left(g\, e^{U/k_BT}\right)\right] = k(r)g(r) \quad . \tag{B2}$$

Integration yields

$$De^{-U/k_BT} r^2 \frac{d}{dr}\left(g\, e^{U/k_BT}\right)\Bigg|_{r=\sigma}^{R} = \int_{\sigma}^{R} k(r)g(r)r^2 dr \quad . \tag{B3}$$

The flux is given by $4\pi r^2 D$ times the l. h. s. of eq 10, and so the l. h. s. of (B3) is $1/4\pi$ times the flux at $r = R$ minus that at $r = \sigma$. The condition of zero net flux across the $r = \sigma$ boundary (eq 10) implies that in the l. h. s. of eq B3 the term at the lower limit $r = \sigma$ vanishes. The unimolecular rate constant k(r) is, as discussed in the text, a rapidly decreasing function of r. For r greater than some distance σ', where $(\sigma' - \sigma)$ is a small quantity, k(r) is essentially zero. Therefore for $R > \sigma'$ the r. h. s. of eq B3 may be approximately replaced by its limit at $R \to \infty$, and because of the vanishing of the l. h. s. of eq B3 at its lower limit, we then have (writing r instead of R)

$$De^{-U/k_BT} r^2 \frac{d}{dr}\left(g\, e^{U/k_BT}\right) = \int_{\sigma}^{\infty} k(r)g(r)r^2 dr \qquad (r > \sigma') \quad . \tag{B4}$$

Substituting eq 4 for the integral over r into (B4) allows one to rewrite the latter as

$$De^{-U/k_BT} r^2 \frac{d}{dr}\left(g\, e^{U/k_BT}\right) = k_{obs}/4\pi \qquad (r > \sigma') \quad . \tag{B5}$$

Rearranging eq B5 and integrating from σ' to ∞ yields

$$\frac{k_{obs}}{4\pi D} \int_{\sigma'}^{\infty} e^{U/k_BT} \frac{dr}{r^2} = \left(g(r)\, e^{U/k_BT}\right) \Big|_{r=\sigma'}^{\infty} \quad . \tag{B6}$$

The potential U(r) vanishes, by definition, as $r \to \infty$, and we require $\lim g(r) = 1$ as $r \to \infty$. Thus, we obtain

$$k_{obs}/k'_{diff} = 1 - g(\sigma') \exp(U(\sigma')/k_BT) \quad , \tag{B7}$$

where

$$k'_{diff} = 4\pi D / \int_{\sigma'}^{\infty} e^{U/k_BT} r^{-2}\, dr \quad . \tag{B8}$$

We now proceed to evaluate the second term in the r. h. s. of eq B7 in terms of the activation controlled rate constant k_{act}. If the product $\exp(U(r)/k_BT)g(r)$ varies only slowly for $\sigma < r < \sigma'$, then k_{obs} is given (using eq 4) approximately by eq B9.

$$k_{obs} \cong 4\pi g(\sigma')\, e^{U(\sigma')/k_BT} \int_{\sigma}^{\infty} k(r) r^2 e^{-U(r)/k_BT}\, dr \tag{B9}$$

which, using eq 5, becomes

$$g(\sigma')\ \exp(U(\sigma')/k_BT) \simeq k_{obs}/k_{act} \quad . \tag{B10}$$

If we substitute eq B10 into eq B7 we obtain

$$k_{obs}/k'_{diff} \cong 1 - k_{obs}/k_{act} \quad . \tag{B11}$$

Because $(\sigma' - \sigma)$ is a small quantity, k'_{diff} is approximately equal to k_{diff}, where k_{diff} is defined as in eq B8, but with σ in place of σ'. Substituting k_{diff} for k'_{diff} in eq B11 and rearranging yields eq 2.

Finally, in Figure 4, to illustrate how much or little $g(r)\ \exp(U(r)/k_BT)$ varies in the interval $\sigma' - \sigma$ we plot $k(r)$, $g(r)$ and $\exp(U(r)/k_BT)$ versus r, for $\Delta G^0 = -1.3$ eV. The quantity σ' is indicated approximately, chosen so that $k(\sigma') = k(\sigma)/3$. The unimolecular rate constant $k(r)$ was calculated in the same way as for the solid line in Figure 1. From the results in Figure 4, the product $g(r)\ \exp[-U(r)/k_BT]$ varies by $\sim 20\%$ over the interval $\sigma < r < \sigma'$. A similarly small change is observed with other values of ΔG^0. This observation suggests that it is adequate to treat $g(r)\ \exp(U(r)/k_BT)$ as constant for $\sigma < r < \sigma'$.

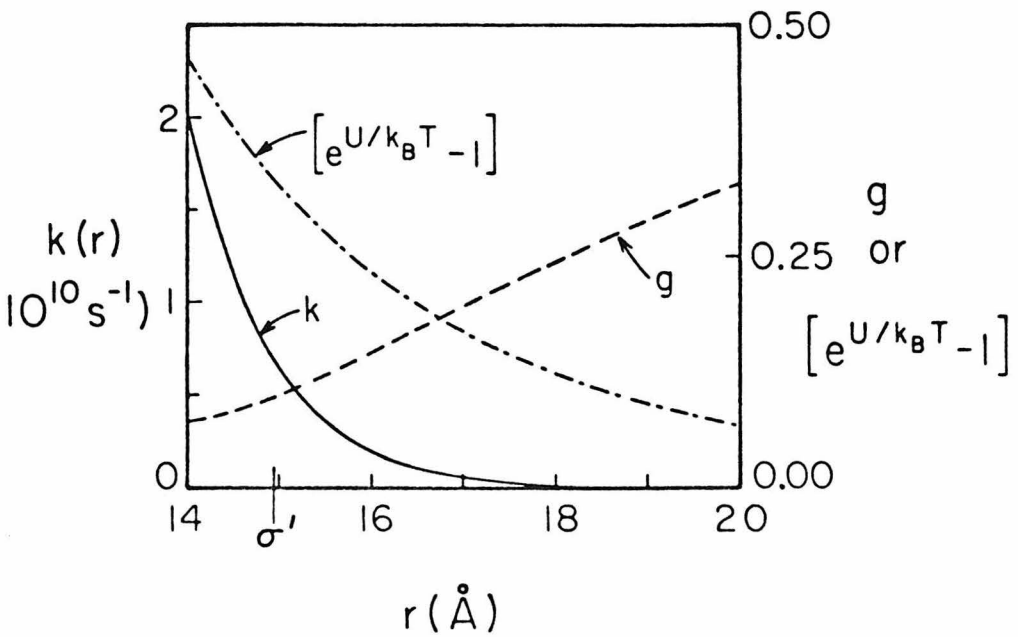

Figure 4. Behavior of k(r), g(r) and $\exp[U(r)/k_BT]$ as a function of r. The calculations are given for the conditions given by the solid line in Figure 1 at $\Delta G^0 = -1.3$ eV. g(r) rises to 0.5 at $r \cong 26$ Å and eventually approaches unity.

Appendix C. 'Experimental' Rate Constant of the Reaction of $Ru(II)(bpy)_3^*$ with $M(III)(bpy)_3$

The 'experimental' rate constant given in the text for reaction (C3) at $\Delta G^0 = 0$ is $\sim 4 \times 10^8\ M^{-1}s^{-1}$. To obtain this value we make use of the self-exchange rate constant ($\sim 10^8\ M^{-1}s^{-1}$) estimated[71] for reaction (C1)

$$Ru(II)bpy_3^* + Ru(III)bpy_3 \rightarrow Ru(III)bpy_3 + Ru(II)bpy_3^* \qquad (C1)$$

and that estimated for reaction (C2), $1.2 \times 10^9\ M^{-1}s^{-1}$.[72] The latter was k_{obs} for the oxidation of $Ru\ bpy_3^{2+}$ by $Ru\ phen_3^{3+}$, for which $\Delta G^0 \cong 0.01$ eV.

$$Ru(II)bpy_3 + Ru(III)bpy_3 \rightarrow Ru(III)bpy_3 + Ru(II)bpy_3 \qquad (C2)$$

Corrected for diffusion using eq 2, the activation rate constant k_{act} for (C2) is about $2 \times 10^9\ M^{-1}s^{-1}$.

The geometric mean of these activation rate constants is $4.5 \times 10^8\ M^{-1}s^{-1}$, and will be used for k_{act} for the reaction

$$Ru(II)bpy_3^* + M(III)bpy_3 \rightarrow Ru(III)bpy_3 + M(II)bpy_3 \qquad (C3)$$

at $\Delta G^0 = 0$. We use the cross-relation[1, 2] to estimate the rate constant for reaction (C3) at $\Delta G^0 = 0$ as the geometric mean of the rate constants for (C1) and (C2). Sutin has argued[73] that the cross-relation should be applicable even for nonadiabatic reactions if the electronic matrix element V(r) for reaction (C3) is equal to the geometric mean of the matrix elements for (C1) and (C2). Assuming that that condition is approximately satisfied, we find $k_{act} = 4.5 \times 10^8\ M^{-1}s^{-1}$ for (C3) at $\Delta G^0 = 0$. Corrected for diffusion using eq 2 this k_{act} yields a k_{obs} for reaction (C3) of $\sim 4 \times 10^8\ M^{-1}s^{-1}$.

Incidentally, the reaction

$$Cr(III)mebpy_3^{3+} + Ru(II)bpy_3 \rightarrow Cr(II)mebpy_3 + Ru(III)bpy_3 \qquad (C4)$$

in 1 M H_2SO_4 has a ΔG^0 very close to zero and has a k_{obs} of $\sim 2 \times 10^8$ $M^{-1}s^{-1}$.[15]

Appendix D. Formation of Other Electronically-Excited States

The possibility of forming other electronically-excited products was also considered. Formation of an electronically excited Ru(II) product is thermodynamically less favorable by 0.3 eV [74, 75] than formation of an excited Ru(III), so Ru(II) products were assumed to be formed in their ground electronic states. The excitation energy for formation of $Os(bpy)_3^{2+}$ is [76, 77] 1.78 eV (similar to that for $Ru(bpy)_3^{2+}$, 1.76 eV), and associated with the excitation is an inner-sphere reorganization energy of about 2 kJ/mol (1/8 of the Stokes shift) [78] at a frequency of $\sim 1300\ cm^{-1}$ (the vibrational spacing observed in the low temperature emission spectrum [76, 78]). The formation of an electronically-excited Os(II) product may be less favorable (or at least no more favorable) than formation of an excited Ru(III) product, depending on the assumptions. [79] Finally, although the excitation energy of $Cr(bpy)_3^{2+}$ is only about [80, 81] 1.05 eV, which is lower than the Ru(III) excitation energy, the reactions to form the electronic ground state of the Cr(II) product already lie in the "normal" (i.e., not inverted) region, and so it would be less favorable to form an electronically-excited Cr(II) product.

References

(1) R. A. Marcus, Discuss. Faraday Soc. 1960,29,21.

(2) R. A. Marcus, J. Chem. Phys. 1965,43,2654.

(3) R. P. Van Duyne and S. F. Fischer, Chem. Phys. 1974,5,183.

(4) J. Ulstrup and J. Jortner, J. Chem. Phys. 1975,63,4358.

(5) N. Kestner, J. Logan, and J. Jortner, J. Phys. Chem. 1974,78,2148.

(6) R. A. Marcus in "Third International Symposium on Oxidases and Related Oxidation-Reduction Systems," T. E. King, H. S. Mason, and M. Morrison, Eds., (Pergamon, New York, 1981).

(7) P. Siders and R. A. Marcus, J. Am. Chem. Soc. 1981,103,748.

(8) A. O. Allen, T. E. Gangwer, and R. A. Holroyd, J. Phys. Chem. 1975,79,25.

(9) A. Henglein, Can. J. Chem. 1977,55,2112.

(10) S. Lipsky, J. Chem. Ed. 1981,58,93.

(11) A. J. Frank, M. Grätzel, A. Henglein, and E. Janata, Ber. Bunsenges Phys. Chem. 1976,80,294.

(12) J. Ulstrup, "Charge Transfer Processes in Condensed Media," Lecture Notes in Chemistry, No. 10, (Springer, New York, 1979) pp. 163-4.

(13) A. J. Frank, M. Grätzel, A. Henglein, and E. Janata Ber. Bunsenges Phys. Chem. 1976,80,547.

(14) C. Creutz and N. Sutin, J. Am. Chem. Soc. 1977,99,241.

(15) B. Brunschwig and N. Sutin, J. Am. Chem. Soc. 1978,100,7568.

(16) J. V. Beitz and J. R. Miller, J. Chem. Phys. 1979,71,4579.

(17) J. R. Miller, private communication.

(18) D. Rehm and A. Weller, Israel J. Chem. 1970,8,259.

(19) L. V. Romashov, Yu. I. Kiryukhin, and Kh. S. Bagdasar'yan, Doklady Phys. Chem. (Engl. Transl.) 1976,230,961.

(20) R. Scheerer and M. Grätzel, J. Am. Chem. Soc. 1977,99,865.

(21) R. Ballardini, G. Varani, M. T. Indelli, F. Scandola, and V. Balzani, J. Am. Chem. Soc. 1978,100,7219.

(22) V. Balzani, F. Bolletta, M. T. Gandolfi, and M. Maestri, Topics Current Chem. 1978,75,1.

(23) J. Eriksen and C. S. Foote, J. Phys. Chem. 1978,82,2659.

(24) E. Vogelmann, S. Schreiner, W. Rauscher, and H. E. A. Kramer, Z. Phys. Chem. N. F. 1976,101,321.

(25) R. A. Marcus, Int. J. Chem. Kinet. 1981,13,865.

(26) A. Weller and K. Zachariasse, Chem. Phys. Letters 1971,10,590.

(27) J. Joussot-Dubien, A. C. Albrecht, H. Gerischer, R. S. Knox, R. A. Marcus, M. Schott, A. Weller, and F. Willig, Life Sci. Res. Rep. 1979,12,129.

(28) R. A. Marcus and N. Sutin, Inorg. Chem. 1975,14,213.

(29) R. R. Dogonadze, A. M. Kuznetsov, and M. A. Vorotyntsev, Z. Phys. Chem. (Wiesbaden) 1976,100,1.

(30) S. Efrima and M. Bixon, Chem. Phys. Letters, 1974, 25,34; and Chem. Phys. 1976,13,447.

(31) W. Schmickler, J. Chem. Soc., Faraday Trans. 2 1976,72,307.

(32) R. A. Marcus and Paul Siders, Adv. Chem. Soc. (in press).

(33) R. A. Marcus, Discuss. Faraday Soc. 1960,29,129.

(34) R. M. Noyes, Progr. Reaction Kinetics 1961,1,129.

(35) P. Debye, Trans. Electrochem. Soc. 1942,82,265.

(36) J. Keizer, J. Phys. Chem. 1981,85,940.

(37) M. J. Pilling and S. A. Rice, J. Chem. Soc., Faraday Trans. 2 1975,71,1563; and P. R. Butler, M. J. Pilling, S. A. Rice, and T. J. Stone, Can. J. Chem. 1977,55,2124.

(38) T. R. Waite, J. Chem. Phys. 1958,28,103.

(39) G. Wilemski and M. Fixman, J. Chem. Phys. 1973,58,4009.

(40) We are indebted to Dr. Norman Sutin for calling to our attention the variety of work-term expressions currently used in the literature and for noting several inconsistencies among them.

(41) P. Debye and E. Hückel, Physikal. Z. 1923,24,185.

(42) (a) W. J. Moore, "Physical Chemistry," 4th Edition, (Prentice-Hall, Englewood Cliffs, 1972), Chap. 10, for the case $a_1 = a_2$; S. Wherland and H. B. Gray, Proc. Nat'l Acad. Sci. USA 1976,73,2950;

(b) G. Scatchard and J. G. Kirkwood, Physik. Zeit. 1932,33,297.

(43) S. Levine and G. P. Dube, Trans. Faraday Soc. 1939, 35,1125; G. P. Dube and S. Levine, Trans. Faraday Soc. 1939,35,1141.

(44) R. A. Marcus, Ann. Rev. Phys. Chem. 1964,15,155; R. A. Marcus, J. Chem. Phys. 1956,24,966; R. A. Marcus, ibidem 1965,43,679.

(45) See P. P. Schmidt, Electrochemistry 1975,5,21 for review.

(46) See reference 12 for review.

(47) V. G. Levich in "Physical Chemistry: An Advanced Treatise," Vol. 9B, H. Eyring, D. Henderson, and W. Jost, Eds., (Academic, New York, 1970).

(48) V. G. Levich and R. R. Dogonadze, Coll. Czech. Chem. Comm. 1961,26,193.

(49) R. R. Dogonadze, A. M. Kuznetsov, and M. A. Vorotyntsev, Phys. Status Solidi B 1972,54,125,425.

(50) P. Siders and R. A. Marcus, J. Am. Chem. Soc. 1981,103,741.

(51) R. R. Dogonadze, A. M. Kuznetsov, and A. A. Chernenko, Russ. Chem. Rev. (Engl. Transl.) 1965,34,759.

(52) The entropy of reaction that is treated by the non-adiabatic formula, eqs 11 and 12, arises, in the harmonic oscillator approximation, from any non-cancelling changes in the vibration frequencies that typically occur in oxidation-reductions. However, the inner-sphere contribution to ΔS^{o} is usually minor, and for the polar solvent no changes in frequency are used. [47,50,51] The actual ΔS^{o} is in large part due to reorganization of the solvent molecules, and this effect (e.g., reflected in electrostriction) is neglected in the harmonic oscillator treatment of the solvent (with fixed ionic radii). Because of the low frequencies involved, solvent reorganization can to a good approximation be treated classically at ordinary temperatures. The correct classical treatment of the solvent can be recovered simply be replacing ΔE with ΔG^{o} in (12) when summing over the solvent modes. This is equivalent to the procedure used by Ulstrup and Jortner,[4] who use the classical expression[44] for the relevant Franck-Condon contribution.

(53) D. Draegert, N. Stone, B. Curnutte, and D. Williams, J. Opt. Soc. Am. 1966,56,64.

(54) F. Franks, Editor, "Water: A Comprehensive Treatise," Vol. 1, (Plenum, New York, 1972).

(55) J. Jortner, J. Chem. Phys. 1976,64,4860.

(56) J. J. Hopfield, Proc. Nat'l Acad. Sci. USA 1974,71,3640.

(57) I. V. Alexandrov, R. F. Khairutdinov, and K. I. Zamaraev, Chem. Phys. 1978,32,123.

(58) The familiar WKB formula (A. Messiah, "Quantum Mechanics," Vol. I (Wiley, New York, 1966, Chap. VI .) for the probability of an electron of mass m tunneling from σ to r through a potential V, when E is the total energy of the electron, is $T \propto \exp\{-(2/\hbar)\int_{\sigma}^{r}[2m(V(\rho)-E)]^{\frac{1}{2}}d\rho\}$. If in the case of a nonadiabatic electron transfer $E - V(\rho)$ is taken to be roughly the binding energy B of the transferred electron, then $T \propto \exp\{-(2/\hbar)(2mB)^{\frac{1}{2}}(r-\sigma)\}$. Comparison with (11) and (17) indicates $\alpha \simeq 2(2mB)^{\frac{1}{2}}/\hbar$. For B = 2 eV , this expression yields $\alpha = 1.5\ \text{Å}^{-1}$.

(59) M. D. Newton, Int. J. Quant. Chem.: Quant. Chem. Symp. 1980,14,363.

(60) S. P. Dolin, R. R. Dogonadze, and E. D. German, J. Chem. Soc., Faraday Trans. 1 1977,73,648; S. U. M. Khan, P. Wright, and J. O'M. Bockris, Sov. Electrochem. (Engl. Transl.) 1977,13,774.

(61) K. L Zamaraev, R. F. Khairutdinov, and J. R. Miller, Kinetika i Kataliz 1980,21,616; Kinetics and Catalysis (Engl. Transl.) 1980,21,448.

(62) M. K. Gordon, Sandia Laboratories Report, SAND75-0211. For a discussion of the algorithm, see L. F. Shampine and M. K. Gordon, "Computer Solution of Ordinary Differential Equations," (Freeman, San Francisco, 1975).

(63) N. Sutin in "Tunneling in Biological Systems," B. Chance, D. C. DeVault, H. Frauenfelder, J. R. Schrieffer, N. Sutin, Eds.,(Academic, New York, 1979) p.201.

(64) "Handbook of Chemistry and Physics," R. C. Weast, Ed., 56th Edition (CRC, Cleveland, 1975).

(65) I. Ruff and M. Zimonyi, Electrochemica Acta 1973,18,515.

(66) In the calculations for the formation of an electronically-excited $Ru(bpy)_3^{3+}$ product we have used the same V(r) as we did for the calculations involving ground electronic-state products. The lowest excited electronic state of $Ru(bpy)_3^{2+}$ is a metal-to-ligand charge transfer state (see ref. 76 below, also F. E. Lytle and D. M. Hercules, J. Am. Chem. Soc. 1969,91,253 and R. A. Palmer and T. S. Piper, Inorg. Chem. 1966,5,864), while the lowest excited electronic state of $Ru(bpy)_3^{3+}$ has been characterized as a ligand-to-metal charge transfer state (B. Mayoh and P. Day, Theoret. Chim. Acta 1978,49,259 and S. F. Mason, Inorg. Chim. Acta Rev. 1968,2,89). Because of the nature of the Ru(II) and Ru(III) excited states, it might be appropriate to use a different V(r) for ground-state and excited products, but the necessary data are lacking.

(67) F. C. Collins and G. Kimball, J. Colloid. Sci. 1949,4,425.

(68) M. R. Flannery, Phys. Rev. Letters 1981,47,163.

(69) J. C. Curtis, J. S. Bernstein, R. H. Schmehl, and T. J. Meyer, Chem. Phys. Letters 1981,81,48.

(70) (a) J. W. van Leeuwen, F. J. M. Mofers, and E. C. I. Veerman, Biochim. Biophys. Acta 1981,635,434, cf eq 5;

(b) W. H. Koppenol, C. A. J. Vroonland, and R. Braams, ibidem 1978,503,499.

(71) C.-T. Lin, W. Bottcher, M. Chou, C. Creutz, and N. Sutin, J. Am. Chem. Soc. 1976,98,6536.

(72) R. C. Young, F. R. Keene, and T. J. Meyer, J. Am. Chem. Soc. 1977,99,2468.

(73) N. Sutin, Acc. Chem. Res. 1968,1,225.

(74) G. Hager and G. Crosby, J. Am. Chem. Soc. 1975,97,7031.

(75) C.-T. Lin, W. Bottcher, M. Chou, C. Creutz, and N. Sutin, J. Am. Chem. Soc. 1976,98,6536.

(76) F. Zuloago and M. Kasha, Photochem. Photobiol. 1968,7,549.

(77) C.-T. Lin and N. Sutin, J. Phys. Chem. 1976,80,97.

(78) G. A. Crosby, D. M. Klassen, and S. L. Sabath, Mol. Crystals 1966,1,453.

(79) E.g., if one assumes λ_{in} for formation of an excited Ru(III) product to be 15.5 kJ/mol, in the absence of specific knowledge to the contrary, while that for formation of an excited Os(II) product is 8 kJ/mol, and if one sets λ_{in} for formation of unexcited Ru(III) equal to[7] 15.5 kJ/mol, one calculates the rate of formation of excited Ru(III) and unexcited Os(II) to be 2.5 times faster than that of unexcited Ru(III) and excited Os(II). Throughout, a $\lambda_{out}(\sigma) = 54$ kJ/mol, a $D = 3.0\times10^{-6}$ cm^2s^{-1} and a $\sigma = 14$ Å were used, together with the r-dependent λ_{out} and a given V(r) ($V(\sigma)$ = 0.0045 eV and $\alpha = 1.5$ $Å^{-1}$). V(r) may of course differ for these reactions.

(80) E. König and S. Herzog, J. Inorg. Nucl. Chem. 1970,32,585.

(81) I. Fujita, T. Yazaki, Y. Torii, and H. Kobayashi, Bull. Chem. Soc. Japan 1972,45,2156.

CHAPTER 5

A MODEL FOR ORIENTATION EFFECTS IN ELECTRON TRANSFER

Introduction

The relative orientation of the donor and acceptor in an electron-transfer reaction may have observable effects on the electron-transfer rate in some systems. For example, the primary photoinduced electron transfer in photosynthetic reaction centers may be influenced by the orientation of the reactants. In plant photosystem II the acceptor is probably a pheophytin (1,2) and the donor may be a substituted chlorophyll *a* monomer (2,3). Both of those molecules are large and noticeably nonspherical, suggesting that there may be one or more preferred orientations for electron transfer. There is evidence that another biologically important electron transfer, that between hemes in cytochromes, also shows a large dependence on the mutual orientation of the hemes' porphyrin rings (4).

Synthetic systems may also show significant orien-

tation effects. For example, electron transfer between cofacial porphyrins has been observed to be very rapid (5,6). Systems involving porphyrins held in other orientations are under study (7). In these systems the electron transfer is between sites that are chemically linked. But to the extent that the pi orbitals involved at the donor and acceptor sites are electronically isolated, the electron transfers may be treated using the usual outer-sphere formalism.

It is with systems such as these in mind that we have set out to develop a model theoretical system within which to learn about the nature and magnitude of orientation effects on electron-transfer rates.

The rate constant for electron transfer between reactants A and B at fixed separation and relative orientation can be described by the Golden-Rule rate constant.

$$k = \frac{2\pi}{\hbar} |V_{AB}|^2 \times (\text{Franck-Condon sum}) \qquad (1)$$

The Franck-Condon sum has been discussed in detail in preceding chapters of this thesis. This chapter will focus on the dependence, within the theoretical model to be described below, of V_{AB} on the separation and relative orientation of A and B.

The treatment of an isolated site A or B (at infinite separation, say) will be described first at some length. Then the matrix element V_{AB} for electron transfer between a weakly interacting A-B pair will be described and the results of some calculations will be presented.

Single-Site Wave Functions

The Model

Before describing the interaction of sites (e.g. molecules or electronically isolated chromophores) A and B I will describe the wave functions associated with an isolated site. The wavefunctions to be described are one-electron wavefunctions. That is, only the transferable electron is considered explicitly. The potential in which this electron moves is modelled as an oblate-spheroidal square well. A cross-section of the potential is sketched in Figure 1. The potential is symmetric in ϕ, the angle of rotation about the Z axis. The cross-section is an ellipse having semimajor axis a, semiminor axis b, and eccentricity $e \equiv \sqrt{a^2-b^2}/a$. The potential V is zero outside the well and has a constant negative value inside the well.

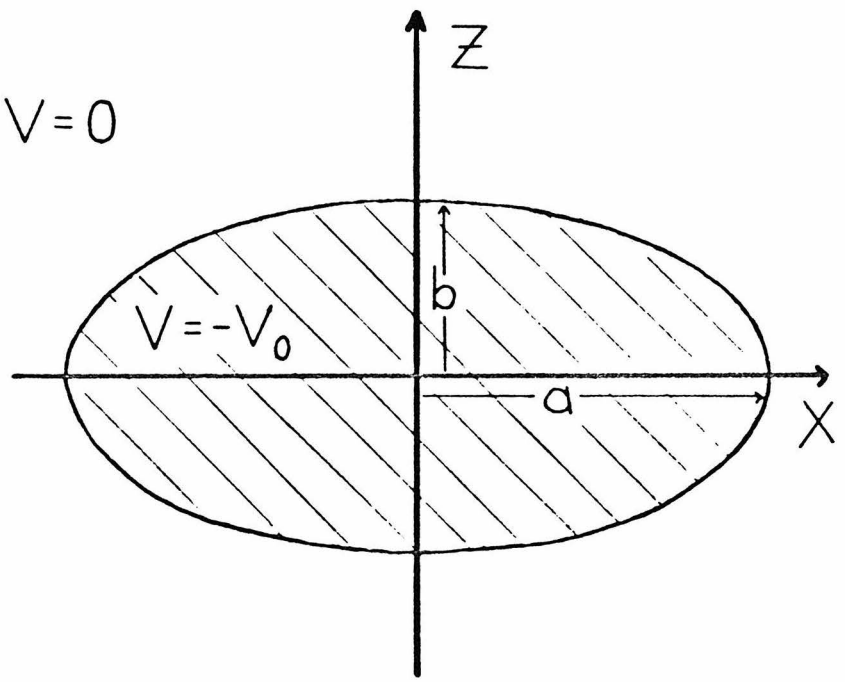

Figure 1. Potential well for a single site.

It is convenient to use oblate spheroidal coordinates as defined in equation 2.

$$\begin{aligned} x &= \frac{1}{2} d(1+\xi^2)^{\frac{1}{2}} (1-\eta^2)^{\frac{1}{2}} \cos\phi \\ y &= \frac{1}{2} d(1+\xi^2)^{\frac{1}{2}} (1-\eta^2)^{\frac{1}{2}} \sin\phi \\ z &= \frac{1}{2} d\,\xi\,\eta \end{aligned} \tag{2}$$

The scale factor d can be chosen so that the surface of the potential well is described by the single radial coordinate ξ. With $d = 2\sqrt{a^2-b^2}$ we have

$$V = \begin{cases} -V_o \; ; \; \xi \leqslant \xi_o \equiv 2b/d \\ 0 \quad ; \; \xi \geqslant \xi_o \end{cases} . \tag{3}$$

Contours of the coordinate system are presented in Figure 2. The angular coordinate ϕ has its usual definition as in spherical coordinates. The surface $\xi = 0$ is a disc of diameter d. The surface $\eta = 0$ is the x-y plane with a circular aperture.

Spherical coordinates r and θ are given in terms of oblate-spheroidal coordinates in equation 4.

$$\begin{aligned} r &= \frac{d}{2} (1 + \xi^2 - \eta^2)^{\frac{1}{2}} \\ \cos\theta &= \xi\,\eta\,(1 + \xi^2 - \eta^2)^{-\frac{1}{2}} \end{aligned} \tag{4}$$

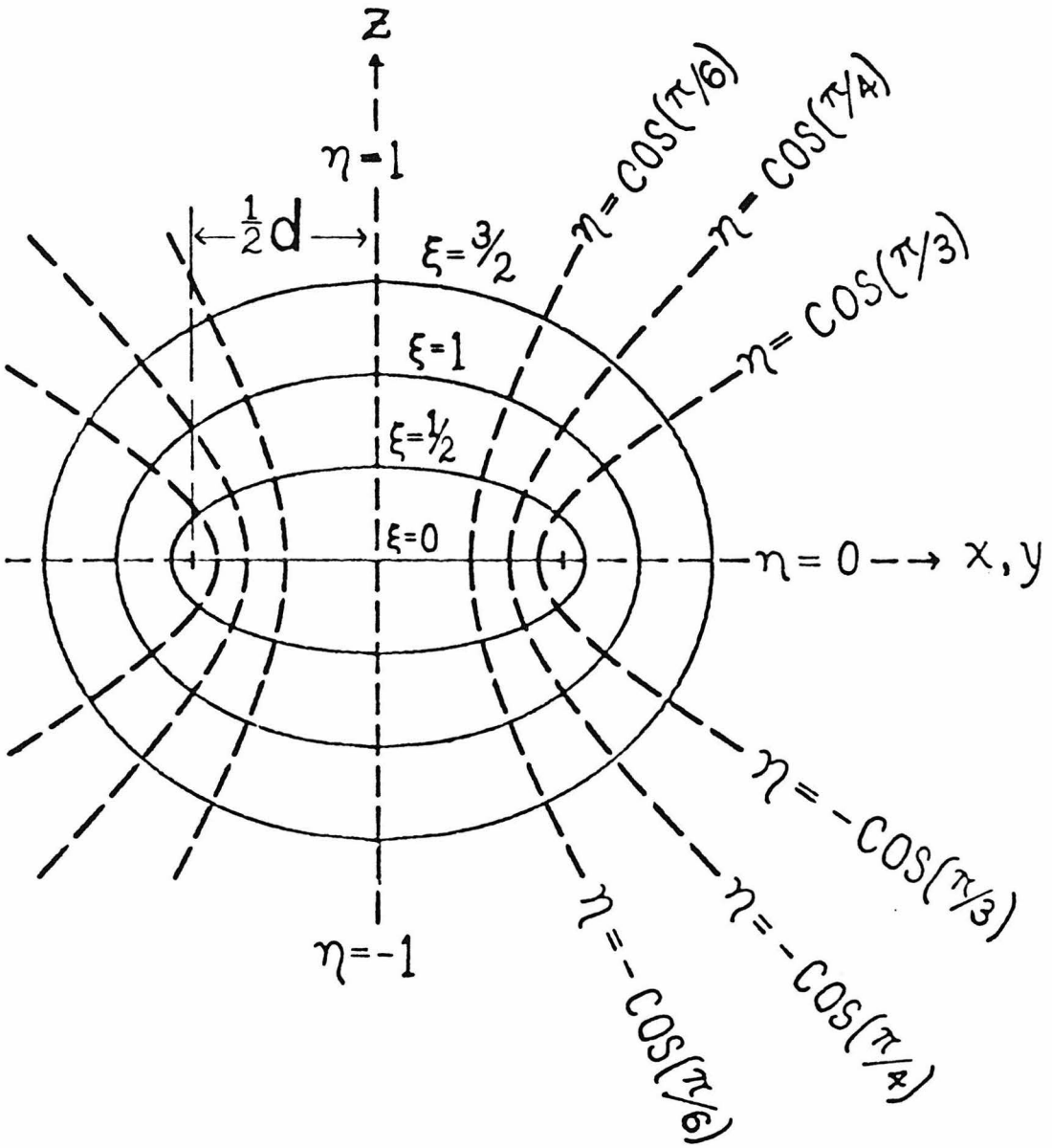

Figure 2. Oblate-spheroidal coordinate system.

Contours of ξ are indicated by solid lines. The dashed lines are contours of η. The contours are invariant with respect to rotation by any angle ϕ about the z axis.

It is clear from equation 4 that the oblate-spheroidal coordinates become asymptotically spherical at a large distance from the origin in the sense that $\xi \to 2r/d$ and $\eta \to \cos\theta$ as $r \to \infty$.

Oblate-Spheroidal Wave Functions

The single-site electronic wavefunctions sought are bound-state solutions to Schrödinger's equation with the potential specified in equation 3. Schrödinger's equation may be written as a pair of Helmholtz's equations, one to be satisfied inside the well and one outside the well.

$$(\nabla^2 + k^2)\Psi = 0 \quad \text{with} \tag{5}$$

$$k^2 = \begin{cases} \frac{2m}{\hbar^2}(E + V_o) \; ; \; \xi \leqslant \xi_o \\ \frac{2m}{\hbar^2} E \qquad ; \; \xi \geqslant \xi_o . \end{cases}$$

In equation 5, m is the mass of the electron. ($2m/\hbar^2 = 0.2624665\ eV^{-1}\text{Å}^{-2}$.)

A solution Ψ^{in} is valid inside the well and a solution Ψ^{out} is valid outside the well. Then the wavefunction will be

$$\Psi = \begin{cases} \Psi^{in} & ; \ \xi \leqslant \xi_o \\ \Psi^{out} & ; \ \xi \geqslant \xi_o . \end{cases} \tag{6}$$

The function Ψ^{in} can be separated as

$$\Psi^{in}(\xi,\eta,\phi) = R^{in}(\xi)\ S^{in}(\eta)\ \Phi(\phi);\ \xi \leqslant \xi_o . \tag{7}$$

Helmholtz's equation separates accordingly.

$$\frac{d^2\Phi}{d\phi^2} + m^2\Phi = 0 \tag{8}$$

$$\frac{d}{d\eta}\{(1-\eta^2)\frac{dS^{in}}{d\eta}\} + \{\eta^2 k_{in}^2 - \frac{m^2}{1-\eta^2} + \lambda_m^{in}\}S^{in} = 0 \tag{9}$$

$$\frac{d}{d\xi}\{(1+\xi^2)\frac{dR^{in}}{d\xi}\} + \{\xi^2 k_{in}^2 + \frac{m^2}{1+\xi^2} - \lambda_m^{in}\}R^{in} = 0 \tag{10}$$

Any choice of k_{in}^2 (that is, of energy) yields a sequence of discrete eigenvalues λ_{mn}^{in}. The subscript n serves to order these eigenvalues. It is convenient to choose n = m, m+1, ... because in the limit $b \to a$ (i.e., the limit in which the oblate-spheroidal well becomes spherical) $\lambda_{mn}^{in} \to n(n+1)$. Thus in the spherical limit n is the quantum number of the total angular momentum.

Equations 8 through 10 for a particular k_{in}^2 yield a set of solutions

$$\{ \psi^{in} = R_{mn}^{in}(\xi;k_{in}^2)\, S_{mn}^{in}(\eta;k_{in}^2) \begin{matrix}\cos(m\phi)\\ \sin(m\phi)\end{matrix} ; n \geq m \geq 0 \} . \quad (11)$$

The inner radial functions $R_{mn}^{in}(\xi;k_{in}^2)$ can be evaluated through their expansions in spherical Bessel functions $j_{n'}(\frac{1}{2}d\, k_{in}\, \xi)$. The angular functions $S_{mn}^{in}(\eta;k_{in}^2)$ can be evaluated through their expansions in associated Legendre functions $P_{n'}^{m}(\eta)$.

The function ψ^{out} can similarly be separated as

$$\psi^{out}(\xi,\eta,\phi) = R^{out}(\xi)\, S^{out}(\eta)\, \Phi(\phi) \; ; \xi \geq \xi_o . \quad (12)$$

The separated equations are identical to equations 8 - 10 with the label "in" replaced by "out." The following set of solutions is obtained:

$$\{ \psi^{out} = R_{mn}^{out}(\xi;k_{out}^2)\, S_{mn}^{out}(\eta;k_{out}^2) \begin{matrix}\cos(m\phi)\\ \sin(m\phi)\end{matrix} ; n \geq m \geq 0 \} . \quad (13)$$

The outer radial functions $R_{mn}^{out}(\xi;k_{out}^2)$ can be evaluated through their expansions in modified spherical Bessel functions $k_{n'}(\frac{1}{2}d\,|k_{out}|\xi)$. The outer angular functions $S_{mn}^{out}(\eta;k_{out}^2)$ can be evaluated through their expansions in associated Legendre functions $P_{n'}^{m}(\eta)$.

The radial and angular functions R_{mn} and S_{mn}, their expansion coefficients, and the eigenvalues λ_{mn} are discussed by Flammer (8) and by Hodge (9). Flammer's book contains detailed discussion and numerous tables

of eigenvalues and expansion coefficients. Hodge's article contains an algorithm for obtaining the expansion coefficients and eigenvalues. Hodge's algorithm is easily programmed and worked well in the calculations described later in this chapter.

Quantization in the limit $V_o \to \infty$

In the limiting case $V_o \to \infty$ quantization is easy. In this case the wavefunction must vanish for $\xi \geq \xi_o$. Hence the wavefunction is simply

$$\psi^{\infty}_{mn} = \begin{cases} \psi^{in}_{mn} \; ; \; \xi \leq \xi_o \\ 0 \quad ; \; \xi \geq \xi_o \end{cases} . \tag{14}$$

Allowed energy levels E_{mn} are those for which $k^2_{in}(E_{mn})$ is such that

$$R^{in}_{mn}(\xi_o ; k^2_{in}) = 0. \tag{15}$$

Energy levels E_{mn} for which $m > 0$ are doubly degenerate.

In the spherical limit $b \to a$ the allowed energy levels are simply those energies E_{mn} for which $(-b\,k_{in})$ is a zero of the nth spherical Bessel function. Energy levels for several m and n are plotted in Figure 3 as functions of the well's eccentricity $e = \sqrt{a^2 - b^2}\,/a$.

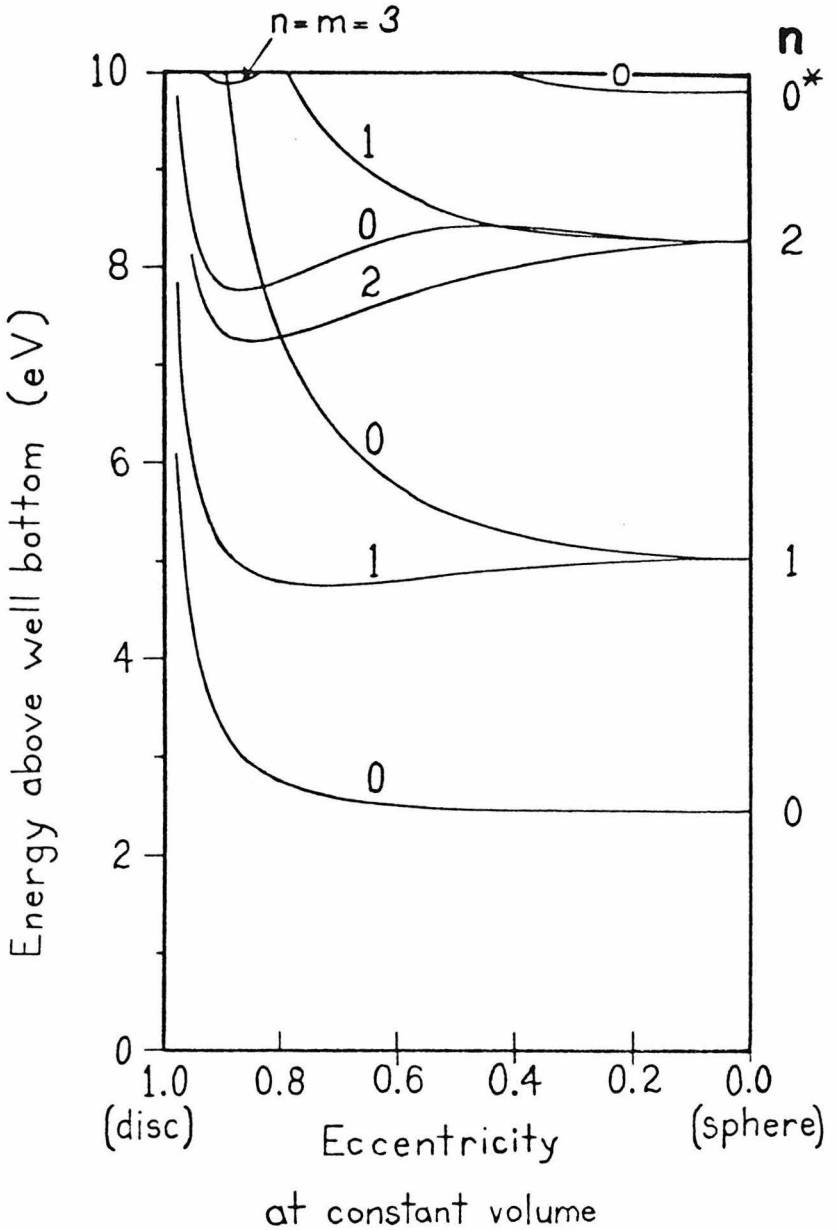

Figure 3. Energies versus eccentricity in the limit $V_o \to \infty$. The well has a constant volume of 251.25 Å^3. Energy levels $E_{mn} \leq 10$ eV above the well bottom are labeled with n along the right-hand side and with m above individual curves. The energy level labeled n=0* has a 'radial' (ξ-type) nodal surface. The asterisk is to indicate the presence of a nodal surface of that type.

In Figure 3 the volume of the well is held constant as e changes. The volume of an oblate spheroid is $V = \frac{4}{3}\pi (a^2 b)^{1/3}$. Thus as the eccentricity e increases from 0 to 1 the semiminor axis b decreases to approach zero and the semimajor axis a approaches infinity. The effective radius $R \equiv (a^2 b)^{1/3}$ for which Figure 3 was plotted is $R = 3.9145$ Å.

An oblate-spheroidal square well has been proposed as a model for the potential in which a nucleon moves in the nucleus (10). In this context energy levels have been calculated previously in the limit $V_o \to \infty$(11).

Quantization for Finite V_o

Wave functions for which V_o is finite have spatial extent beyond the boundary of the well. Such spatial extent is essential if two wells are to transfer an electron due to long-range electronic interaction. Quantization of the energy in the case of finite V_o can be accomplished by requiring continuity of the wave function and its gradient at the boundary, i.e., at $\xi = \xi_o$. It is however not possible to achieve continuity using the separated wave functions given in equations 11 and 13. Rather the wave function can be expanded using the sets of functions in equations 11 and 13 as basis functions.

$$\Psi_{mn}(\xi,\eta,\phi;E) = N_{mn}^{-1} \begin{pmatrix} \cos m\phi \\ \sin m\phi \end{pmatrix} \tag{16}$$

$$\times \begin{cases} \sum_{i=0}^{\infty} c_i^{in} R_{m,m+r}^{in}(\xi;k_{in}^2) S_{m,m+r}^{in}(\eta;k_{in}^2) ; & \xi \leqslant \xi_o \\ \sum_{i=0}^{\infty} c_i^{out} R_{m,m+r}^{out}(\xi;k_{out}^2) S_{m,m+r}^{out}(\eta;k_{out}^2) ; & \xi \geqslant \xi_o \end{cases}$$

In equation 16 $r = 2i+s$ where $s\equiv 0$ for wave functions even with respect to η and $s\equiv 1$ for wave functions odd with respect to η. The index n has the same parity as m+r and serves to index the wave functions Ψ_{mn}. It is convenient to again choose $n = m, m+1, \ldots$ since in the spherical limit (see equation 17) n recovers its spherical meaning as the quantum number of the total angular momentum.

$$\lim_{b \to a} \Psi_{mn}(\xi,\eta,\phi;E) \propto \begin{pmatrix} \cos m\phi \\ \sin m\phi \end{pmatrix} P_n^m(\eta) \tag{17}$$

$$\times \begin{cases} j_n(k_{in}r)\, k_n(|k_{out}|a) ; & r \leqslant a \\ j_n(k_{in}a)\, k_n(|k_{out}|r) ; & r \geqslant a \end{cases}$$

The factor N_{mn} in equation 16 is a normalization factor which is computed numerically using Gauss-Legendre and Gauss-Laguerre quadratures.

The allowed energies for given m and n and $b < a$ can be obtained by requiring that the wave function and its gradient be continuous at the boundary. Because the boundary surface is a function of only one variable ξ, continuity of $\nabla\Psi$ at ξ_o requires only continuity of Ψ and continuity of $\partial\Psi/\partial\xi$ at ξ_o. Equations 18 and 19 express the continuity (quantization) condition.

$$\lim_{\xi\to\xi_o^-} \Psi_{mn}(\xi,\eta,\phi;k_{in}^2) = \lim_{\xi\to\xi_o^+} \Psi_{mn}(\xi,\eta,\phi;k_{out}^2) \qquad (18)$$

$$\lim_{\xi\to\xi_o^-} \frac{\partial}{\partial\xi}\Psi_{mn}(\xi,\eta,\phi;k_{in}^2) = \lim_{\xi\to\xi_o^+} \frac{\partial}{\partial\xi}\Psi_{mn}(\xi,\eta,\phi;k_{out}^2) \qquad (19)$$

Thus quantization of the energy involves matching the two expansions given in equation 16, and their partial derivatives with respect to ξ, at $\xi = \xi_o$.

We have adopted the following method for determining the energies E_{mn} for which equations 18 and 19 are satisfied. Each outer angular function $S_{mn}^{out}(\eta;k_{out}^2)$ is expanded in the complete set of inner angular functions $S_{mn}^{in}(\eta;k_{in}^2)$. At this point Ψ_{mn} is represented as an expansion in $S_{mn}^{in}(\eta;k_{in}^2)$ both for $\xi \leqslant \xi_o$ and for $\xi \geqslant \xi_o$. Equating the two expansions term-by-term at $\xi = \xi_o$ yields equation 20.

$$\underline{c}^{in} = \underline{\underline{M}}_E \, \underline{c}^{out} \qquad (20)$$

In equation 20 the vector $\underline{c}^{in} = (c_o^{in}, c_1^{in}, \ldots.)$ and the vector $\underline{c}^{out} = (c_o^{out}, c_1^{out}, \ldots.)$ where c_i^{in} and c_i^{out} are defined in equation 16. Both vectors are of infinite dimension but are in practice truncated, of course. The elements of the matrix $\underline{\underline{M}}_E$, where the subscript E indicates the matrix's dependence on the energy, are given in equation 21.

$$(\underline{\underline{M}}_E)_{ij} = \frac{\langle S_{mp}^{out} \mid S_{mq}^{in} \rangle}{\langle S_{mq}^{in} \mid S_{mq}^{in} \rangle} \times \frac{R_{mp}^{out}(\xi_o;\ k_{out}^2)}{R_{mq}^{in}(\xi_o;\ k_{in}^2)} \tag{21}$$

where $p = m + 2j + s;\ j \geq 0$, and

$q = m + 2i + s;\ i \geq 0.$

Similarly requiring continuity of the gradient yields the matrix equation

$$\underline{c}^{in} = \underline{\underline{M}}'_E\ \underline{c}^{out} \tag{22}$$

where

$$(\underline{\underline{M}}'_E)_{ij} = \frac{\langle S_{mp}^{out} \mid S_{mq}^{in} \rangle}{\langle S_{mq}^{in} \mid S_{mq}^{in} \rangle} \times \frac{\frac{d}{d\xi_o} R_{mp}^{out}(\xi_o;\ k_{out}^2)}{\frac{d}{d\xi_o} R_{mq}^{in}(\xi_o;\ k_{in}^2)} \tag{23}$$

and again $p = m + 2j + s;\ j \geq 0$, and

$q = m + 2i + s;\ i \geq 0.$

Equations 20 and 22 together yield equation 24.

$$\underline{c}^{out} = (\ \underline{\underline{M}}_E^{-1}\ \underline{\underline{M}}'_E\ )\ \underline{c}^{out} \tag{24}$$

Thus $\underline{c}^{out}$ is an eigenvector of the matrix $(\underline{\underline{M}}_E^{-1}\,\underline{\underline{M}}_E')$ having unit eigenvalue. In practice energy levels and expansion coefficients are found by iterating on equation 24 to obtain an eigenvector associated with an eigenvalue of 1. This eigenvector is $\underline{c}^{out}$. The inner expansion coefficients $\underline{c}^{in}$ are then obtained using equation 20.

Several energy levels are shown in Figure 4 as functions of eccentricity at constant volume. The levels were calculated for a well depth $V_o = 10$ eV and an effective radius $R \equiv (a^2 b)^{1/3} = 3.9145\,\text{Å}$. Figure 4 is thus directly comparable to Figure 3 for which $V_0 = \infty$.

The energy levels are shown as functions of V_o in Figure 5. For these calculations, $a = 4.85\,\text{Å}$ and $b = 2.55\,\text{Å}$, which implies $e = 0.8506$. The value of a was chosen as an estimate of the in-plane radius of porphine, and is the same as the a used by Platt (12) to treat porphine as a $2a \times 2a$ square. The value $b = 2.55\,\text{Å}$ was chosen to give a reasonable height to the spheroidal well. The average height of a spheroid is $h = \frac{2}{3} b$. The interplane spacing in graphite, which may be used to estimate the 'thickness' of a pi orbital, is $\simeq 3.4\,\text{Å}$. The value of b chosen is such that $h = \frac{2}{3} b = \frac{1}{2}(3.4\text{Å})$.

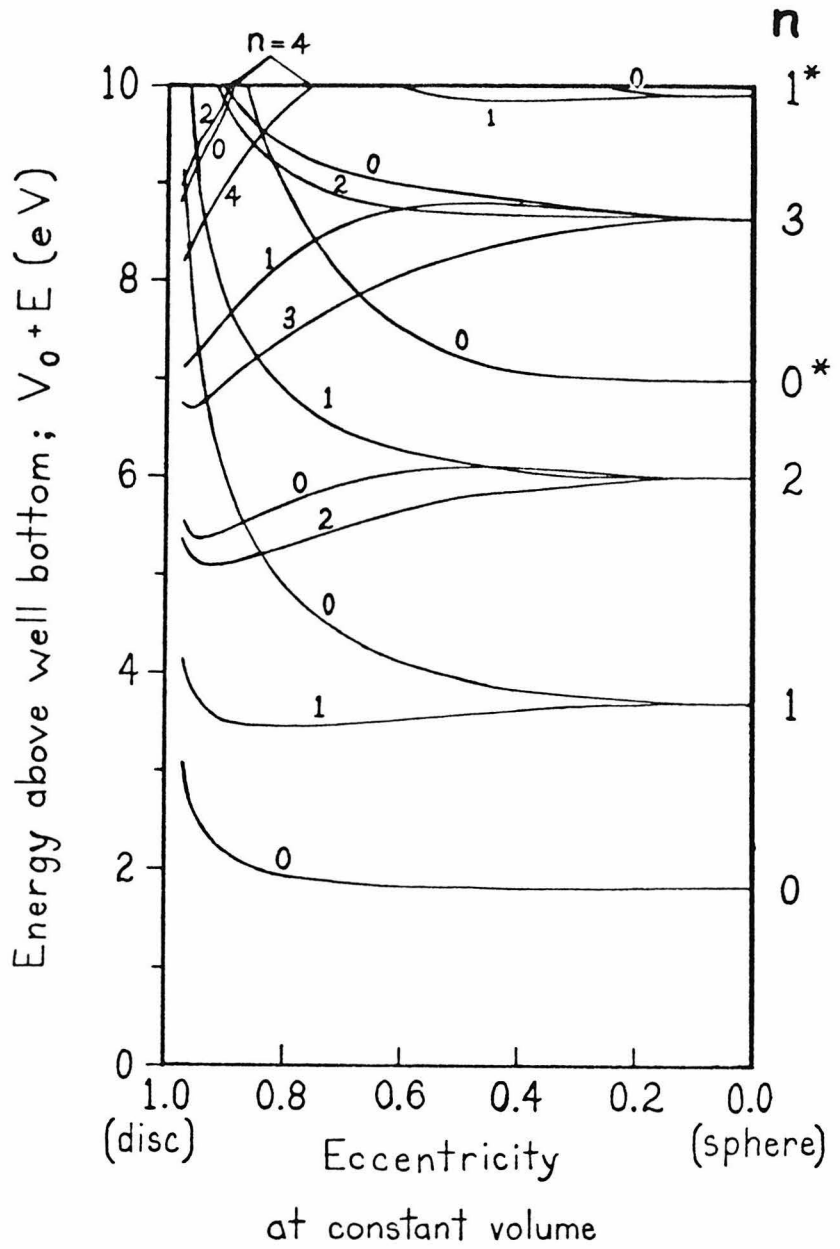

Figure 4. Energies versus eccentricity for V_0 = 10 eV. The well has a constant volume of 251.25 Å^3. Energy levels E_{mn} are labeled with n along the right-hand side. An asterisk indicates a state having a ξ-type ('radial') nodal surface. The value of m is indicated for each curve.

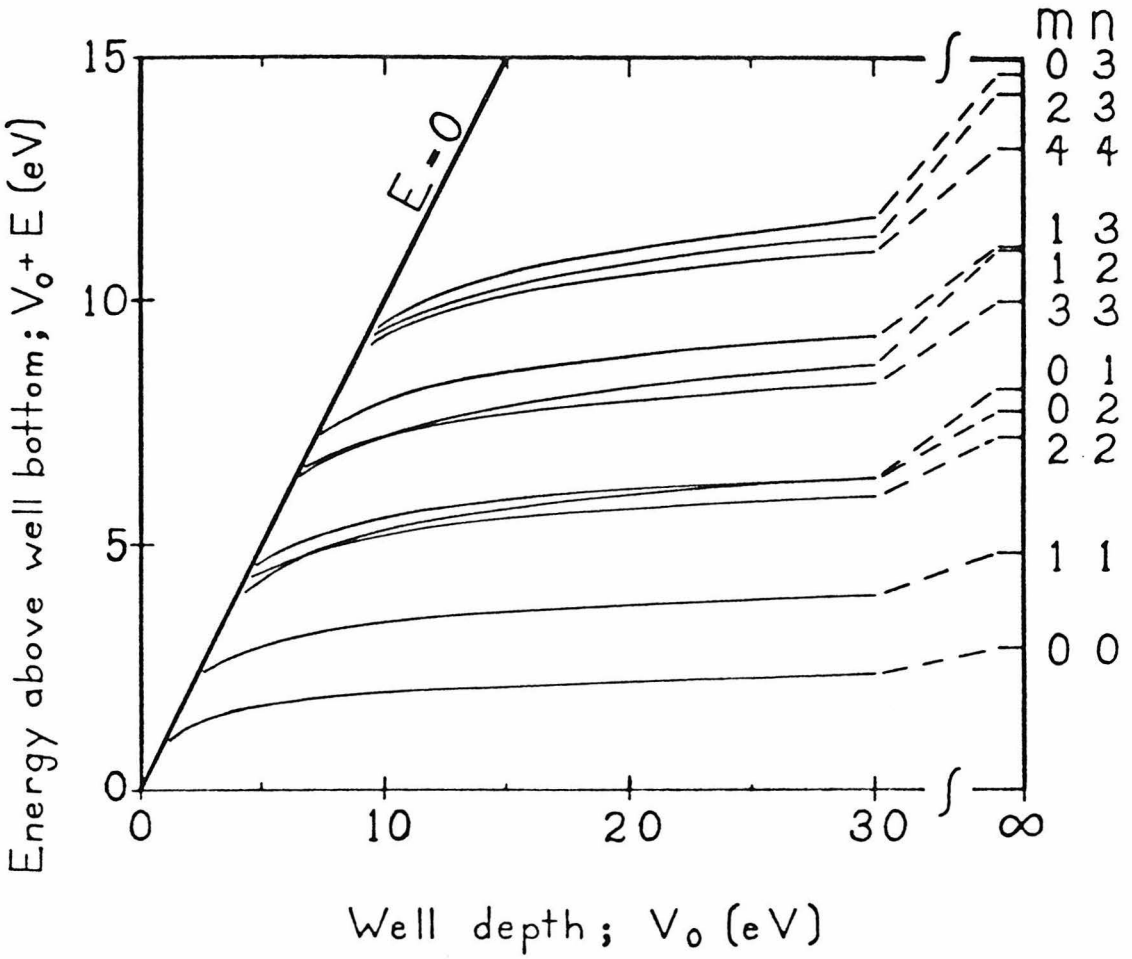

Figure 5. Energies versus well depth.

a = 4.85 Å. b = 2.55 Å. Contour plots of the wavefunctions corresponding to these energy levels at V_o = 10 eV are shown in the following figures.

Several plots of contours of wave functions are shown in Figures 6 through 10. These are plots of wave functions for which energies at well-depth V_o=10 eV are shown in Figure 4. Each wavefunction corresponds to a different (m,n) pair and is the lowest-energy function for that pair. Although the nodal structure of these wavefunctions is roughly the same as that obtained using spherically symmetric potentials, the wavefunctions are noticeably nonspherical.

Large-r Behavior of the Wavefunctions

At a large radial distance each of the outer radial functions has the asymptotic form given in equation 25.

$$R_{mn}^{out}(\xi;k_{out}^2) \sim \frac{2}{\alpha r} e^{-\alpha r/2} \quad \text{as } r \to \infty \qquad (25)$$

$$\text{where } \alpha \equiv 2|k_{out}| = 2\left(\frac{2m}{\hbar^2}|E|\right)^{\frac{1}{2}}.$$

Hence the wavefunction Ψ_{mn} at a fixed large r and fixed ϕ is

$$\Psi_{mn} \propto \sum_{i=0}^{\infty} c_i^{out} S_{m,m+r}^{out}(\eta;\, k_{out}^2) \,. \qquad (26)$$

We can examine the angular dependence of Ψ_{mn} at large r by projecting Ψ_{mn} in equation 26 on the associ-

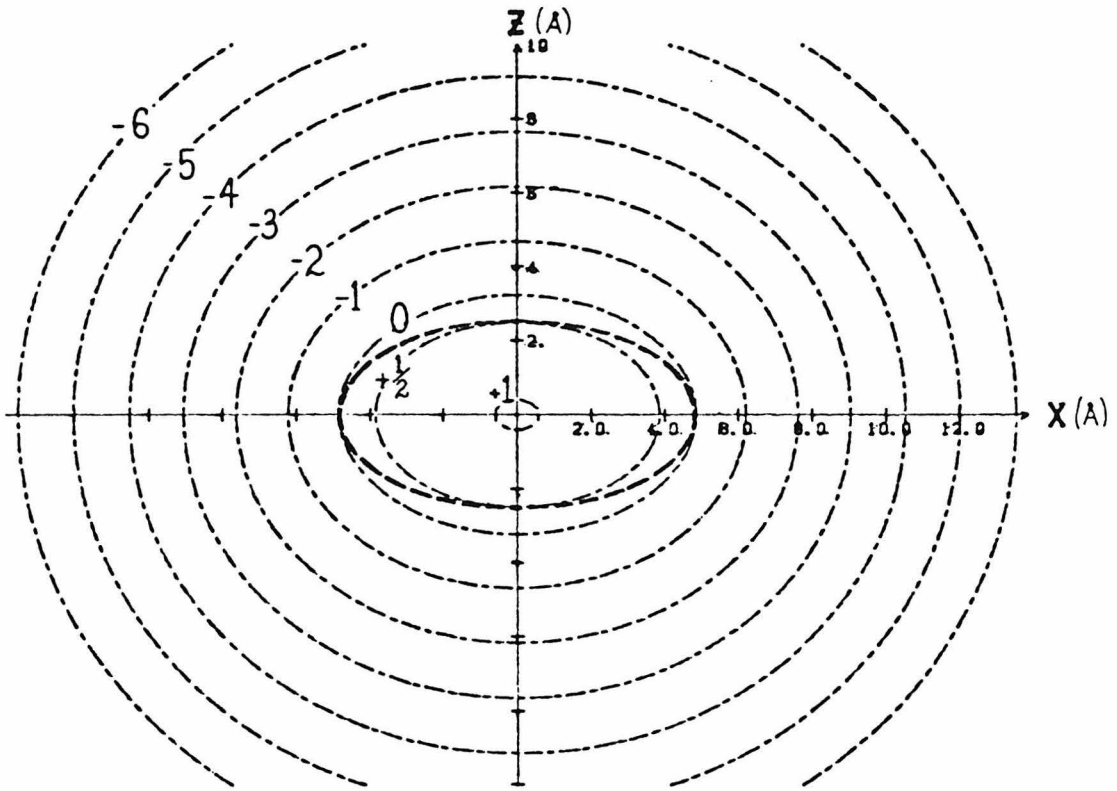

Figure 6. Contours of Ψ_{mn} for m=0, n=0.

V_o = 10 eV. E = - 7.98 eV. a = 4.85 Å. b = 2.55 Å.
The heavy dashed line is the well boundary.
The contours are labeled with $\log_{10}|\Psi_{00}|$.

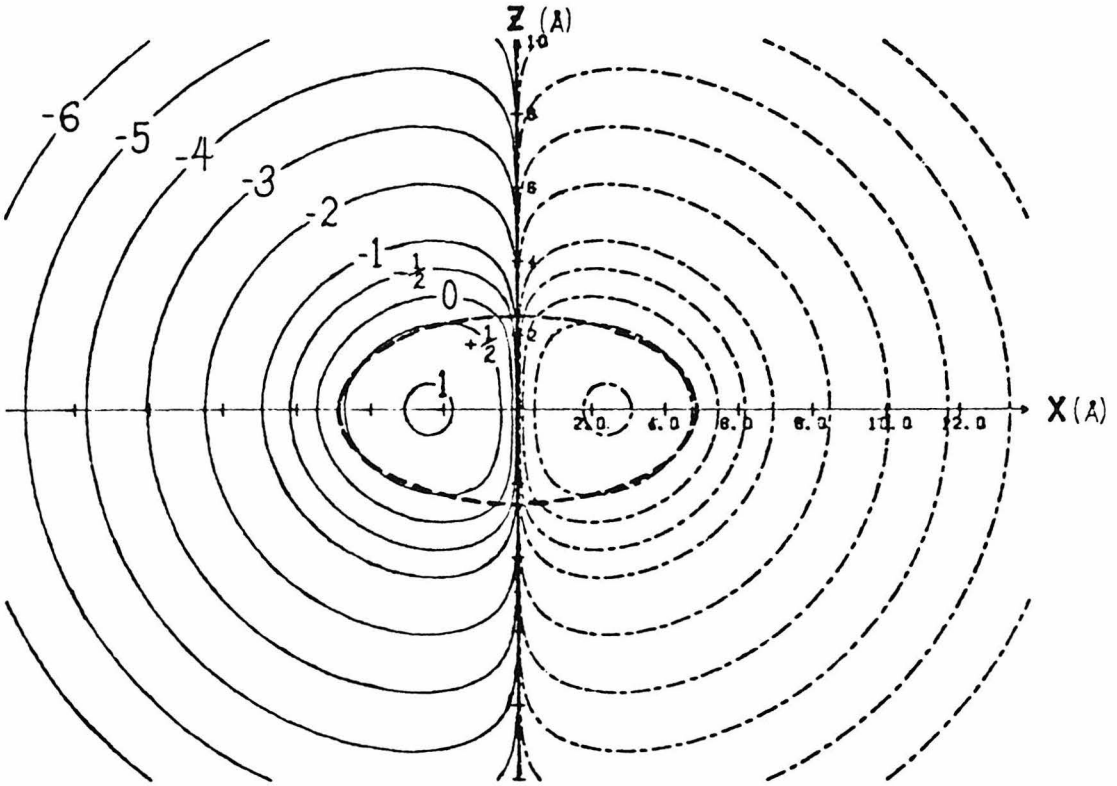

Figure 7. Contours of Ψ_{mn} for m=1, n=1.

V_o = 10 eV. E = - 6.55 eV. a = 4.85 Å. b = 2.55 Å.
The heavy dashed line is the well boundary.
The contours are labeled with $\log_{10}|\Psi_{11}|$.
Dashed contours indicate $\Psi_{11} < 0$. Solid
contour lines are for $\Psi_{11} > 0$.

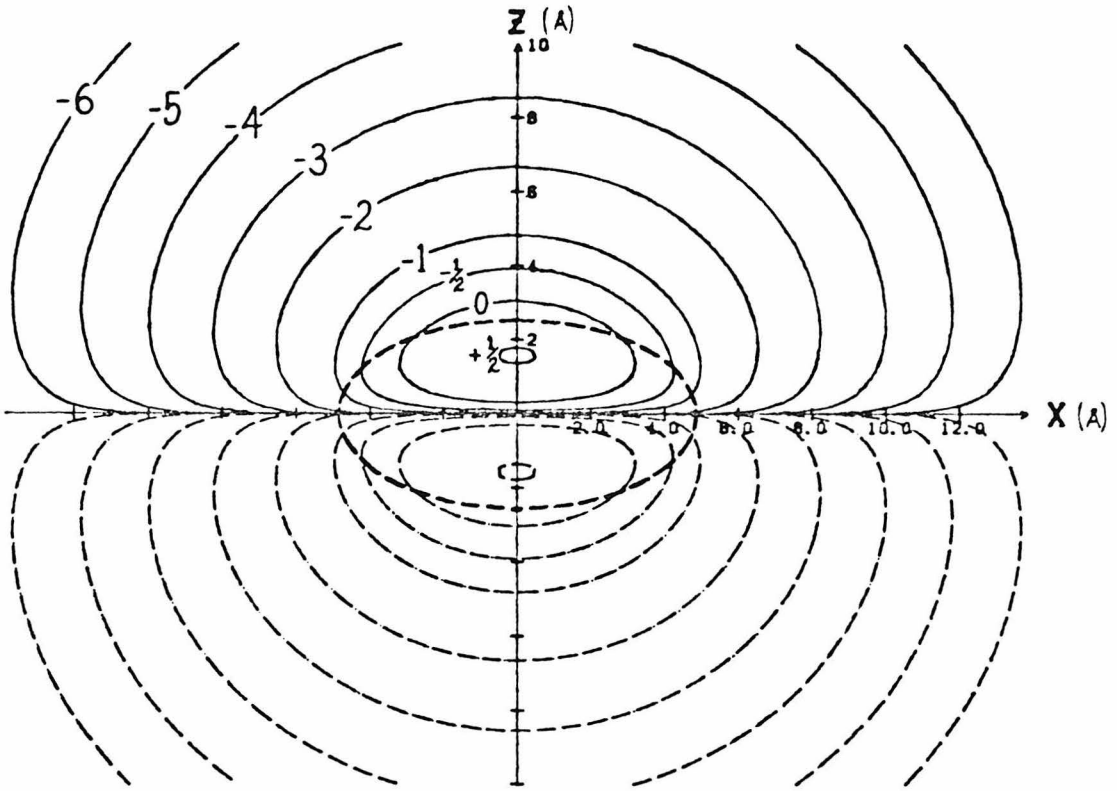

Figure 8. Contours of Ψ_{mn} for m=0, n=1.

V_o = 10 eV. E = - 4.70 eV. a = 4.85 Å. b = 2.55 Å.
The heavy dashed line is the well boundary.
The contours are labeled with $\log_{10}|\Psi_{01}|$.
Dashed contours indicate $\Psi_{01} < 0$. Solid
contours are for $\Psi_{01} > 0$.

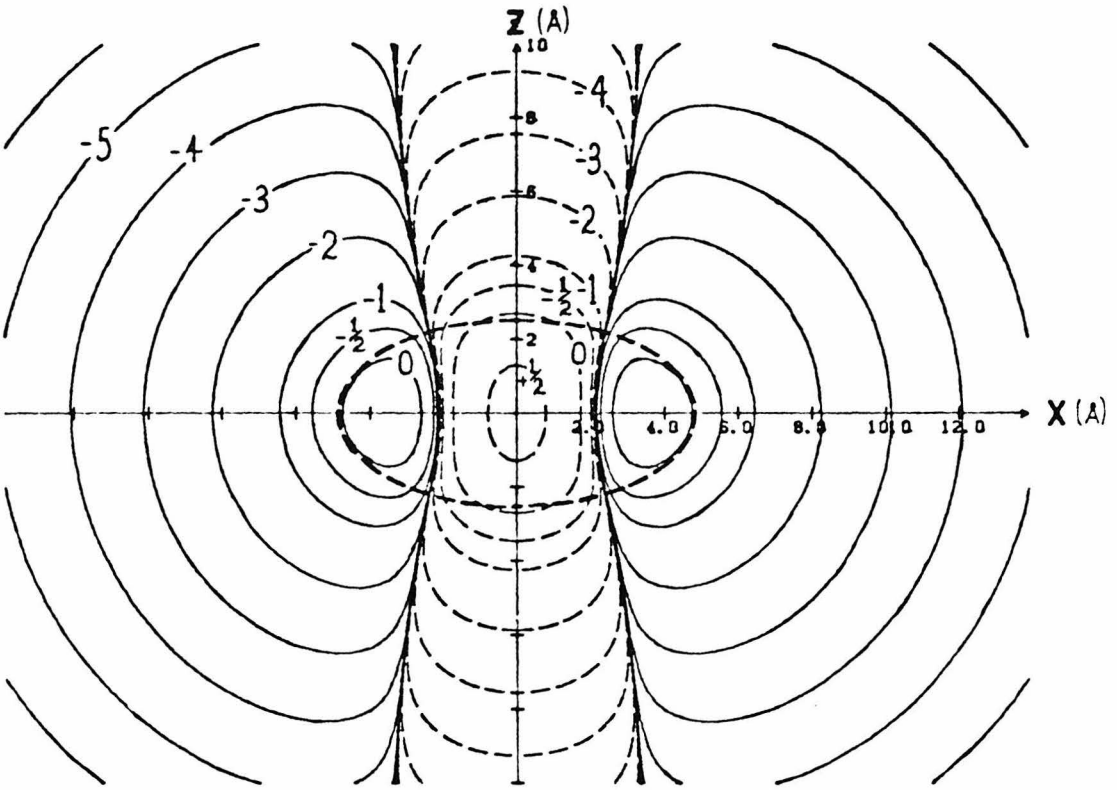

Figure 9. Contours of Ψ_{mn} for m=0, n=2.

V_o = 10 eV. E = - 4.44 eV. a = 4.85 Å. b = 2.55 Å.
The heavy dashed line is the well boundary.
The contours are labeled with $\log_{10}|\Psi_{02}|$.
Dashed contours indicate $\Psi_{02} < 0$. Solid
contours are for $\Psi_{02} > 0$.

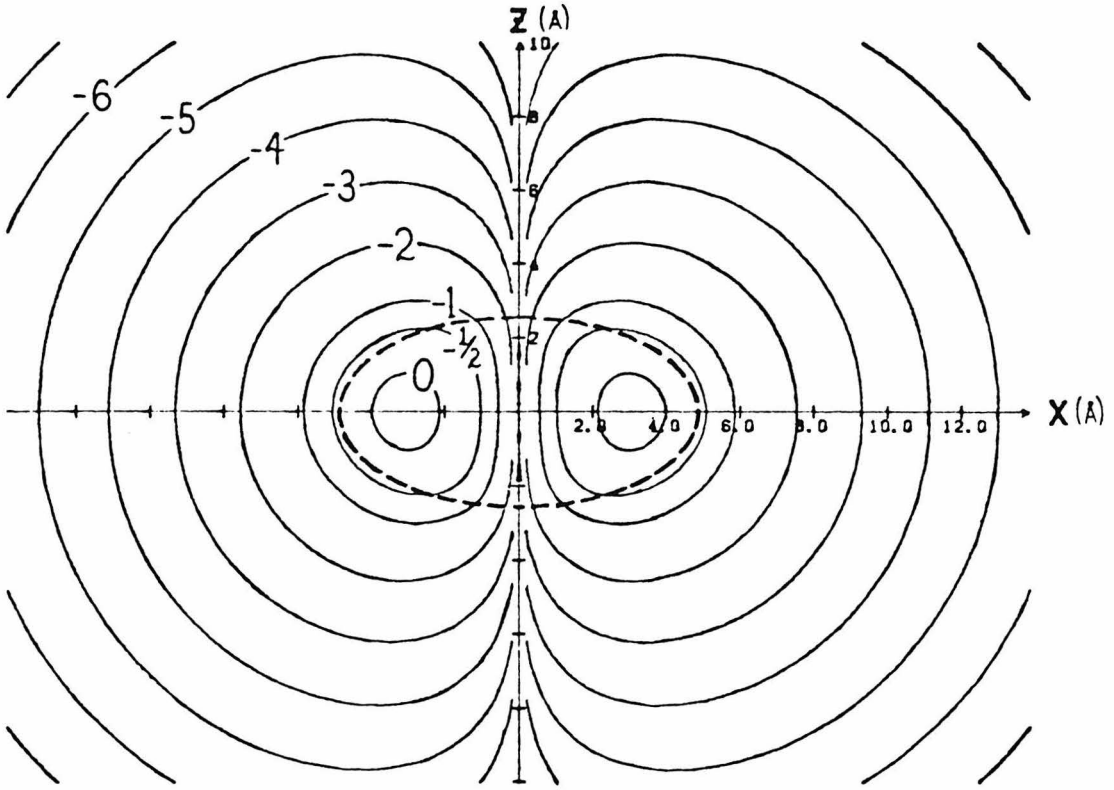

Figure 10. Contours of Ψ_{mn} for m=2, n=2.

V_o = 10 eV. E = - 4.82 eV. a = 4.85 Å. b = 2.55 Å.
The heavy dashed line is the well boundary.
The contours are labeled with $\log_{10}|\Psi_{22}|$.

ated Legendre polynomials $P_n^{m'}(\eta)$; $n' \geq m$. Recall (equation 4) that for large r $\eta \sim \cos\theta$. If the large-r angular probability distribution were insensitive to the non-zero eccentricity of the spheroidal well, then we would find $|\langle P_n^{m'}|\Psi_{mn}\rangle|^2 \propto \delta_{n'n}$, but that is not found. Even at asymptotically large distances the electron 'sees' the nonsphericity of the potential well. Calculated projections squared are presented in Figure 11 for the case m=0, n=2 and $V_o = 10$ eV. These projections are plotted for wells of three eccentricities, all with effective radius $R = 3.9145$ Å. The quantity plotted is the square of a normalized projection, as defined in equation 27, at asymptotically large radial distance.

$$\mathcal{P}_{n'} \equiv \frac{\langle \Psi_{mn}|P_n^{m'}\rangle}{\langle P_n^{m'}|P_n^{m'}\rangle} \Bigg/ \sum_i \frac{\langle \Psi_{mn}|P_i^m\rangle}{\langle P_i^m|P_i^m\rangle} \qquad (27)$$

Electron Transfer Between Sites

The electronic states of an electron in the potential of a single molecule (electron site) can be described using the spheroidal-well model discussed in the preceding section of this chapter. A system

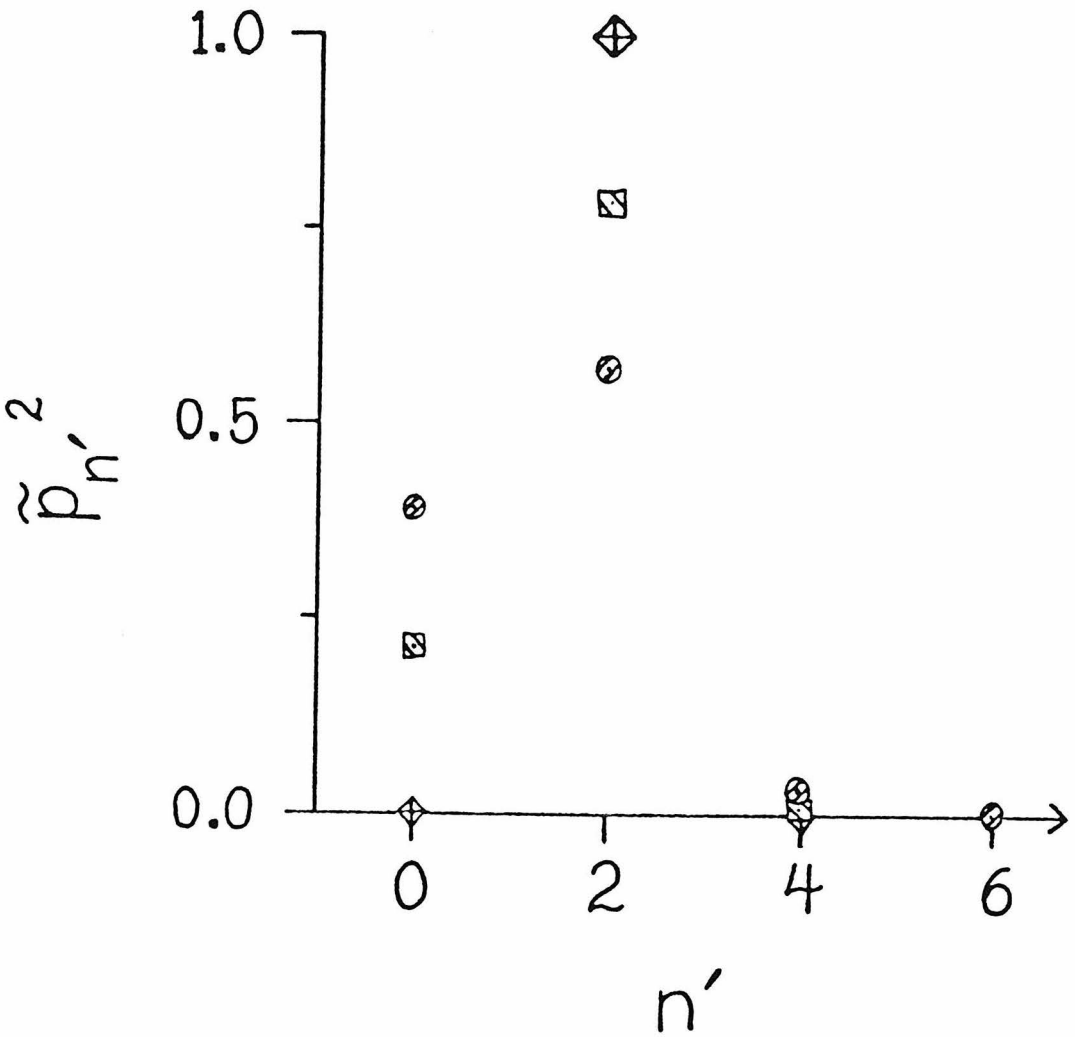

Figure 11. Normalized projections $|\langle\Psi_{02}|P_n^{o},\rangle|^2$ in lim $r \to \infty$.

The quantity $\tilde{P}_n$, is defined in equation 27. e is the eccentricity of the well, at a constant volume of 251.25 A^3. For these calculations V_o = 10 eV. The symbols correspond to the following eccentricities e:

◆ e = 0.1, E = -4.006 eV

▧ e = 0.5, E = -3.922 eV

⊘ e = 0.9, E = -4.565 eV

consisting of two such wells (site A and site B) and one electron (the 'transferable' electron) can be used to model electron transfer between a pair of molecules A and B. The rate constant for electron transfer (reaction 28)

$$A^- + B \xrightarrow{k} A + B^- \qquad (28)$$

is given in equation 1, within the Golden-Rule and Condon approximations. That rate constant is for transfer between sites having specific and fixed orientations and relative separation. In order to use equation 1, nuclear coordinates and an associated set of vibrational states has been assumed to be present in the wells and the intervening medium, but will not be dealt with explicitly in what follows. It is the dependence of the rate constant, and in particular of the electronic matrix element V_{AB}, on the separation and orientation of the reactants that will be examined in the remainder of this chapter.

The matrix element V_{AB} is to be calculated within the model system consisting of two oblate-spheroidal square wells (labeled A and B) and one transferable electron.

The zeroth-order problem is that in which the two wells do not interact (e.g., the infinite-separation limit). Only the following two zeroth-order electronic states will be considered:

(i) The electronic state for the electron on site A, uninfluenced by site B. The wavefunction for this state is denoted ψ^{A}_{mn}. The subscripts m and n index angular momentum in the sense described previously in this chapter. The wavefunction is given in equation 16, with the origin of coordinates at the center of well A, and with ξ_o defining the boundary of well A. The value of V_o (as in equation 3) appropriate to site A is denoted V^{A}_{o}.

(ii) The electronic state for the electron on site B, uninfluenced by site A. The wavefunction associated with this state is denoted $\psi^{B}_{m',n'}$. The subscripts m′ and n′ index the angular momentum. The primes are only to distinguish these numbers from the m and n that characterize the wavefunction on site A. The function $\Psi^{B}_{m',n'}$ is given in equation 16, with m′ and n′ replaced by m and n there, with the origin of coordinates located at the center of well B, and with ξ_o defining the boundary of well B. The value of V_o appropriate to site B is denoted V^{B}_{o}.

The electronic matrix element V_{AB} appropriate to the present model is given in equation A.34 of the appendix. It is presented in a more explicit form in equation 29.

$$V_{AB} = (H_{AB} - S_{AB}H_{AA}) / (1 - S_{AB}^2) \qquad (29)$$

$$H_{AB} = -V_o^B \int_{\text{well } B} \psi^B_{m',n'} \psi^A_{mn} \, dv_B$$

$$H_{AA} = -V_o^B \int_{\text{well } B} (\psi^A_{mn})^2 \, dv_B$$

$$S_{AB} = \int_{\text{all space}} \psi^B_{m',n'} \psi^A_{mn} \, dv$$

Calculated Results

The results of several calculations of V_{AB} are discussed below. In all calculations that follow the two wells (A and B) are identical, i.e. $V_o^A = V_o^B \equiv V_o$ and for both wells $a = 4.85$ Å and $b = 2.55$ Å. Furthermore the same wavefunction is used in each well. That is, ψ^A_{mn} and $\psi^B_{m',n'}$ can be superimposed by translating and rotating ψ^A_{mn}. (This of course implies $m'=m$ and $n'=n$.)

The energy with which a state is bound is important in determining the rate at which its wavefunction decays outside the well (i.e., in the tunneling region). The radial dependence of each wavefunction Ψ^{A}_{mn} and Ψ^{B}_{mn} is asymptotic at large radial distance r to $2\times\exp(-\alpha r/2)/(\alpha r)$, where $\alpha = 2\sqrt{-2mE}/\hbar$. (This asymptotic dependence follows from equations 16 and 25.) Thus V_{AB} will decay radially as $P\times\exp(-\alpha r/2)$, where P is some function of r^{-1}, at large separation r of A and B. (In the spherical limit $b \to a$ P is a polynomial.) Finally then the rate constant k (see equation 1) is expected to be asymptotically proportional to $P^2\times\exp(-\alpha r)$ at large r. Frequently the factor P^2 is neglected and a simple exponential decay, $k \sim \exp(-\alpha r)$, is assumed.

The value of α has been inferred from experimental measurements of the electron-(14,15) or hole-(16) transfer rate between aromatic molecules and ions in low-temperature glass matrices. The values found range from about 1.0 to 1.5 Å^{-1}. In the calculations below V_o is treated as a parameter and is adjusted so that the energy E of the zeroth-order states Ψ^{A}_{mn} and Ψ^{B}_{mn} yields a specific desired value of $\alpha = 2\sqrt{-2mE}/\hbar$.

Orientation Effect at Contact

The present model can be used to predict the orientation dependence of electron transfer between two molecules in contact. Such a configuration is sketched in Figure 12. The orientation angle θ describes the available configurations for which the major axes and the minor axes of the two spheroidal wells are parallel. These configurations may span part of the range of relative orientations available to chlorophyll and pheophytin in a photosynthetic reaction center, although the correspondence of that system with the present model is rough at best.

The matrix element V_{AB} is plotted versus θ in Figure 13. The results of two calculations are shown. For the solid line, the lowest-energy pi states (m=0, n=1) were used in each well. The well depth V_o=5.6540 eV was chosen so that E_{01}=-1.15 eV, which yields $\alpha = 1.1$ Å^{-1}. For the dashed line the ground state (m=n=0) was used in each well, and V_o=2.5937 eV was chosen so that again E_{00}=-1.15 eV. The dashed line is included in Figure 13 to indicate the importance of the wells' nonspherical shape. Were the wells spherical, V_{AB} would be independent of θ for the m=n=0 state.

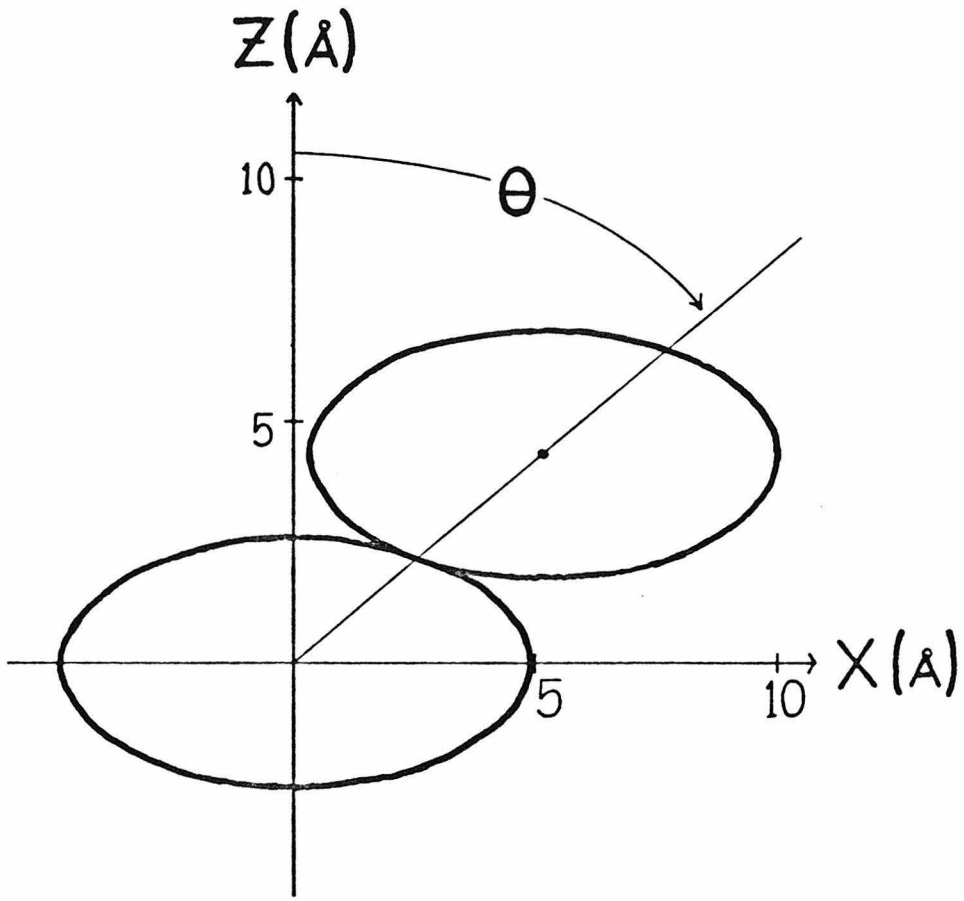

Figure 12. Orientation at contact.

The major and minor axes of both ellipses lie in the plane of the figure. The major axes of wells A and B are parallel, and the minor axes of wells A and B are parallel. The angle θ is the angle plotted on the abscissae of Figures 13 and 14.

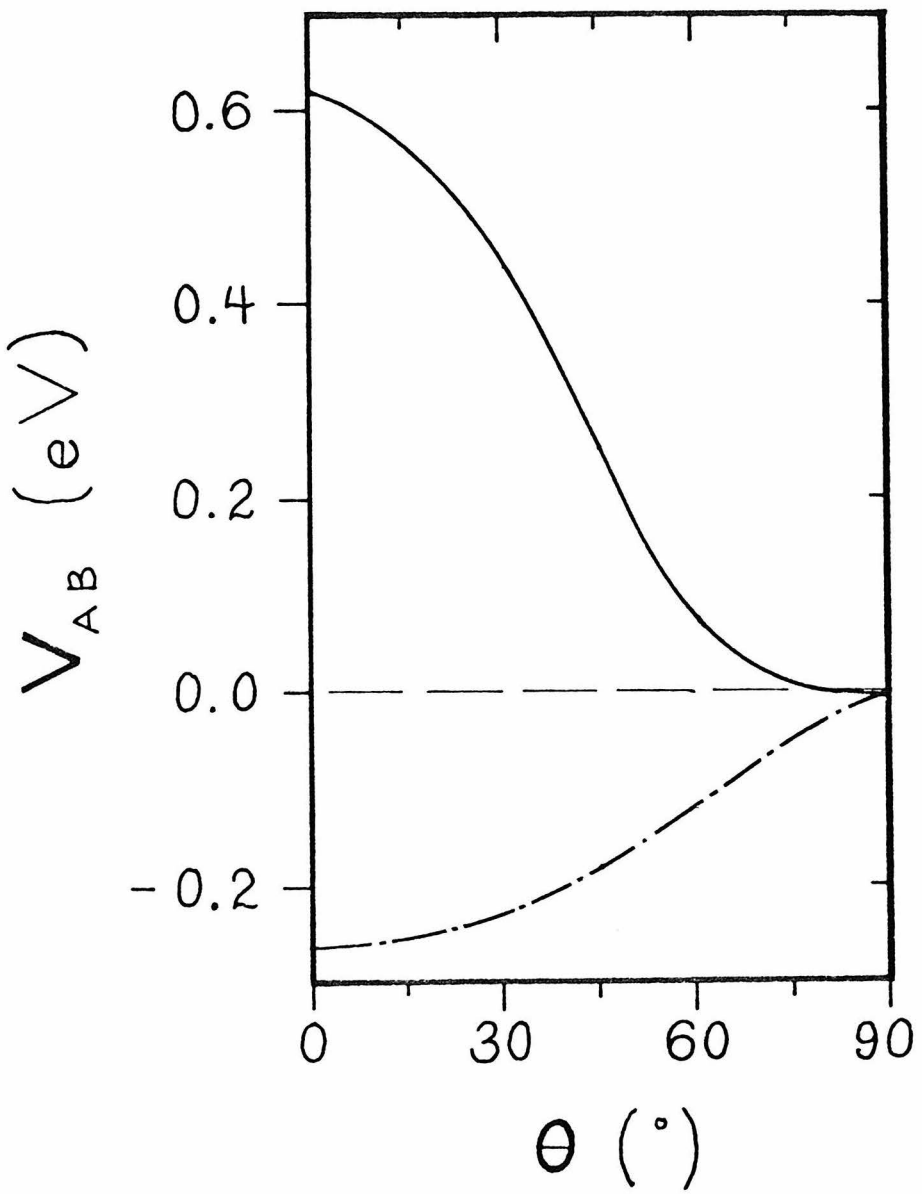

Figure 13. Orientation effect at contact for E = - 1.15 eV.

V_{AB} is the matrix element defined in equation 29. The angle θ is defined in Figure 12. For the solid line m=0, n=1 and V_o = 5.6540 eV in both wells. For the dashed line m=0, n=0, and V_o = 2.5937 eV in both wells.

Figure 14 is analogous to Figure 13, but for Figure 14 $\alpha = 1.45\ \text{Å}^{-1}$ (E = -2.00 eV). This energy corresponds to $V_o = 6.7789$ eV for the pi state and $V_o = 3.6012$ eV for the sigma state.

Orientation Effect at a Distance

Figures 15 and 16 present H_{AB} (defined in equation 29) as a function of orientation angle θ for wells separated by 19.85 Å center-to-center. At this large separation H_{AB} and V_{AB} are nearly identical because the 'correction' factors $S_{AB}H_{AA}$ and S_{AB}^2 (see equation 29) are very small. Both Figure 15 and Figure 16 were plotted using the lowest-energy pi state (m=0,n=1) in each well, and with $a = 4.85$ Å, $b = 2.55$ Å. For Figure 15 $V_o = 5.654$ eV, E = -1.15 eV and $\alpha = 1.1\ \text{Å}^{-1}$. For Figure 16 $V_o = 6.7789$ eV, E = -2.00 eV and $\alpha = 1.45\ \text{Å}^{-1}$.

Three different sets of orientations are considered. These orientations are illustrated at the top of the figures, with the lines indicating the major axes of the spheroidal wells. The wells' minor axes are perpendicular to the lines and lie in the plane of the figures.

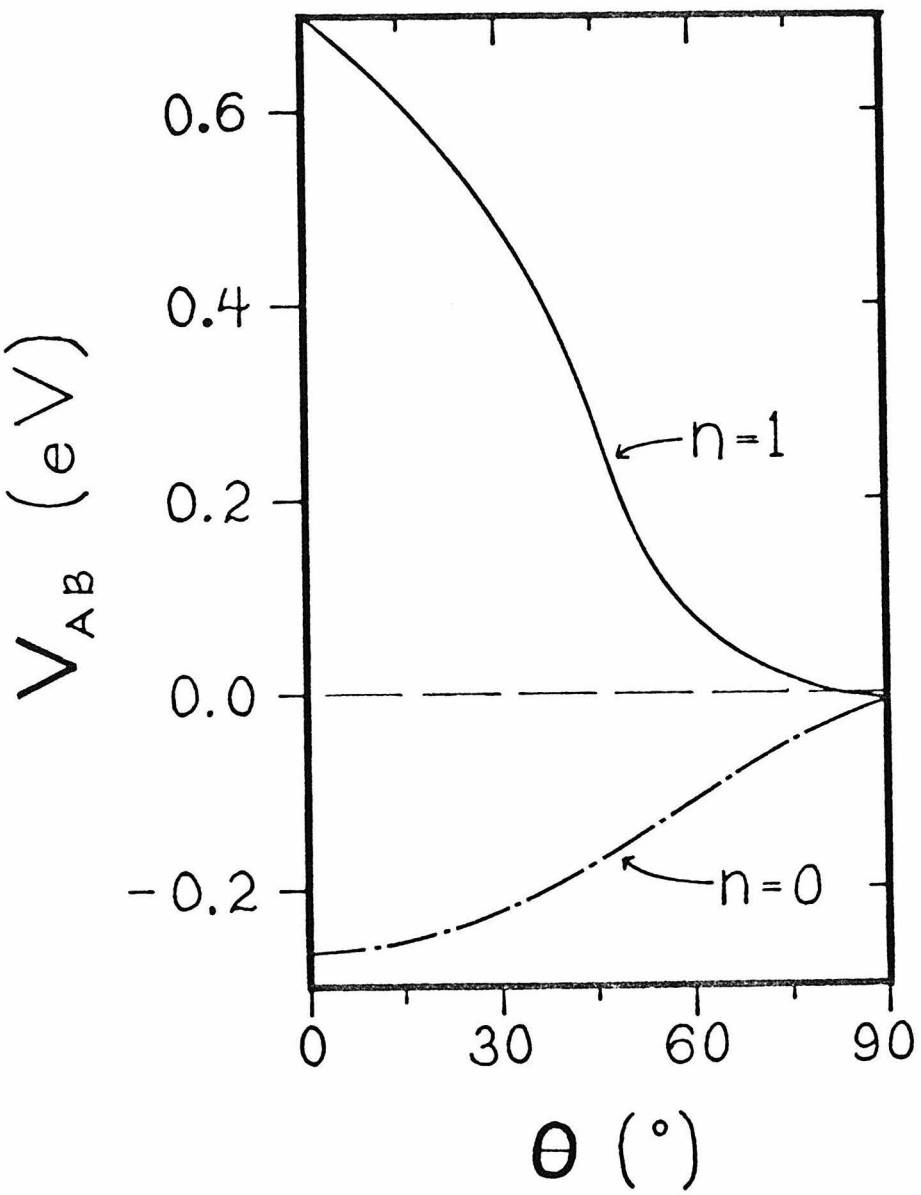

Figure 14. Orientation effect at contact for E = - 2.00 eV.

V_{AB} is the matrix element defined in equation 29. The angle θ is defined in Figure 12. For the solid line m=0, n=1 and V_o = 6.7789 eV in both wells. For the dashed line m=0, n=0 and V_o = 3.6012 eV in both wells.

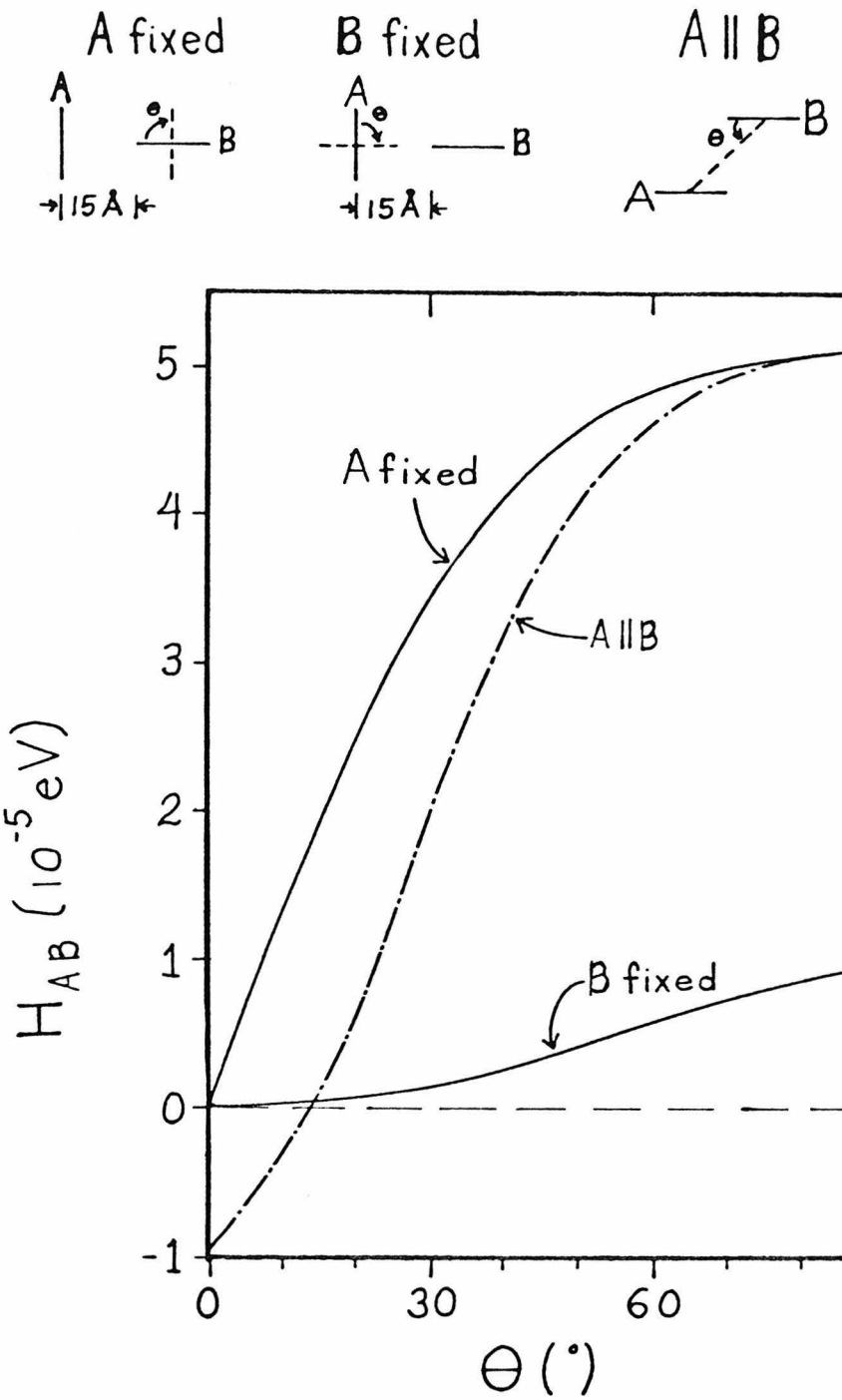

Figure 15. Orientation effect at a distance; E = - 1.15 eV.

In both the A and the B well m=0, n=1, and V_o = 5.6540 eV. H_{AB} is defined in equation 29. The sketches at the top of the figure show the meaning θ has for each of the three sets of configurations. The major and minor axes of both well A and well B lie in the plane of the sketches.

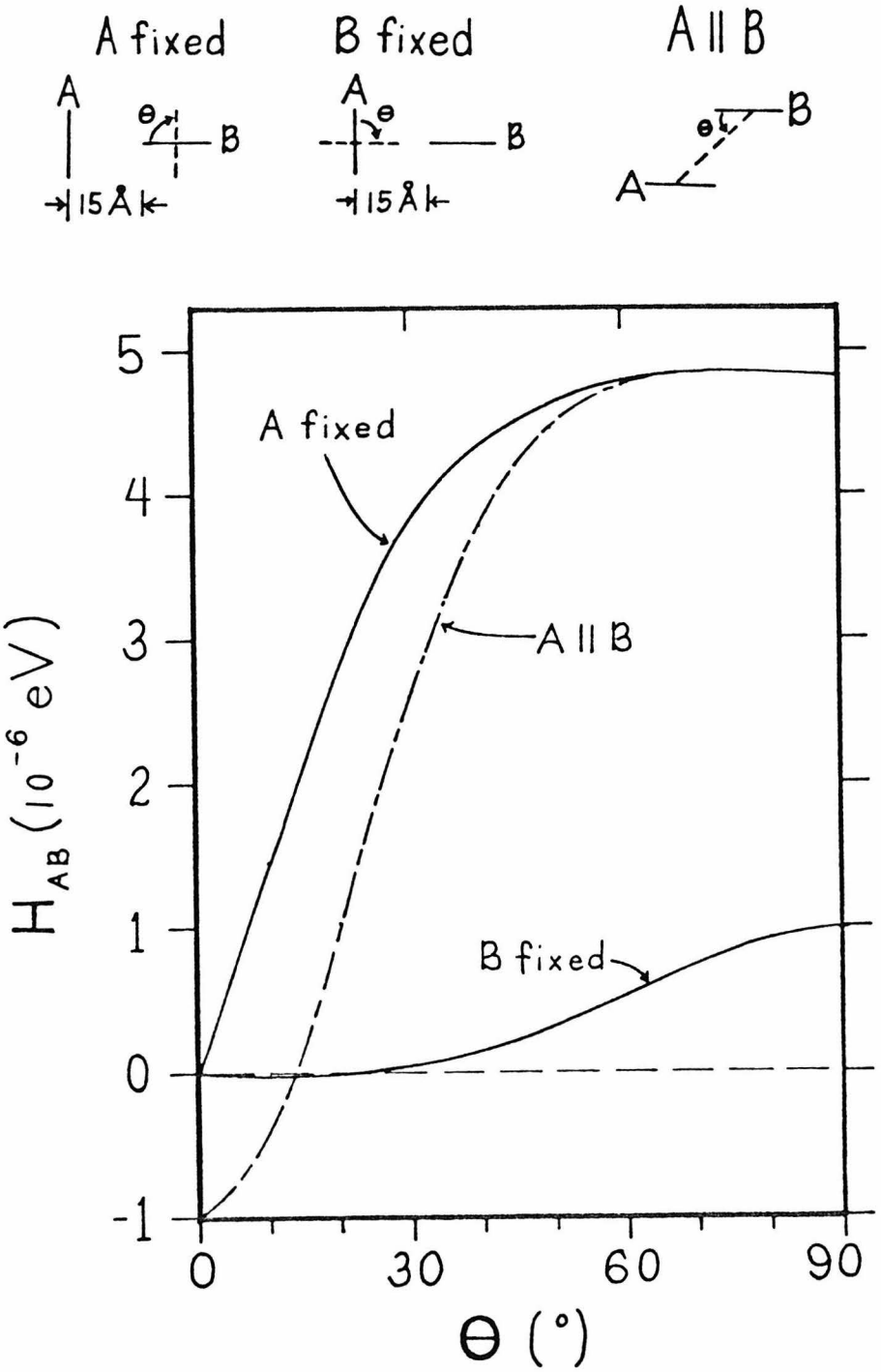

Figure 16. Orientation effect at a distance; E = - 2.00 eV.

In both the A and the B well m=0, n=1, and V_o = 6.7789 eV. H_{AB} is defined in equation 29. The sketches at the top of the figure show the meaning θ has for each of the three sets of configurations. The major and minor axes of both wells lie in the plane of the sketches.

Conclusion

A model electron-transfer system involving nonspherical (specifically oblate-spheroidal) donor and acceptor sites and a transferable electron has been presented. The wavefunctions for the isolated donor and acceptor have been discussed at length. The electronic matrix element for electron transfer has been described and the results of several calculations presented.

Possible orientation effects in the context of the tunneling of trapped electrons in glassy matrices have been considered previously (17,18,19). These theoretical studies considered tunneling between spherically symmetric potential wells. The present chapter considers sites which are inherently orientable (because of their nonspherical symmetry) and so presumably better represent the aromatic systems toward which this study is aimed.

Thus a machinery has been developed for the calculation of orientation effects, especially for electron transfer between large aromatic molecules. Perhaps the model can be applied to synthetic electron-transfer systems, or to certain electron transfers of biological interest, where the relative orienta-

tion and separation are subject to some control. Specific applications of the model may be the subject of future work.

APPENDIX A

GOLDEN-RULE RATE CONSTANT

Consider a system consisting of an electron and a pair of sites, site A and site B. These sites are electronic potential wells. The coordinates of the electron are denoted q. Some nuclear (e.g., vibrational) coordinates Q are associated with each well and with the medium in which site A and site B reside. If the electron initially resides on site A, then the electron may hop to site B due to interaction between the electron wavefunctions localized on site A and on site B.

An approximate rate constant $k_{B \leftarrow A}$ for the electron transfer from A to B is derived in this appendix. The derivation follows closely Kestner, Logan and Jortner's slightly more general treatment given in Appendix A of reference 20. A derivation is presented here in the interest of clarity and because the treatment in reference 20 is flawed by several minor errors.

The total Hamiltonian is given in equation A.1.

$$H = T_e(q) + T_n(Q) + V_{eA}(q;Q) + V_{eB}(q;Q) + V(Q) \qquad (A.1)$$

where

$$V_{eA} = \begin{cases} -V_o^A & ; \ q \text{ in well A} \\ 0 & ; \ q \text{ elsewhere} \end{cases} \qquad (A.2)$$

and

$$V_{eB} = \begin{cases} -V_o^B & ; \ q \text{ in well B} \\ 0 & ; \ q \text{ elsewhere} \end{cases} . \qquad (A.3)$$

The potentials V_{eA} and V_{eB} are the potentials for the electron interacting with site A and with site B, respectively. For the purposes of this chapter V_{eA} and V_{eB} have the simple form indicated in equations A.2 and A.3. More general potentials would not appreciably complicate the derivation that follows. $V(Q)$ is a strictly internuclear potential. T_e and T_n are the electronic and nuclear kinetic-energy operators.

Two zeroth-order electronic Hamiltonians H_{eA} and H_{eB} can be defined. These describe the system with the electron localized on site A or on site B, respectively.

$$H_{eA} = T_e(q) + V_{eA}(q;Q) + V(Q) \qquad (A.4)$$

$$H_{eB} = T_e(q) + V_{eB}(q;Q) + V(Q) \qquad (A.5)$$

The total Hamiltonian can be written as in equation A.6. The potential of site B can be viewed as a pertur-

$$H = H_{eA}(q,Q) + V_{eB}(q;Q) \tag{A.6}$$

bation that will induce electron transfer from the zeroth-order states localized on site A. Similarly the potential of site A could be treated as perturbing the states localized on site B.

Two sets of Born-Oppenheimer electronic wavefunctions, $\{\Psi_{Ai}\}$ and $\{\Psi_{Bj}\}$, can be defined as in equations A.7 and A.8. The wavefunctions Ψ_{Ai} (indexed by i)

$$H_{eA}\ \Psi_{Ai}(q;Q) = E_{Ai}(Q)\ \Psi_{Ai}(q;Q) \tag{A.7}$$

$$H_{eB}\ \Psi_{Bj}(q;Q) = E_{Bj}(Q)\ \Psi_{Bj}(q;Q) \tag{A.8}$$

form a complete set of electronic wavefunctions localized on site A. Similarly $\{\Psi_{Bj}\}$ is a complete set of B-localized electronic states.

The wavefunction Ψ, which is a solution of Schrödinger's equation for the total Hamiltonian H, can be expanded in the union $\{\Psi_{Ai},\ \Psi_{Bj}\}$ of sets of localized electronic states. Such an expansion is given in equation A.9, where the subscript α spans

$$\Psi(q,Q,t) = \sum_{\alpha} \chi_{\alpha}(Q,t)\ \Psi_{\alpha}(q,Q) \tag{A.9}$$

both Ai and Bj. In equation A.10 Ψ has been substituted into Schrödinger's equation.

$$i\hbar \frac{\partial}{\partial t} \Psi = H \Psi \qquad \text{(A.10)}$$

The expansion A.9 can be substituted into equation A.10. Equation A.11 is then obtained by left-multiplying by Ψ^*_β (where $\beta \in \{Ai,Bj\}$) and integrating over the electronic coordinates q (typically a 3-vector) through their domain v.

$$\begin{aligned} i\hbar \int_v \Psi^*_\beta \left(\frac{\partial}{\partial t} \sum_\alpha \chi_\alpha \Psi_\alpha\right) dq \;&=\; \int_v \Psi^*_\beta \sum_{\alpha \in \{Ai\}} \chi_\alpha H_{eA} \Psi_\alpha \; dq \\ &+ \int_v \Psi^*_\beta \sum_{\alpha \in \{Bj\}} \chi_\alpha H_{eB} \Psi_\alpha \; dq \\ &+ \int_v \Psi^*_\beta \sum_\alpha \chi_\alpha U_{e\alpha} \Psi_\alpha \; dq \\ &+ \int_v \Psi^*_\beta \sum_\alpha T_n \chi_\alpha \Psi_\alpha \; dq \end{aligned}$$

$$\text{where} \qquad U_{e\alpha} = \begin{cases} V_{eB} \; ; \; \alpha \in \{Ai\} \\ V_{eA} \; ; \; \alpha \in \{Bj\} \end{cases} \qquad \text{and}$$

$$\begin{aligned} i\hbar \sum_\alpha \langle \beta | \alpha \rangle \frac{\partial}{\partial t} \chi_\alpha \;&=\; \sum_\alpha E_\alpha \chi_\alpha \langle \beta | \alpha \rangle \;+\; \sum_\alpha \chi_\alpha \langle \beta | U_{e\alpha} | \alpha \rangle \\ &+ \sum_\alpha \langle \beta | T_n \chi_\alpha | \alpha \rangle \end{aligned} \qquad \text{(A.11)}$$

The so-called 'Born-Oppenheimer breakdown operator' L is defined in equation A.12. For a nucleus of mass

$$[T_n, \chi_\alpha]\ \Psi_\alpha = (L\Psi_\alpha)\ \chi_\alpha \qquad (A.12)$$

M, the position of which is described by a single cartesian coordinate Q, for example,

$$L\Psi_\alpha = -\frac{\hbar^2}{2M}\left\{\frac{\partial^2\Psi_\alpha}{\partial Q^2} + 2\frac{\partial\Psi_\alpha}{\partial Q}\frac{\partial}{\partial Q}\right\} \quad . \qquad (A.13)$$

The operator L defined in equation A.12 can be used in equation A.11 to yield equation A.14.

$$\sum_\alpha S_{\beta\alpha}\left\{T_n + E_\alpha(Q) - i\hbar\frac{\partial}{\partial t}\right\}\chi_\alpha(Q,t) =$$

$$-\sum_\alpha \langle\beta|U_{e\alpha}|\alpha\rangle\,\chi_\alpha - \sum_\alpha \langle\beta|L|\alpha\rangle\,\chi_\alpha \qquad (A.14)$$

where $S_{\beta\alpha} \equiv \langle\beta|\alpha\rangle$.

The elements $S^{-1}_{\alpha\beta}$ of the inverse of the overlap matrix are defined by equation A.15.

$$\sum_\beta S^{-1}_{\alpha\beta}\, S_{\beta\gamma} = \delta_{\alpha\gamma} \qquad (A.15)$$

Left-multiplying equation A.14 by $S^{-1}_{\gamma\beta}$ and summing over β yields equation A.16.

$$\{T_n + E_\gamma - i\hbar\frac{\partial}{\partial t}\}\chi_\gamma = -\sum_\alpha\sum_\beta S^{-1}_{\gamma\beta}\{\langle\beta|U_{e\alpha}|\alpha\rangle + \langle\beta|L|\alpha\rangle\}\chi_\alpha \qquad (A.16)$$

Regrouping terms in equation A.16 yields equation A.17.

$$\{T_n + E_\gamma + \sum_\beta S^{-1}_{\gamma\beta}\langle\beta|U_{e\gamma} + L|\gamma\rangle - i\hbar\frac{\partial}{\partial t}\}\chi_\gamma$$

$$= -\sum_{\alpha\neq\gamma}\sum_\beta S^{-1}_{\gamma\beta}\langle\beta|U_{e\alpha}+L|\alpha\rangle\chi_\alpha \qquad (A.17)$$

In order to simplify the treatment, the problem is restricted to only two electronic states, $|A\rangle$ and $|B\rangle$. In this approximation, and neglecting matrix elements of L, equation A.17 simplifies to equation A.18 for the case γ=A. The choice γ=B leads to an equation identical to A.18 but with labels A and B interchanged; namely equation A.19.

$$\{T_n + E_A + S^{-1}_{AA}\langle A|V_{eB}|A\rangle + S^{-1}_{AB}\langle B|V_{eB}|A\rangle - i\hbar\frac{\partial}{\partial t}\}\chi_A =$$

$$-\{S^{-1}_{AB}\langle B|V_{eA}|B\rangle + S^{-1}_{AA}\langle A|V_{eA}|B\rangle\}\chi_B \qquad (A.18)$$

$$\{T_n + E_B + S^{-1}_{BB}\langle B|V_{eA}|B\rangle + S^{-1}_{BA}\langle A|V_{eA}|B\rangle - i\hbar\frac{\partial}{\partial t}\}\chi_B =$$

$$-\{S^{-1}_{BA}\langle A|V_{eB}|A\rangle + S^{-1}_{BB}\langle B|V_{eB}|A\rangle\}\chi_A \qquad (A.19)$$

A set of zeroth-order nuclear wave functions

$$\{\chi^o_{A\nu}(Q)\, e^{-itE^o_{A\nu}/\hbar},\ \nu=0,1,\ \ldots.\} \qquad (A.20)$$

corresponds to equation A.18, satisfying equation A.21. The index ν is a vibrational quantum number.

$$\{T_n + E_A + S_{AA}^{-1}\langle A|V_{eB}|A\rangle + S_{AB}^{-1}\langle B|V_{eB}|A\rangle - E_{A\nu}^{o}\}\,\chi_{A\nu}^{o} = 0 \qquad (A.21)$$

There is an analogous set of zeroth-order nuclear wavefunctions

$$\{\,\chi_{B\omega}^{o}(Q)\,e^{-itE_{B\omega}^{o}/\hbar}\;;\;\omega=0,1,\ldots.\,\} \qquad (A.22)$$

corresponding to equation A.19 and satisfying equation A.23.

$$\{T_n + E_B + S_{BB}^{-1}\langle B|V_{eA}|B\rangle + S_{BA}^{-1}\langle A|V_{eA}|B\rangle - E_{B\omega}^{o}\}\chi_{B\omega}^{o} = 0 \qquad (A.23)$$

The nuclear wavefunctions χ_A and χ_B can be expanded in the zero-order basis of equations A.20 and A.22, as in equations A.24 and A.25.

$$\chi_A(Q,t) = \sum_{\nu} C_{A\nu}(t)\,\chi_{A\nu}^{o}(Q)\,e^{-itE_{A\nu}^{o}/\hbar} \qquad (A.24)$$

$$\chi_B(Q,t) = \sum_{\omega} C_{B\omega}(t)\,\chi_{B\omega}^{o}(Q)\,e^{-itE_{B\omega}^{o}/\hbar} \qquad (A.25)$$

Equations A.24 and A.25, when substituted into equations A.18 and A.19, yield equations A.26 and A.27.

$$i\hbar \frac{\partial}{\partial t} C_{A\nu} = \sum_{\omega} C_{B\omega}(t)\{\langle A\nu|S_{AB}^{-1}\langle B|V_{eA}|B\rangle + S_{AA}^{-1}\langle A|V_{eA}|B\rangle\ |B\omega\rangle\}e^{-i(E^{o}_{B\omega} - E^{o}_{A\nu})t/\hbar} \tag{A.26}$$

$$i\hbar \frac{\partial}{\partial t} C_{B\omega} = \sum_{\nu} C_{A\nu}(t)\{\langle B\omega|S_{BA}^{-1}\langle A|V_{eB}|A\rangle + S_{BB}^{-1}\langle B|V_{eB}|A\rangle\ |A\nu\rangle\}e^{-i(E^{o}_{A\nu} - E^{o}_{B\omega})t/\hbar} \tag{A.27}$$

From this point the derivation follows a standard route to a Golden-Rule rate expression. Consider transitions from an initial state $|A\nu\rangle$ to a final state $|B\omega\rangle$, assuming that $C_{A\nu'} = \delta_{\nu,\nu'}$ and that $C_{B\omega}(t=0) = 0$ for all ω. With V_{AB} defined as in equation A.28, this assumption applied to equation A.27 yields equation A.29.

$$V_{AB} \equiv S_{AB}^{-1}\langle A|V_{eB}|A\rangle + S_{BB}^{-1}\langle B|V_{eB}|A\rangle \tag{A.28}$$

$$C_{B\omega} = \langle B\omega|V_{AB}|A\nu\rangle \times \begin{cases} \dfrac{e^{-i(E^{o}_{A\nu} - E^{o}_{B\omega})t/\hbar} - 1}{E^{o}_{A\nu} - E^{o}_{B\omega}}; & E^{o}_{A\nu} \neq E^{o}_{B\omega} \\ -it/\hbar; & E^{o}_{A\nu} = E^{o}_{B\omega} \end{cases} \tag{A.29}$$

If the rate constant for transitions $A\nu \rightarrow B\omega$ is defined as in equation A.30, then equation A.29 yields the state-to-state rate constant given in equation A.31.

$$k_{B\omega \leftarrow A\nu} \equiv \lim_{t\to\infty} \{ \frac{1}{t} |C_{B\omega}|^2 \} \qquad (A.30)$$

$$k_{B\omega \leftarrow A\nu} = \frac{2\pi}{\hbar} |\langle B\omega | V_{AB} | A\nu \rangle|^2 \, \delta(E^o_{A\nu} - E^o_{B\omega}) \qquad (A.31)$$

It is the matrix element in equation A.28 that is given, with a few errors, in equation I.5 of reference 20.

The total rate constant for transitions from site B to site A can be constructed as the Boltzmann-weighted sum over the state-to-state rate constants $k_{B\omega \leftarrow A\nu}$.

$$k_{B\leftarrow A} = \frac{2\pi}{\hbar Q_A} \sum_{\nu} \sum_{\omega} e^{-E^o_{A\nu}/k_B T} |\langle B\omega | V_{AB} | A\nu \rangle|^2 \, \delta(E^o_{A\nu} - E^o_{B\omega}) \qquad (A.32)$$

In equation A.32 Q_A is a nuclear partition function for the case when the electron is localized on site A. Equation A.32 may be simplified by applying the Condon approximation, in which the electronic matrix element V_{AB} is removed from the integral over nuclear coordinates, yielding equation A.33.

$$k_{B\leftarrow A} = \frac{2\pi}{\hbar Q_A} |V_{AB}|^2 \sum_{\nu} \sum_{\omega} e^{-E^o_{A\nu}/k_B T} |\langle B\omega | A\nu \rangle|^2 \delta(E^o_{A\nu} - E^o_{B\omega}) \qquad (A.33)$$

Equation A.28 for V_{AB} may be transformed to the more familiar form of equation A.34 (reference 21, for example, uses V_{AB} in the form of equation A.34) by noting that, within the present treatment in which only two electronic states are considered, $S_{BA}^{-1} = - S_{AB}/(1 - S_{AB}^{2})$ and $S_{BB}^{-1} = 1/(1 - S_{AB}^{2})$, where $S_{AB} \equiv \langle A|B\rangle$, and it is assumed that $\langle A|A\rangle = \langle B|B\rangle = 1$.

$$V_{AB} = \{ \langle B|V_{eA}|A\rangle - S_{AB}\langle A|V_{eB}|A\rangle \}/(1 - S_{AB}^{2}) \qquad (A.34)$$

References

(1) V. V. Klimov, A. V. Klevanik, V. A. Shuvalov, and A. A. Krasnovsky, FEBS Letters 1977, 82,183-186.

(2) J. Fajer, M. S. Davis, A. Forman, V. V. Klimov, E. Dolan, and B. Ke, J. Am. Chem. Soc. 1980,102,7143-7145.

(3) M. S. Davis, A. Forman, and J. Fajer, Proc. Nat'l Acad. Sci. USA 1979,76,4170-4174.

(4) S. Schichman and H. B. Gray, to be published.

(5) T. L. Netzel, P. Kroger, C. K. Chang, I. Fujita, and J. Fajer, Chem. Phys. Letters 1979, 67,223-228.

(6) T. L. Netzel, M. A. Bergkamp, and C. K. Chang, J. Am. Chem. Soc. 1982,104,1952-1957.

(7) G. McLendon, private communication.

(8) C. Flammer, "Spheroidal Wave Functions" (Stanford Univeristy Press, Stanford, 1957).

(9) D. B. Hodge, J. Math. Phys. 1970,11,2308-2312.

(10) J. Rainwater, Phys. Rev. 1950,79,432-434.

(11) S. Granger and R. D. Spence, Phys. Rev. 1951, 83,460-461.

(12) J. R. Platt, J. Chem. Phys. 1954,22,1448-1455.

(13) R. T. Morrison and R. N. Boyd, "Organic Chemistry," (Allyn and Bacon, Boston, 1973), Third Ed., page 968.

(14) I. V. Alexandrov, R. F. Khairutdinov, and K. I. Zamaraev, Chem. Phys. 1978,32,123-141.

(15) R. K. Huddleston and J. R. Miller, J. Phys. Chem. 1982,86,1347-1350.

(16) J. R. Miller and J. V. Beitz, J. Chem. Phys. 1981,74,6746-6756.

(17) S. A. Rice and M. J. Pilling, Progr. React. Kinet. 1978,9,93-194.

(18) B. Brocklehurst, J. Phys. Chem. 1979,83,536-543.

(19) A. B. Doktorov, R. F. Khairutdinov, and and K. I. Zamaraev, Chem. Phys. 1981,61, 351-364.

(20) N. R. Kestner, J. Logan, and J. Jortner, J. Phys. Chem. 1974,78,2148-2166.

(21) M. D. Newton, Int'l J. Quant. Chem. : Quant. Chem. Symposium 1980,14,363-391.